HIGHWAY RESEARCH RECORD

Number 386

Traffic Safety Barriers, Lighting Supports, and Dike Slopes

11 reports

HIGHWAY RESEARCH BOARD
NATIONAL RESEARCH COUNCIL
NATIONAL ACADEMY OF SCIENCES—NATIONAL ACADEMY OF ENGINEERING

1972
HIGHWAY RESEARCH BOARD

OFFICERS

Alan M. Voorhees, *Chairman*
William L. Garrison, *First Vice Chairman*
Jay W. Brown, *Second Vice Chairman*
W. N. Carey, Jr., *Executive Director*

EXECUTIVE COMMITTEE

A. E. Johnson, *Executive Director, American Association of State Highway Officials* (ex officio)
F. C. Turner, *Federal Highway Administrator, U.S. Department of Transportation* (ex officio)
Carlos C. Villarreal, *Urban Mass Transportation Administrator, U.S. Department of Transportation* (ex officio)
Ernst Weber, *Chairman, Division of Engineering, National Research Council* (ex officio)
D. Grant Mickle, *President, Highway Users Federation for Safety and Mobility* (ex officio, Past Chairman 1970)
Charles E. Shumate, *Executive Director, Colorado Department of Highways* (ex officio, Past Chairman 1971)
Hendrik W. Bode, *Gordon McKay Professor of Systems Engineering, Harvard University*
Jay W. Brown, *Director of Road Operations, Florida Department of Transportation*
W. J. Burmeister, *Executive Director, Wisconsin Asphalt Pavement Association*
Howard A. Coleman, *Consultant, Missouri Portland Cement Company*
Douglas B. Fugate, *Commissioner, Virginia Department of Highways*
William L. Garrison, *Edward R. Weidlein Professor of Environmental Engineering, University of Pittsburgh*
Roger H. Gilman, *Director of Planning and Development, Port of New York Authority*
George E. Holbrook, *E. I. du Pont de Nemours and Company*
George Krambles, *Superintendent of Research and Planning, Chicago Transit Authority*
A. Scheffer Lang, *Department of Civil Engineering, Massachusetts Institute of Technology*
John A. Legarra, *Deputy State Highway Engineer, California Division of Highways*
William A. McConnell, *Director, Product Test Operations Office, Product Development Group, Ford Motor Company*
John J. McKetta, *Department of Chemical Engineering, University of Texas*
John T. Middleton, *Deputy Assistant Administrator, Office of Air Programs, Environmental Protection Agency*
Elliott W. Montroll, *Albert Einstein Professor of Physics, University of Rochester*
R. L. Peyton, *Assistant State Highway Director, State Highway Commission of Kansas*
Milton Pikarsky, *Commissioner of Public Works, Chicago*
David H. Stevens, *Chairman, Maine State Highway Commission*
Alan M. Voorhees, *President, Alan M. Voorhees and Associates, Inc.*
Robert N. Young, *Executive Director, Regional Planning Council, Baltimore*

HIGHWAY RESEARCH RECORD

Number 386

Traffic Safety Barriers, Lighting Supports, and Dike Slopes

11 reports
prepared for the
51st Annual Meeting

Subject Areas

22 Highway Design
27 Bridge Design
51 Highway Safety

HIGHWAY RESEARCH BOARD
DIVISION OF ENGINEERING NATIONAL RESEARCH COUNCIL
NATIONAL ACADEMY OF SCIENCES—NATIONAL ACADEMY OF ENGINEERING

Washington, D.C. 1972

NOTICE

The studies reported herein were not undertaken under the aegis of the National Academy of Sciences or the National Research Council. The papers report research work of the authors done at the institution named by the authors. The papers were offered to the Highway Research Board of the National Research Council for publication and are published herein in the interest of the dissemination of information from research, one of the major functions of the HRB.

Before publication, each paper was reviewed by members of the HRB committee named as its sponsor and was accepted as objective, useful, and suitable for publication by NRC. The members of the committee were selected for their individual scholarly competence and judgment, with due consideration for the balance and breadth of disciplines. Responsibility for the publication of these reports rests with the sponsoring committee; however, the opinions and conclusions expressed in the reports are those of the individual authors and not necessarily those of the sponsoring committee, the HRB, or the NRC.

Although these reports are not submitted for approval to the Academy membership or to the Council of the Academy, each report is reviewed and processed according to procedures established and monitored by the Academy's Report Review Committee.

ISBN 0-309-02056-5

Price: $3.80

Available from

Highway Research Board
National Academy of Sciences
2101 Constitution Avenue, N.W.
Washington, D.C. 20418

CONTENTS

FOREWORD

The 11 papers in the RECORD deal with the design and testing of roadside appurtenances such as traffic safety barriers, luminaire and motorist-aid call-box supports, and various ground forms for transverse earthen dikes and sloping grates for culverts in highway medians. These papers will be of interest to highway engineers concerned with improving the safety aspects of the roadside environment.

Hayes, Ivey, Hirsch, and Viner report on the design and favorable full-scale tests of a hybrid traffic safety barrier, composed of a steel drum crash cushion backed by concrete median barriers, for use at bridge piers in medians. The crash cushions act as energy absorbers for frontal impacts and as redirection barriers for angle impacts into the front of piers. The concrete barriers redirect angle impacts into the sides of or between the piers.

Ivey, Buth, Hirsch, and Viner describe the development and results of recent vehicle crash tests of an energy-absorbing barrier or crash cushion constructed of lightweight vermiculite concrete. The authors conclude that the barrier is an effective system for protecting motorists from head-on or side-angle impacts with rigid obstacles.

Walker, Young, and Warner report the results of a series of vehicle impact tests of a modified water-cell crash cushion, wherein water cells are progressively replaced by energy-absorbing cartridges constructed of vermiculite concrete. Harness-restrained human drivers in medium-weight vehicles report no discomfort in impacts into this barrier at speeds greater than 50 mph.

The results of three full-scale vehicle impact tests of an energy-absorbing barrier employing sand-filled frangible plastic barrels are reported by Nordlin, Stoker, and Doty. Sedans weighing 4,700 lb impacted the nose of this barrier head on and at a 15-deg angle. A 1,900-lb sedan impacted the nose head on. The barrier performed satisfactorily in these tests.

The fifth paper reports on full-scale vehicle crash tests of luminaire supports conducted to evaluate their behavior on impact and to develop quantitative information for comparison with pendulum tests of identical supports. The authors, Buth and Ivey, conclude that a definitive relation between change-in-momentum values for pendulum tests and full-scale vehicle tests was not obtained.

Martinez and Hairston evaluated the results of vehicle collisions into various roadside motorist-aid call-box assemblies. This study was carried out with the aid of a mathematical model verified by pendulum and full-scale vehicle crash tests. The authors concluded that vehicle velocity and momentum changes due to the collision of 2,000- to 5,000-lb vehicles impacting at speeds of 20 to 60 mph were well within established tolerable limits.

The approach ends of guardrails and median barriers have offered less protection to motorists than the length-of-need section of the installation. Bronstad and Michie report on the encouraging results of end-on full-scale vehicle impact tests into a new guardrail terminal design. The new terminal provides the necessary end anchorage strength yet appears to offer greatly improved safety advantages.

Walker and Warner report the results of full-scale vehicle crash tests performed to evaluate a lapped W-section, strong-post guardrail or median barrier employing energy-absorbing cartridges constructed of vermiculite concrete. The authors concluded that a standard weight sedan can survive impacts into this barrier at a speed of 60 mph and an angle of 21 deg without complete loss of steering control.

Nordlin, Stoker, Hackett, and Doty report the results of full-scale vehicle impact tests on a bridge barrier rail consisting of two $3\frac{1}{2}$-in. square tubular steel rails mounted 14 and 27 in. above the pavement on 6-WF-25-steel posts bolted to the edge of a concrete deck. The authors conclude that this design with post spacing at 8 ft will

satisfactorily retain and redirect a 4,500-lb impacting vehicle at a speed of 60 mph and an angle of 15 deg.

Ross and Post used a mathematical computer simulation technique to investigate the dynamic behavior of a selected automobile negotiating various ground forms in the vicinity of the sloping inlet or outlet grate for a culvert. These simulations provided information on dynamic tire forces, accelerations, and translational and rotational motion of the automobile. For some ground forms, roll-over occurred as illustrated by computer graphic displays.

The last paper by Dunlap and Grote evaluates the safety hazard of earthen dikes to errant vehicles impacting and/or traversing them. The main analysis tool was a 14-degree-of-freedom digital computer program with a special modification to simulate a vehicle traversing soft soil. The preceding paper and this one demonstrate that mathematical simulations provide a rapid and economical means of analytically investigating the many parameters involved in a vehicle negotiating various ground forms.

—E. F. Nordlin

HYBRID BARRIER FOR USE AT BRIDGE PIERS IN MEDIANS (MODULAR CRASH CUSHION PLUS CONCRETE MEDIAN BARRIER)

Gordon G. Hayes, Don L. Ivey, and T. J. Hirsch, Texas Transportation Institute, Texas A&M University; and
John G. Viner, Federal Highway Administration

A traffic safety barrier for use at bridge piers in roadway medians has been designed and crash-tested. The hybrid system consists of steel drum crash cushions that have smooth transitions to concrete median barriers. The system is narrow enough to allow installation in relatively restricted median areas under highway overpasses. The crash cushions, which are located in front of the outermost bridge piers, act as energy absorbers for frontal impacts and as redirection barriers for angle impacts. The concrete median barrier serves as a redirection barrier for "interior" angle impacts. Two vehicles were directed into the side of the crash cushion at 10 and 20 deg to test the system in the crash cushion median barrier transition area. The vehicles were redirected smoothly and showed no spin-out or overturning tendency. Without structural repairs to the barrier after the 10-deg test, a lightweight vehicle was directed head on into the crash cushion and was brought to a stop in an acceptable manner.

•BRIDGE piers in roadway medians at highway overpass structures present a rigid-object hazard to passing motorists. The probability of injury to occupants of a vehicle that violates the median in the overpass area can be greatly reduced by adding an energy-absorbing device to the front of the outermost bridge piers.

The use of guardrails at such locations is not a wholly satisfactory solution because a substantial portion of the length of these median installations are end-treatments, and all currently available guardrail end-treatments are quite hazardous themselves (1). The hybrid crash cushion and concrete median barrier discussed in this report is one possible alternative to current treatments at these locations.

An impact attenuator that has a compatible transition to a concrete median barrier system was designed, constructed, and tested under a contract with the Federal Highway Administration (FHWA). These evaluation tests consisted of crashing two vehicles at angles of 10 and 20 deg into the side of the system and one vehicle head on into the crash cushion.

DESCRIPTION OF BARRIER SYSTEM

Two simulated concrete bridge piers were installed for the tests. The protective installation shown in Figure 1 is a combination of a shaped concrete median barrier (2) and a variation of the modular crash cushion (3, 4). This cushion was designed by the Structures and Applied Mechanics Division of FHWA with the assistance of the Texas Transportation Institute (TTI).

The crash cushion was composed of 55-gallon steel drums with holes in the tops and bottoms to reduce the crush strength. Plywood panels (2 ft high and 4 ft long) covered with sheet metal were attached to the side of the crash cushion adjacent to oncoming traffic to provide a redirection capability for vehicles that strike a glancing blow. These redirection panels are attached to the drums in a fish-scale fashion and telescope in a head-on collision without altering barrier crush characteristics.

Sponsored by Committee on Traffic Safety Barriers and Sign, Signal and Lighting Supports.

These 2- by 4-ft panels were chosen in preference to the 3- by 8-ft panel scheme used in earlier development tests (4) and in the demonstration conducted by U.S. Steel to minimize the ramping of the vehicle that was noted in these impacts. The 2- by 4-ft panel was inspired by Hensen's (5) use of 2- by 3-ft panels in the design of a barrier for use in Denver, Colorado. It was felt that the 2-ft high panels, centered on the 34¾-in. drums, would decrease ramping by offering a smaller smooth surface. It was anticipated that the tops and bottoms of the drum would probably lip over the panel edges during impact and retard any ramping tendency. Also, it was felt that the lower trailing corners of these 2- by 4-ft panels were not as likely to scrape against the ground and cause a tendency toward ramping in this fashion.

Steel cables gave the cushion and redirection panels lateral stability for side impacts. The cables were passed through eyebolts in the support posts so that the drums, support posts, and redirection panels could slide along the cables during a head-on collision. The ¾-in. wire rope cables were located at the top rolling hoop of the steel drum to encourage a slight downward wedging action (again to decrease ramping tendencies) of the panels during side impacts. This feature was suggested by the U.S. Steel demonstration tests conducted by TTI.

As shown in Figure 1, the support cables on the left (looking from the front of the crash cushion) were arranged differently. The two ¾-in. cables were located between the first and second columns of drums to eliminate vehicle snagging at the cable anchorage in the event a "reverse" impact occurred from traffic in the other lanes. No plywood redirection panels were used on the left side in this installation. If panels had been used on the left side, they would have had to be hinged at their rearward edge to redirect vehicles moving from the rear to the front. The outside top edge of the concrete median barrier was aligned with the side face of the steel drums (adjacent to front-to-rear traffic) so that unnecessary contact with the drums would be avoided.

The concepts for this barrier called for as narrow a barrier as possible to allow its use where space is restricted as well as to offer a smaller target to an errant vehicle in order to reduce the number of collisions with the barrier. For this reason, the shaped concrete median barrier was selected as an element of the hybrid barrier.

The number of drums per row toward the rear of the barrier was increased in previous designs for steel drum crash cushion tests to stop 2,000- to 4,500-lb impacting vehicles with acceptable decelerations and to avoid the use of an unnecessarily long barrier. This resulted in barrier designs that had four to six drums per row at the rear of the barrier. In those tests, all of the drums had the same crushing strength (same gauge and hole cutout pattern). This could be referred to as a monomodular design concept. The crash cushion used in these tests consisted of three columns of drums with relatively "soft" drums on the crash-cushion nose, "medium stiff" drums in the center, and "stiff" drums in the rear of the crash cushion.

The crush characteristics of these drums and the corrugated metal pipe segments used in this design are given elsewhere (6). It was recognized that the use of two or more different gauge drums with identical hole cutout patterns could result in confusion in the field. To minimize the possibility of such field problems occurring, we used the same gauge drums with varying hole cutout patterns. Data on crush resistances for various hole cutout patterns are given elsewhere (6).

The resulting design had the same number of drums in each row, which permitted the cables to be kept straight in plan view, as is desirable, and the side of the crash cushion to be aligned parallel to the roadway. This had the advantage of reducing the angle of impact with the side of the barrier in a given collision as compared with the previously discussed design.

The concrete median portion of this barrier is an adaptation of the GM shaped concrete section. In an earlier test (a 63-mph, 25-deg impact into a 32-in. high New Jersey shaped concrete median barrier) reported by Nordlin (2), portions of the sheet metal of the vehicle lipped over the top of the barrier. Because the concept of the hybrid barrier discussed in this report called for a design in which the concrete median section of the barrier could be placed as close as possible to the bridge piers, the concrete median barrier height was increased to 40 in. as shown in Figure 1. This modified GM shape had an upper face that was 25 in. high with a 3⅞-in. offset as compared to the 16⅞-in.

height and $2\frac{7}{8}$-in. offset of the standard GM shape. The purpose of this change was primarily to improve barrier performance for collisions involving pickup trucks and heavier vehicles. Evaluation of this aspect of the barrier design was beyond the scope of this investigation.

PHOTOGRAPHIC INSTRUMENTATION

Four high-speed cameras were used in Tests A and B. One camera was located perpendicular to the initial path of the vehicle, one parallel to the crash-cushion centerline, one perpendicular to the crash-cushion centerline, and one overhead. In Test C, a head-on impact, two cameras were located perpendicular to the crash-cushion centerline (and vehicle path), and one was mounted overhead. Three documentary cameras were used in all tests.

The high-speed motion pictures of the tests had timing marks on the edge of the film from which film speed, and therefore elapsed time, could be computed. Each test vehicle had a stadia board and several targets on it to facilitate the measurement of vehicle movement. The average speed of the vehicle over a desired interval could then be obtained from time-displacement determinations. These measurements were made along the path of the vehicle. The lateral motion of the vehicle (perpendicular to the crash cushion) was determined from the overhead or end-view cameras.

ELECTROMECHANICAL INSTRUMENTATION

In Tests A and B, transverse and longitudinal accelerometers were mounted on short flanges welded to each longitudinal frame member just behind the front seat. In Test C, only longitudinal accelerometers were included on the vehicle. Throughout this report, longitudinal decelerations indicate accelerations toward the rear of the vehicle, and transverse decelerations indicate accelerations toward the right of the vehicle (deceleration = negative acceleration). In all tests, an anthropometric dummy was secured in the driver's seat by a lap belt connected to a load cell that sensed lap belt force. In Test C, a head-on impact, biaxial accelerometers were mounted in the head of the dummy. The signals from the various transducers were transmitted by telemetry to a ground station and recorded on magnetic tape. The accelerometer data were passed through an 80-Hz low-pass active filter to reduce the effects of "ringing."

DESCRIPTION OF TESTS

Test A

A 4,150-lb Ford sedan was directed obliquely into the side of the crash cushion at a speed of 56.7 mph. The vehicle's approach path made a 20-deg angle with the centerline of the crash cushion. The impact point was selected such that the driver's seat was directed at the center of the front bridge pier. With this impact point, it was thought that maximum barrier deflection would occur in the vicinity of the transition between the crash cushion and the shaped concrete barrier and thus provide the most meaningful test for this transition. The left front end of the vehicle contacted the crash cusion at the rear edge of the fifth fender panel from the front, as shown in Figure 2. Both the maximum deformation of the crash cushion and the maximum vehicle decelerations occurred at roughly 0.150 sec after impact. As desired, the front end of the vehicle was near the bridge pier-median barrier transition at this time. Figure 3 shows sequential photographs from an end view. Elapsed times are not shown in Figure 3 because the camera used in the test does not incorporate timing marks on the film.

The vehicle redirected smoothly. The residual lateral deformation of the side of the crash cushion was 16 in. Seven steel drums and eight fender panels were damaged. Figure 4 shows the vehicle after the test. The left front of the vehicle was deformed 18 in. longitudinally and 16 in. transversely. The damage to the left front wheel caused the vehicle to swerve in an arc to the left after loss of contact with the barrier.

The vehicle deceleration data are given in Tables 1 and 2. The average lateral deceleration (from contact until the vehicle was parallel to the barrier centerline) calculated from high-speed film over a period of 0.27 sec was about 4 g. The accelerometers indicated a maximum longitudinal deceleration of 14.4 g and a maximum transverse

Figure 1. Crash cushion median barrier system.

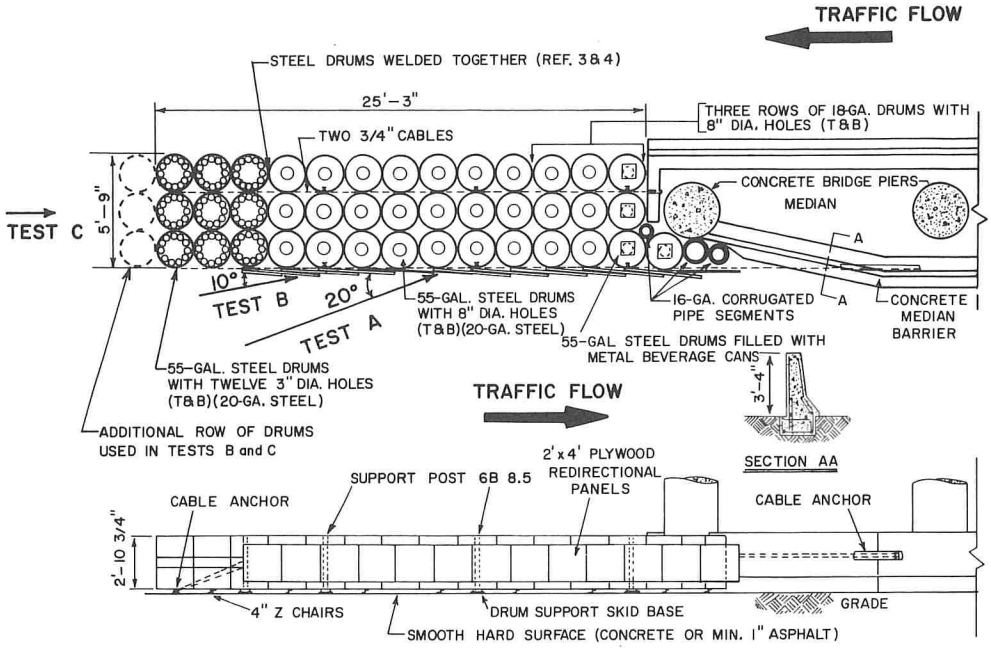

Figure 2. Barriers before and after Test A (oblique view).

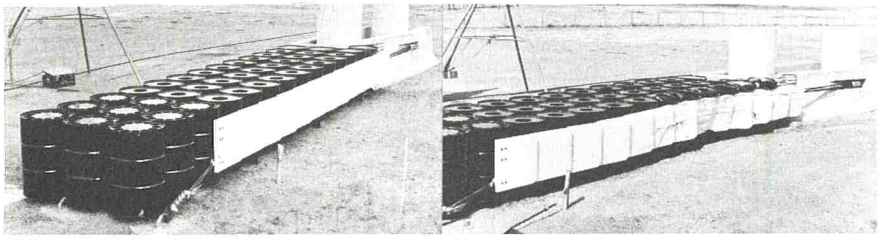

Figure 3. Sequential photographs of Test A (view parallel to barrier).

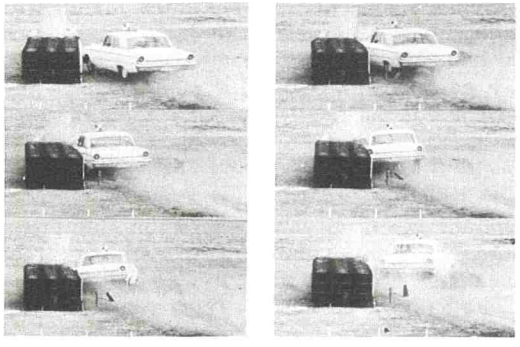

Figure 4. Vehicle after Test A.

deceleration of 10.4 g. The average longitudinal deceleration was 2.6 g over a period of 0.46 sec, and the average transverse deceleration was 2.0 g over a period of 0.46 sec.

Test B

In this test, a 3,990-lb 1964 Dodge sedan struck the barrier 10 deg to the centerline at a speed of 62.3 mph. The purpose of this test was to evaluate the transition between the crash cushion and the shaped concrete barrier under test conditions (60 mph, 10 deg) that have caused vehicle ramping and near overturn in previous tests. The crash cushion had been restored to its original condition with the exception of one corrugated steel pipe at the edge of the concrete backup wall that was not replaced. In addition, another row of steel drums was added to the front of the crash cushion. As in Test A, the impact point was selected such that the driver's seat was aimed at the center of the bridge pier.

Figure 5 shows the barrier after the test, and Figure 6 shows sequential photographs of the test. The damage to the crash cushion was slight. The redirection was very smooth, with only a slight ramping of the left front end of the vehicle observed. The vehicle left the barrier at an angle of about 5 deg to the centerline of the crash cushion; the tracks of the vehicle as it left the barrier can be seen in Figure 5. The damage to the vehicle is shown in Figure 7. The vehicle was driven away from the site after the test, which indicates, along with the small angle of departure, that a driver could have maintained control after the impact.

The accelerometer data showed that the maximum longitudinal deceleration was 3.4 g and the maximum transverse deceleration was 11.0 g. The average longitudinal and transverse decelerations over a period of about 0.4 sec were 0.8 and 2.0 g respectively. The high-speed film showed that the average longitudinal deceleration was 2.5 g and the average deceleration perpendicular to the crash cushion was 3.0 g. Parallelism occurred at 0.19 sec.

Test C

Damage reports from field installations indicate that more than one collision can occur before the damage is discovered and the crash cushion repaired. To evaluate the performance of the crash cushion after an angle impact, we conducted the final test of the series without restoring the crash cushion except for painting and reshaping some of the fender panels. (The shape of these panels does not have a significant effect in head-on impacts.)

A 1965 Simca weighing 1,790 lb struck the crash cushion head on at a speed of 55.8 mph. At test time, the crash cushion had a bow in it from the previous test; the maximum deformation was 9 in. The condition of the crash cushion before and after the test is shown in Figure 8. The damaged fender panels can be seen in Figure 9 (t = 0.000 sec). The front end of the lightweight, rear-engine vehicle was deformed 11 in. at the bumper level, and the hood was pushed back but did not penetrate the windshield.

The vehicle's forward motion stopped in 0.257 sec, after 11.3 ft of travel. The average deceleration over this interval, inferred from the films, was 9.2 g. The vehicle rebounded 1.8 ft. The average deceleration, inferred from the accelerometers, over a period of 0.356 sec was 7.2 g.

In this test, the resultant from the biaxial accelerometers in the dummy's head was plotted and graphically integrated piecemeal to obtain an index to compare to a published injury criterion called the Gadd Severity Index (7). This index is defined as follows:

$$SI = \int_0^t a^n \, dt$$

where

a = acceleration in g,
t = time in seconds, and
n = an exponent greater than unity.

Table 1. Film analysis data.

Factor	Test A	Test B	Test C
Vehicle weight, lb	4,150	3,990	1,790
Impact angle, deg	20	10	0
Initial speed, fps	83.1	91.4	81.8
Initial speed, mph	56.7	62.3	55.8
Final speed, fps	45.6	75.9	0[a]
Final speed, mph	31.1	51.7	0[a]
Time in contact, sec	0.513	0.414	0.257[a]
Distance in contact, ft	29.2	31.9	11.3[a]
Average longitudinal deceleration, g			
Vehicle parallel to barrier	4.0[b]	2.5[b]	9.2[a,b]
	3.9[c]	2.4[c]	9.9[c]
Loss of contact	2.6[b]	1.3[b]	8.9[b,d]
	2.3[c]	1.2[c]	7.8[c,d]
Average lateral[e] deceleration, g			
Vehicle parallel to barrier	3.9[b]	3.0[b]	—
	3.2[c]	2.6[c]	—

[a]At end of forward motion in Test C.
[b]Calculated by $(V_1^2 - V_2^2/2gD)$; where V_1 = initial speed, V_2 = speed at point of interest, D = distance traveled by vehicle's CG over interval used, and g = 32.2 ft/sec^2.
[c]Calculated by (1/g) ($\Delta V/\Delta t$), where ΔV = change in speed of vehicle's CG and Δt = time interval.
[d]To end of accelerometer traces (0.5 ft of rebound).
[e]Lateral = perpendicular to barrier centerline.

Table 2. Accelerometer data.

Factor	Test A	Test B	Test C
Vehicle weight, lb	4,150	3,990	1,790
Impact angle, deg	20	10	0
Maximum deceleration,[a] g			
Longitudinal	14.4	3.4	13.8
Transverse	10.4	11.0	—
Average deceleration,[a] g			
Longitudinal	2.6	0.8	7.2
Time interval, sec	0.460	0.411	0.356
Transverse[b]	2.0	2.0	—
Time interval, sec	0.461	0.410	—

[a]Values given are averages of right and left accelerometer outputs.
[b]Transverse to vehicle longitudinal axis.

Figure 5. Barrier after Test B (oblique view).

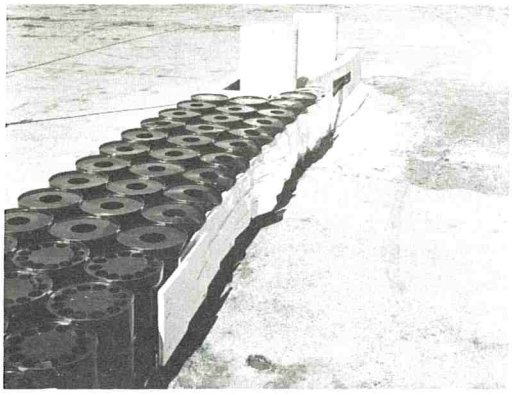

Figure 6. Sequential photographs of Test B (overhead view).

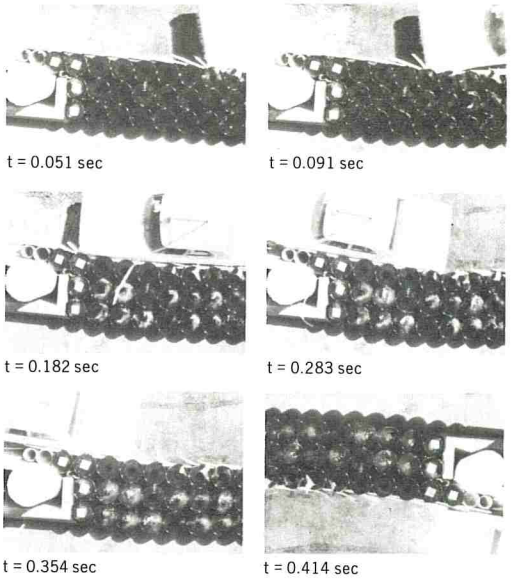

Figure 7. Vehicle before and after Test B.

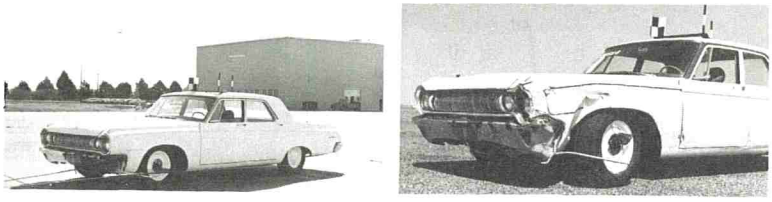

Figure 8. Barrier before and after Test C (end view).

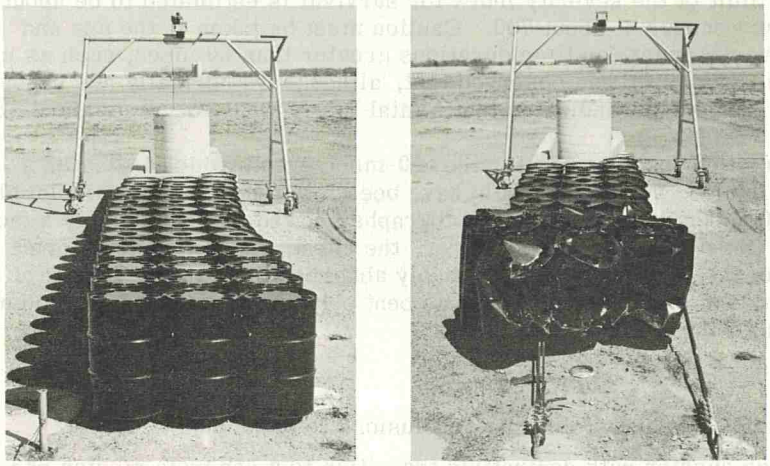

Figure 9. Sequential photographs of Test C (view perpendicular to barrier).

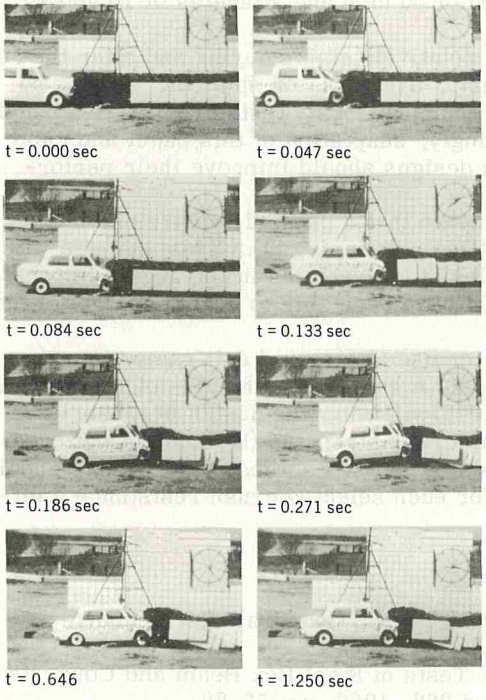

For head-face impacts that last between 1 and 60 msec (8), the exponent n has a value of 2.5; the upper limit of the severity index for survival is estimated to be about 1,000, and moderate injury occurs at about 700. Caution must be taken in the use and interpretation of the severity index for time durations greater than 60 msec, such as in this test. For example, Snyder (8) has observed that, although we normally are exposed to 1 g our entire lives, the formula indicates that a fatal injury would occur in about 16 min.

The severity index for this test was 176 for the 540-msec event, which indicates a low probability of head injury. The index would have been lower had it been calculated over the most severe 60-msec interval. The photographs showed that the dummy's face hit the upper portion of the steering wheel; however, the chest, which hit the steering column and lower part of the steering wheel, probably absorbed most of the energy of the torso motion. The dashboard of the vehicle was bent outward by the steering column, and the driver's seat was shifted forward.

CONCLUSIONS

The results of this study allow the following conclusions to be made:

1. The modular crash cushion with compatible transition to a concrete median barrier performed comparable to previous modular crash cushions in attenuating a head-on vehicle impact.
2. The crash cushion used in this test series with a compatible transition to a concrete median barrier had sufficient lateral strength to smoothly redirect 4,000-lb vehicles impacting the side of the cushion at a speed of 60 mph and at angles of 10 and 20 deg.
3. In angle impacts, the vehicles remained relatively stable during and after the redirection process and showed no tendency to ramp, overturn, or spin out. The 2- by 4-ft redirection panels appear far superior to other previously tested redirection panels used on the steel drum crash cushion. Accordingly, adaptation of this panel and cable arrangement to other steel drum crash cushion designs should improve their performance.
4. The vehicle decelerations in all tests indicate that a properly restrained passenger would have survived the impacts with little or no injury (9). This, coupled with the very stable behavior and low departure angles of the vehicles in the angled impacts, suggests that a properly restrained driver might have been able to regain control of the redirected vehicles.
5. This barrier design can also be adopted for use at elevated exit ramps by using the cable and panel arrangement impacted in Tests A and B on both sides of the barrier.
6. Use of the information presented by White (6) will allow the design of a barrier of this type using all 20-gauge drums with different crash strengths (hole cutout patterns) rather than the combination of 18- and 20-gauge drums used in these tests. This should reduce possible confusion in the field because for each selected crush resistance a different hole cutout pattern would be selected.

REFERENCES

1. Michie, J. D., Calcote, L. R., and Bronstad, M. E. Guardrail Performance and Design. Final Rept. on NCHRP Proj. 15-1(2), Jan. 1970.
2. Nordlin, E. F., and Field, R. N. Dynamic Tests of Steel Box Beam and Concrete Median Barriers. Highway Research Record 222, 1968, pp. 53-88.
3. Hirsch, T. J. Barrel Protective Barrier. Texas Transportation Institute, Texas A&M Research Foundation, Tech. Memo 505-1, July 1968.
4. Hirsch, T. J., Hayes, G. G., and Ivey, D. L. The Modular Crash Cushion. Texas Transportation Institute, Texas A&M Research Foundation, Tech. Memo 505-1S, Aug. 1970.
5. Hensen, R. J. Energy Absorber Designs for Exit Ramp Gores. Denver Research Institute.

6. White, M. D. The Modular Crash Cushion: Design Data From Static Crush Tests of Steel Drums and of Corrugated Steel Pipes. Federal Highway Administration, U. S. Department of Transportation, Progress memo on Contract CPR-11-5851, April 1971.
7. Gadd, C. W. Use of a Weighted-Impulse Criterion for Estimating Injury Hazard. Proc., 10th Stapp Car Crash Conf., SAE, New York, 1966.
8. Snyder, R. G. Human Impact Tolerance. 1970 Internat. Automobile Safety Conf. Compendium, Detroit, May 13-15, 1970; Brussels, Belgium, June 8-11, 1970, pp. 712-782.
9. Patrick, L. M., et al. Knee, Chest, and Head Impact Loads. Proc., 11th Stapp Car Crash Conf., SAE, Anaheim, Oct. 10-11, 1967.

EVALUATION OF CRASH CUSHIONS CONSTRUCTED OF LIGHTWEIGHT CELLULAR CONCRETE

Don L. Ivey, Eugene Buth, and T. J. Hirsch, Texas Transportation Institute, Texas A&M University; and
John G. Viner, Federal Highway Administration

Lightweight cellular concrete crash cushions have now progressed to the the point that experimental installations are being made in the continental United States. This report describes the development of these safety devices and presents the results of the most recent vehicle crash tests. This crash cushion is composed of vermiculite concrete, lightweight welded wire fabric, and cylindrical cardboard forms. At the present stage of development, the crash cushion is an effective system that protects motorists from collisions with rigid obstacles whether they collide in a head-on or side-angle attitude.

•THE feasibility of vehicle crash cushions constructed of lightweight cellular concrete was demonstrated by a series of three head-on vehicle impacts on prototype installations (1). The concrete crash cushion is one of a group of first-generation devices that include the barrel crash cushion, the Fitch inertia barrier, and the Hi-Dro Cell barrier. The evaluation sequence that was followed with all of these systems is (a) feasibility testing, (b) full-scale head-on testing, and (c) side-angle testing. Because of the excellent performance of the concrete cushion in the first three tests conducted, several states were interested in applying the concept to some of their potentially hazardous areas. The basic cushion (2) that was tested under the Federal Highway Administration's 4S Program (Fig. 1, Mod I) and the side-fender panels previously tested as part of barrel crash cushion designs (3) were incorporated in a concrete cushion designed for Florida. The results of two side-angle tests of the system constructed for Florida (Fig. 1, Mod II) were reported to Florida in November 1970 (2).

It was decided that additional tests would be conducted to further evaluate the concrete cushion for both side-angle impacts and head-on impacts involving small vehicles. Further modifications of the cushion were made prior to the final series of tests that resulted in the design shown as Mod II in Figure 1. The most significant concrete cushion designs that have been tested are shown in Figures 2 through 4. This report describes in detail the three tests that were conducted on the Mod III concrete crash cushion.

EXPERIMENTAL PROGRAM

Three full-scale vehicle crash tests (designated D, E, and F) of the Mod III concrete crash cushion (Fig. 4) were conducted in this final test series; the results are given in Table 1. Properties of the concrete used in the various cushions tested are as follows.

Test	Average Compressive Strength (psi)	Average Unit Weight (pcf)
A	50	32
B	71	32
C	57	21
Florida 1 and 2	64	22
D, E, and F	64	22

Sponsored by Committee on Traffic Safety Barriers and Sign, Signal and Lighting Supports.

Figure 1. Evolution of concrete crash cushion.

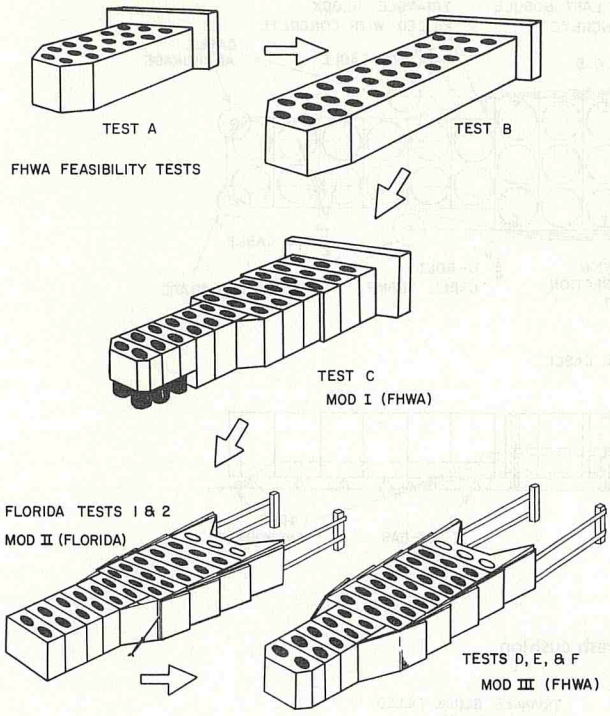

Figure 2. Test C, Mod I concrete crash cushion.

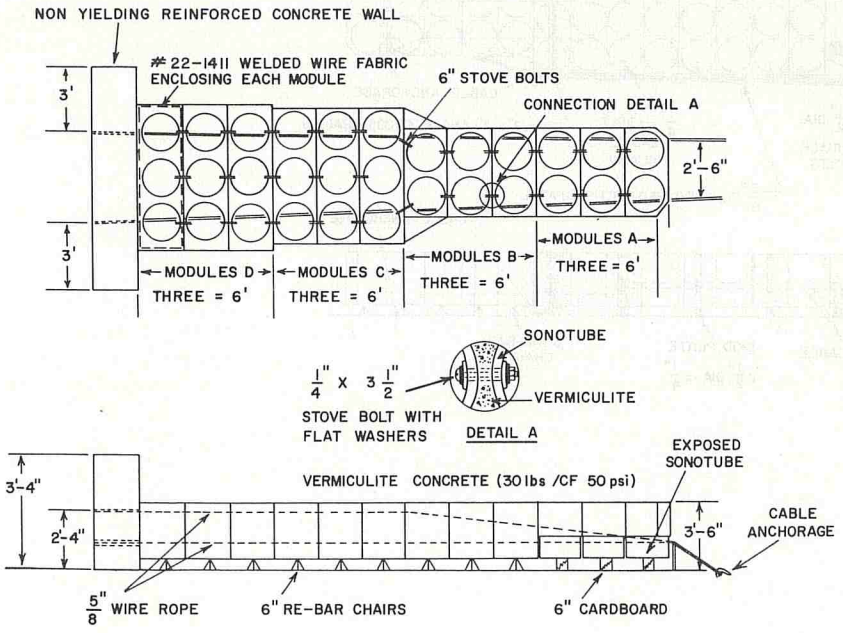

Figure 3. Florida Tests 1 and 2, Mod II concrete crash cushion.

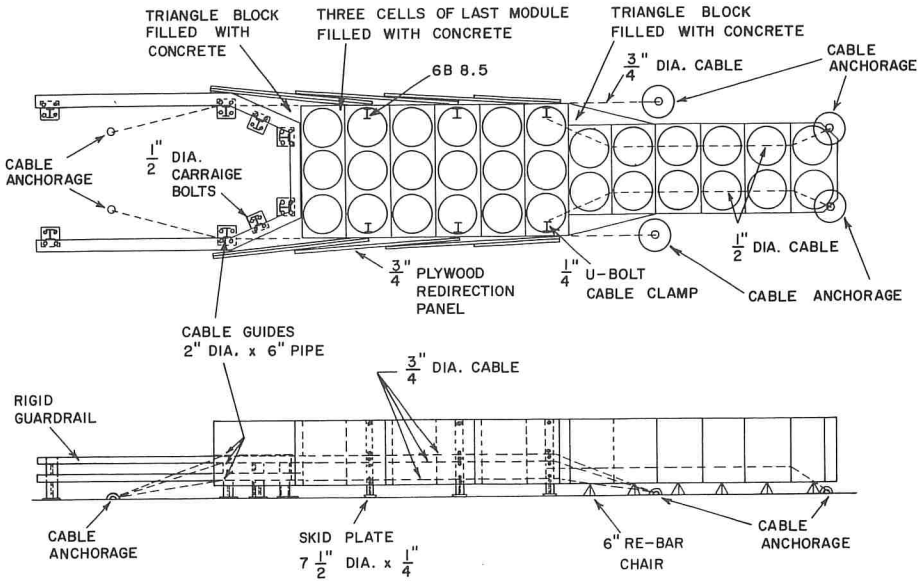

Figure 4. Tests D, E, and F, Mod III concrete crash cushion.

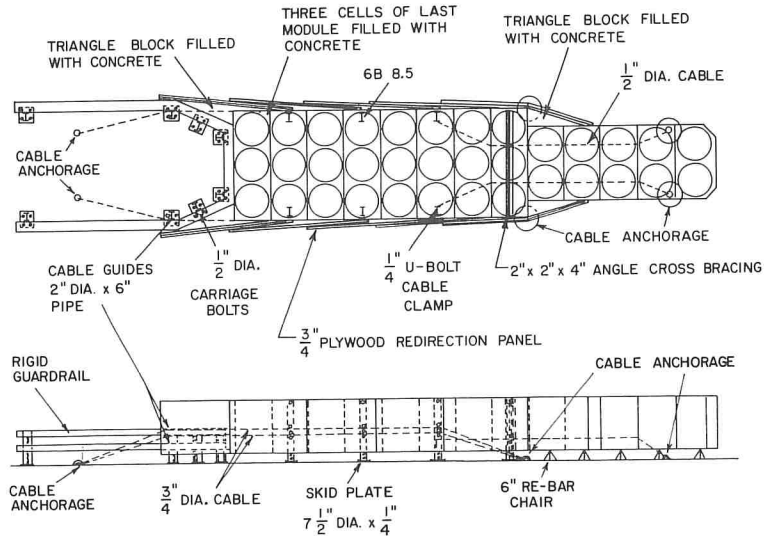

Accelerometers and an impact-o-graph were used on each test to record vehicle decelerations. Statham strain-gauge-type accelerometers were used, and all electronic data were passed through an 80-Hz low-pass active filter. High-speed cameras were also used to record the vehicle position and speed throughout the test.

Test D

In this test a 1963 Chevrolet weighing 3,790 lb was impacted into the cushion at a 10-deg angle from the longitudinal axis of the cushion (Fig. 5). The contact point was 18 ft in advance of the rigid backup rail. The speed at contact was 57.2 mph, and the speed at loss of contact was 49.6 mph. The average longitudinal deceleration was 1.3 g. The distance that the vehicle was in contact with the barrier was 20.4 ft over a period of approximately $\frac{1}{3}$ sec. The vehicle laterally penetrated the barrier a maximum distance of about 2 ft. The vehicle was smoothly redirected, and damage was relatively light (Fig. 6). Figure 7 shows that only five modules were significantly damaged and that the cushion could probably still sustain a head-on impact. The test was considered extremely successful in regard to both passenger safety and vehicle damage.

Test E

In this test a 1962 Chevrolet, weighing 3,820 lb was impacted into a Mod III barrier at a 20-deg side angle. The point of contact was 16 ft in advance of the rigid backup rail. The impact speed was 59.7 mph, and vehicle speed at loss of contact with the barrier was 29.3 mph. This represented an average deceleration of 5.6 g in the longitudinal direction. The vehicle was in contact with the cushion for approximately 16 ft. Photographs of this test are shown in Figures 8 through 10. As the vehicle made contact and slid down the side of the cushion, a slight ramping tendency was observed. This interaction finally culminated in the generation of a high roll-initiating force as the vehicle reached the end of the cushion. The vehicle rolled in a counterclockwise direction (when viewed in the direction of vehicle travel); ramped on the rear of the cushion near the end of the backup rail; traveled beyond the cushion installation, skidding on its left side; rolled clockwise to an upright position; and continued to roll over onto its top. It came to rest approximately 80 ft past the barrier. Although the decelerations, which were caused by vehicle-cushion interaction, were within the range of human tolerance, the roll condition that occurred after the vehicle left the cushion was not within passenger safety limits. This is the only test conducted to date in which an unacceptable reaction of the vehicle occurred. Recommendations for modification of the barrier to preclude the recurrence of this situation are presented later in this paper.

Test F

A 1957 Volvo weighing 2,210 lb was impacted into the cushion head on at a speed of 61 mph. The average longitudinal deceleration was 10.2 g, with a peak longitudinal deceleration of 19 g. The interaction of the vehicle and cushion was considered acceptable. The damage done to the vehicle and cushion is shown in Figures 11 and 12.

The deceleration that occurs with a 2,000-lb vehicle is approximately twice that which occurs with a 4,000-lb vehicle. This is verified by comparing the preceding values with the 6.4 average and 10.4 maximum decelerations observed in Test C (1).

DISCUSSION OF FINDINGS

Of the eight vehicle crash tests that have now been conducted on the concrete crash cushion, all but one have yielded results that appear very favorable in reference to passenger safety. The exception to this was the 20-deg, 59.7-mph, side-angle impact of the Mod III cushion (Test E). In this test the vehicle was subjected to a large moment about the roll axis toward the end of the contact zone. This resulted in a hazardous roll, after contact with the cushion was lost, and the vehicle came to rest upside down. This tendency in side-angle collisions has been noted in other crash tests, such as Test R-E (4) and USS Test 1 (the first test of a series of three tests conducted by United

Table 1. Summary of tests.

Factor	Test D	Test E	Test F
Vehicle			
Year	1963	1962	1957
Make	Chevrolet	Chevrolet	Volvo
Weight, lb	3,790	3,820	2,210
Impact angle, deg	10	20	0
Film data			
Initial speed, V_1, fps	83.9	87.5	89.7
mph	57.2	59.7	61.2
Final speed, V_2, fps	72.7	43.9	0
mph	49.6	29.3	0
Average deceleration[a], G_{avg}, g	1.3	5.6	10.2
Stopping distance or contact distance, S, ft	20.4	16.1	12.2
Time in contact, sec	0.286	0.235	0.364
Accelerometer data			
Longitudinal deceleration			
Peak g	6.2	14.7	19.0
Average g	1.4	4.2	6.4
Time, sec	0.294	0.268	0.446
Transverse deceleration			
Peak g	9.8	12.7	—
Average g	2.4	3.3	—
Time, sec	0.302	0.273	—

[a] $G_{avg} = (V_1^2 - V_2^2)/2gS$

Figure 5. Test D sequential photographs (view parallel with barrier).

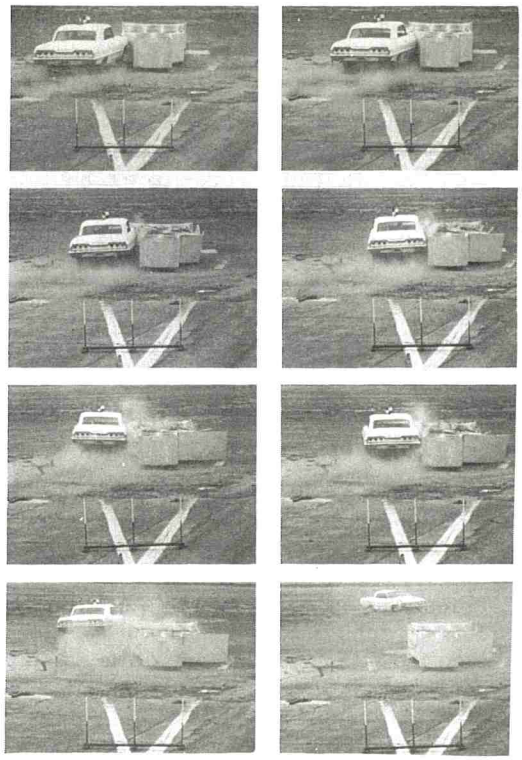

Figure 6. Vehicle after Test B.

Figure 7. Barrier before and after Test D (end view).

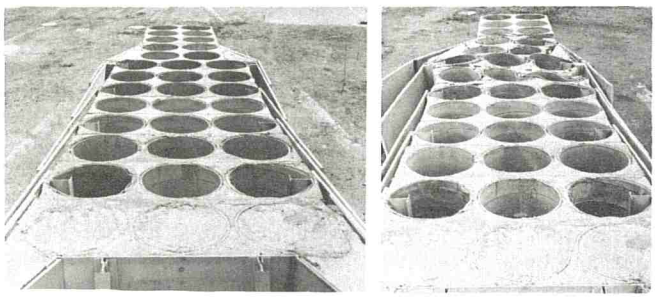

Figure 8. Vehicle before Test E and in final position.

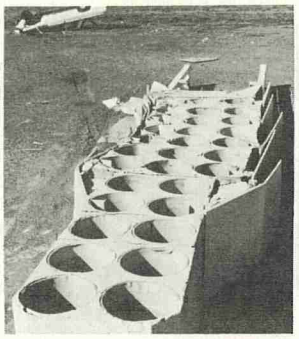

Figure 9. Barrier before and after Test E.

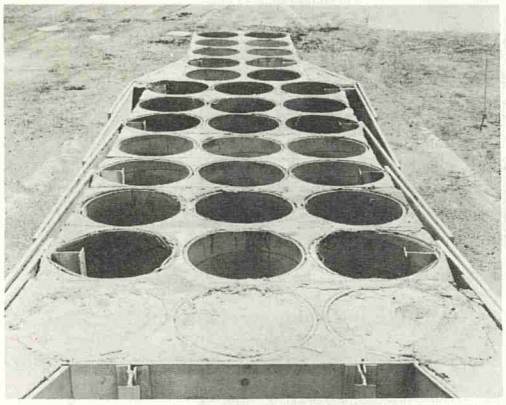

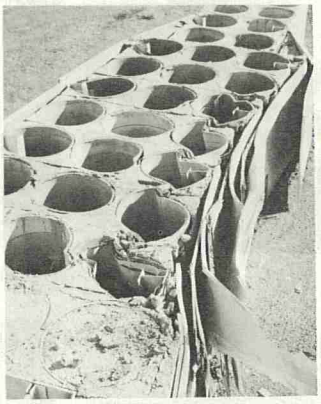

Figure 10. Test E sequential photographs (view perpendicular to barrier).

t = 0 sec

t = 0.104 sec

t = 0.153 sec

t = 0.213 sec

t = 0.315 sec

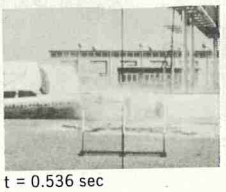

t = 0.536 sec

Figure 11. Vehicle before and after Test F.

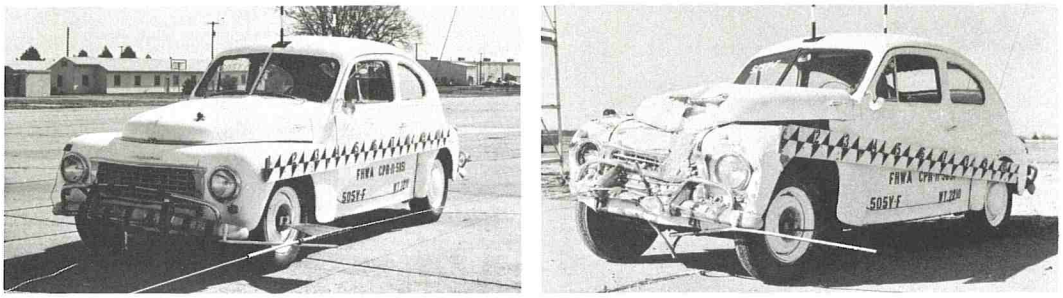

Figure 12. Test F sequential photographs (overhead view).

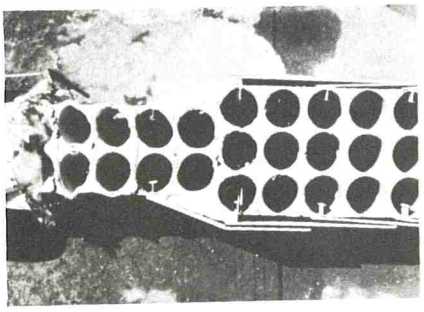

t = 0.031 sec

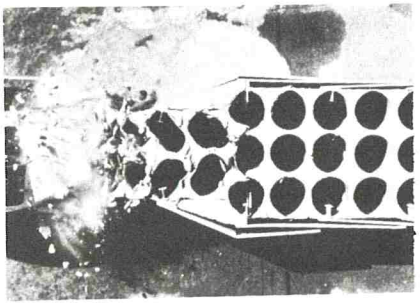

t = 0.064 sec

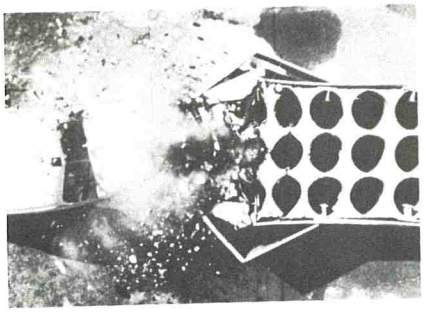

t = 0.130 sec

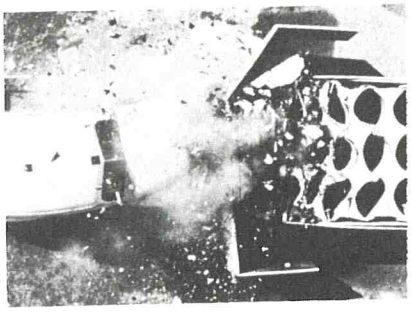

t = 0.199 sec

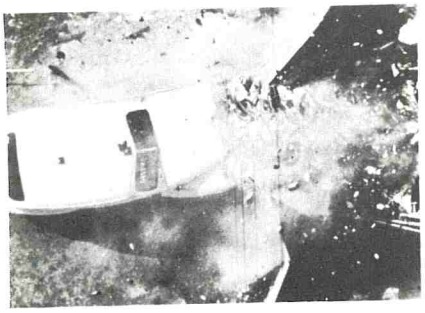

t = 0.380 sec

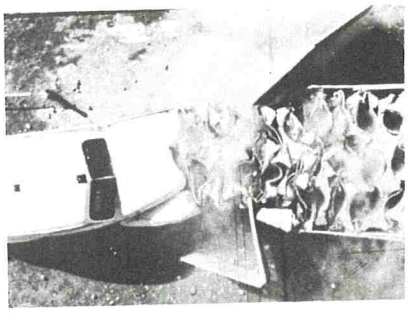

t = 1.480 sec

States Steel Corporation, U.S.S. Contract 6339, Texas A&M Research Foundation Project RF 719, March 1970; no formal publication). In both of these tests, the vehicle contact-wheel appeared to ride up the side panels, which resulted in the vehicle becoming airborne as contact with the barrier was lost. The phenomenon observed in Test E, however, appears to be significantly different from that observed in previous tests. From observation of the high-speed test film, it appeared that the following events occurred:

1. The vehicle contacted the cushion at t = 0 sec (Fig. 10), which is approximately 16 ft in advance of the rigid backup rail.
2. The vehicle began to displace the barrier laterally and slide along the side panels (Fig. 10; t = 0.104 and t = 0.153 sec). There was a slight ramping tendency during this stage, with the contact side of the vehicle rising approximately 1 ft as compared to its elevation at contact. This ramping was less severe than that which occurred in Test R-E and USS Test 1.
3. At t = 0.213 sec (Fig. 10), the vehicle frame appeared to be in a state of severe torsion, as indicated by the sudden elevation of the right front quadrant of the vehicle. It was at this point, where contact with the last module of the cushion was made, that the severe upward thrust on the right front of the vehicle caused the counterclockwise roll motion. The last module of the Mod II and III cushions was made of solid vermiculite, whereas the other modules had sonotube openings. Because of the comparative rigidity of this module, one of the two following events had to occur: (a) The contact area of the vehicle is suddenly forced to the outside to pass the rigid module in a relatively violent redirection (barrier force causes a moment about the yaw axis of the vehicle) (2, Florida Test 1); or (b) the contact area of the vehicle is forced upward to pass over the rigid module resulting in a rolling motion (barrier forces cause a moment about the roll axis of the vehicle). In the slightly elevated position that the right front of the vehicle had achieved in Test E, the path of least resistance was over the final rigid module.

The question remaining to be answered is why this roll phenomenon occurred in Test E but not in Test D or Test 1 of the Florida series. In Test D, the impact angle was only 10 deg, and the vehicle had been almost completely redirected before reaching the solid module. Thus, traumatic force was not necessary to get by the rigid portion of the cushion. In Florida Test 1, the impact angle was 20 deg, as in Test E, but the contact point was only 6 ft in advance of the rigid module. In all other respects, the final 8 ft of the Florida Mod II cushion was identical to the final 8 ft of the FHWA Mod III cushion. It is hypothesized that the ramping that occurred in Test E was initiated when the vehicle struck the cushion at a point where the cables supporting the redirection panels were low; whereas, in Florida Test 1, the cables at the impact point were almost fully elevated. It would therefore appear that the Mod III cushion has a weak point if struck at an angle of 20 deg, close to where the side panels start. No such weakness was demonstrated by tests on the Mod II cushion because the panels extend only 11 ft from the rigid backup rail, and angle hits in advance of the panels result in an acceptable "pocketing" interaction (2, Florida Test 2).

It is believed that this weakness in the Mod III cushion can be overcome by (a) replacing the solid module at the rear of the Mod III cushion with a standard hollow module and (b) elevating the side cables 6 in. at the rear of the cushion. The first step results in reducing the forces imparted to the vehicle at this point in the interaction and reduces the vehicle reaction necessary to get by the final module. The second step results in elevating the vertical position of maximum lateral resistance and thus reduces the slight ramping tendency that has been noted.

CONCLUSION

It has been shown that the lightweight concrete crash cushion can be used to effectively decelerate a vehicle for both the head-on and side-angle crash conditions. Seven of eight tests show deceleration levels within the tolerance of restrained humans. The single test of the Mod III cushion resulted in an undesirable reaction of the vehicle during a cushion impact; modifications to prevent future reactions of this type have been

recommended. Because these proposed modifications have not been tested, full-scale tests incorporating these modifications are planned by FHWA.

The lightweight cellular concrete crash cushion can be installed by semiskilled laborers using one of two methods. The formwork can be placed in the field, and a local vermiculite applicator can supply the necessary concrete; or the precast modular construction method can be used. The cost per installation compares favorably with that of the barrel crash cushion. By using the modular construction technique that permits mass production we can realize considerable savings. Close quality control should be exercised on the geometry of the module and on the vermiculite concrete. Control of batch proportions and unit weight will give predictable crushing strengths. Replacement of segments of the crash cushion after a collision is feasible. For a cast-in-place cushion, the crushed material can be removed, the affected portion of the barrier reformed, and fresh vermiculite placed in the necessary areas. Fast-setting cement will alleviate the problem of curing time. The precast cushion, which has three tube modules weighing approximately 250 lb, could be handled by two men. Modules that are crushed during a collision can be unbolted, removed, and replaced during a low-density traffic period.

The lightweight, low-strength concrete used in these crash cushions exhibits relatively poor durability when it is subjected to cycles of freezing and thawing and allowed to become saturated with water. Several waterproofing agents were tested with limited success (5). The best method of achieving protection to date has been used by Wisconsin. In Milwaukee, rubberized tarpulin covers were used to protect vermiculite cushions against absorbing water and the accumulation of ice and snow in the sonotube voids. There has been no durability problem in Wisconsin on the cushions covered in this way. Additional information about concrete crash cushions can be found in the original report (5).

REFERENCES

1. Ivey, D. L., Buth, E., and Hirsch, T. J. Feasibility of Lightweight Cellular Concrete for Vehicle Crash Cushions. Highway Research Record 306, 1970, pp. 50-57.
2. Ivey, D. L., and Buth, E. Side Angle Collisions With Concrete Vehicle Crash Cushions. Florida Department of Transportation, Texas Transportation Institute, Research Rept. 733, Nov. 1970.
3. Hirsch, T. J., Hayes, G. G., and Ivey, D. L. The Modular Crash Cushion. Texas Transportation Institute, Technical Memo. 505-1S, Aug. 1970.
4. Hayes, G. G., Ivey, D. L., and Hirsch, T. J. Performance of the Hi-Dro Cushion Cell Barrier Vehicle-Impact Attenuator. Highway Research Record 343, 1971, pp. 93-99.
5. Ivey, D. L., Buth, E., Hirsch, T. J., and Viner, J. G. Evaluation of Crash Cushions Constructed of Lightweight Cellular Concrete. Texas Transportation Institute, Technical Memo 505-9S, June 1971.

CRASH TESTS OF AN ARTICULATED ENERGY-ABSORBING GORE BARRIER EMPLOYING LIGHTWEIGHT CONCRETE CARTRIDGES

Grant W. Walker, Dynamics Research and Manufacturing, Inc.;
Bruce O. Young, Energy Absorption Systems, Inc.; and
Charles Y. Warner, National Highway Traffic Safety Administration

The concept of vermiculite concrete energy absorption has been further tested by incorporating cartridges into the Hi-Dro Cell sandwich unit designed for water-cell use. Repeated tests were performed with gradually increased use of the cartridges in place of water cells. Tests up to 55 mph with medium-weight automobiles indicate improved response, especially with regard to the approach to square-wave deceleration pulse. Harness-restrained drivers reported no discomfort in three separate impacts at speeds above 50 mph.

•INITIAL success with the use of vermiculite concrete modules in guardrails has encouraged other highway applications of these modules (1). The following is a report of crash tests performed to evaluate the substitution of vermiculite concrete cartridges for water cells in the Hi-Dro Cushion Cell sandwich gore barrier. The use of this barrier has already proved successful in test and actual conditions (2, 6).

Lightweight concrete crash barriers investigated by the Texas Transportation Institute were found to have acceptable head-on performance and low initial cost (7). No angle tests were conducted.

Experience gained in the development of the hardware for the Hi-Dro Cell sandwich unit suggested that its cost could be reduced by the substitution of vermiculite concrete cartridges for the water cells. The tests reported here cover a development program wherein this was accomplished and the head-on test performance evaluated for speeds up to 56 mph.

Experience gained from angle impacts into several systems using very similar deflection hardware suggests that acceptable angle-impact performance is obtainable. There does not appear to be any technological problem that would prevent equally good angle performance of this system. Crash tests to evaluate angle impact performance have just been initiated. Angle impacts in the 15-deg, 45-mph range have not produced adverse results, but more severe tests are planned.

TEST PROCEDURE

The basic hardware for this test series was a cell sandwich unit that is shown in Figures 1 and 2 (5). Figures 3 through 6 show details of the construction of the cells and cartridges and show their arrangement in the barrier system. Sequential tests were conducted where vermiculite concrete cartridges were gradually substituted for water cells, starting from the nose and working toward the rear. In three tests at speeds above 45 mph, the complete unit was equipped with vermiculite concrete absorbers.

The data were collected in these tests by using techniques similar to those used elsewhere (1). High-speed photometrics were obtained from four ground cameras. Ve-

Sponsored by Committee on Traffic Safety Barriers and Sign, Signal and Lighting Supports.

Figure 1. Impact attenuator with helicell nose section.

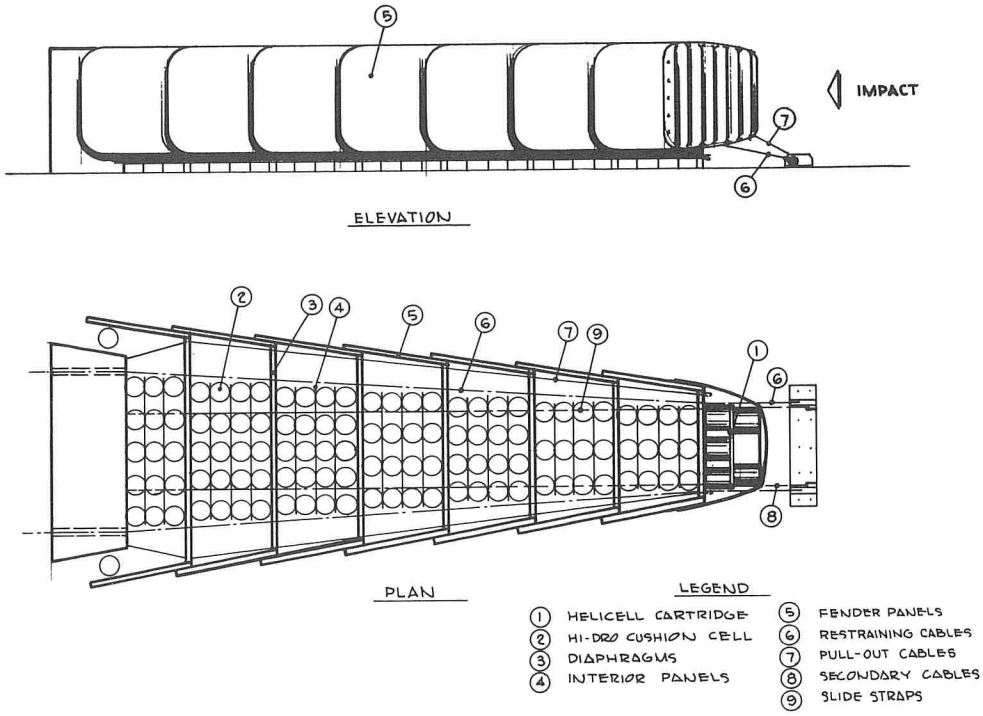

Figure 2. Impact attenuator with helicell cartridges.

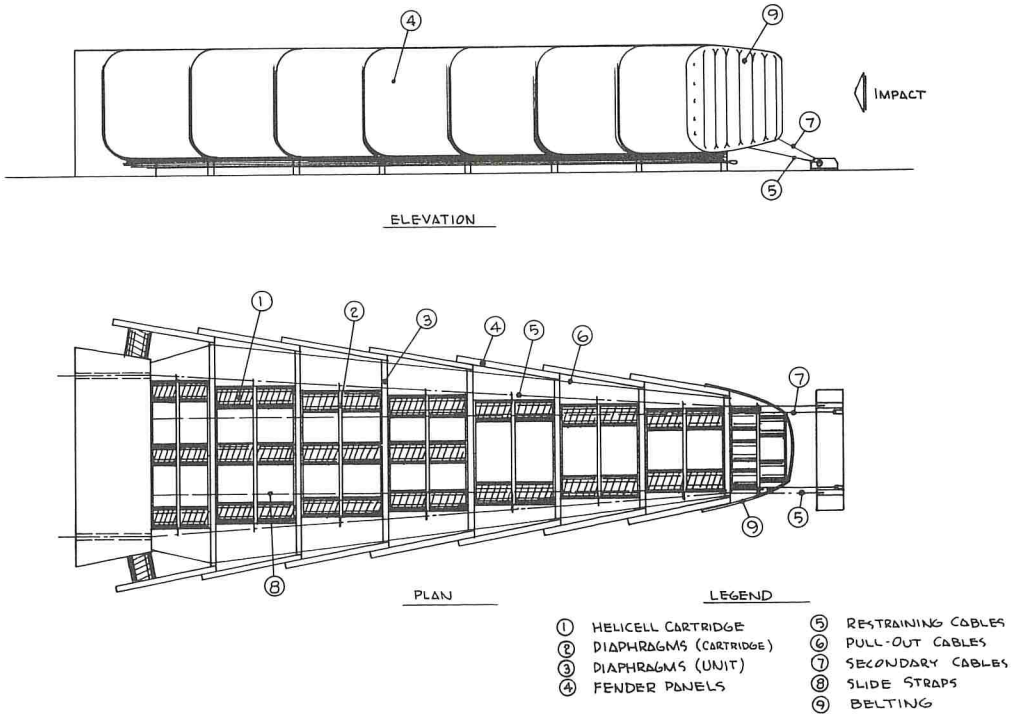

Figure 3. Vermiculite concrete cartridge.

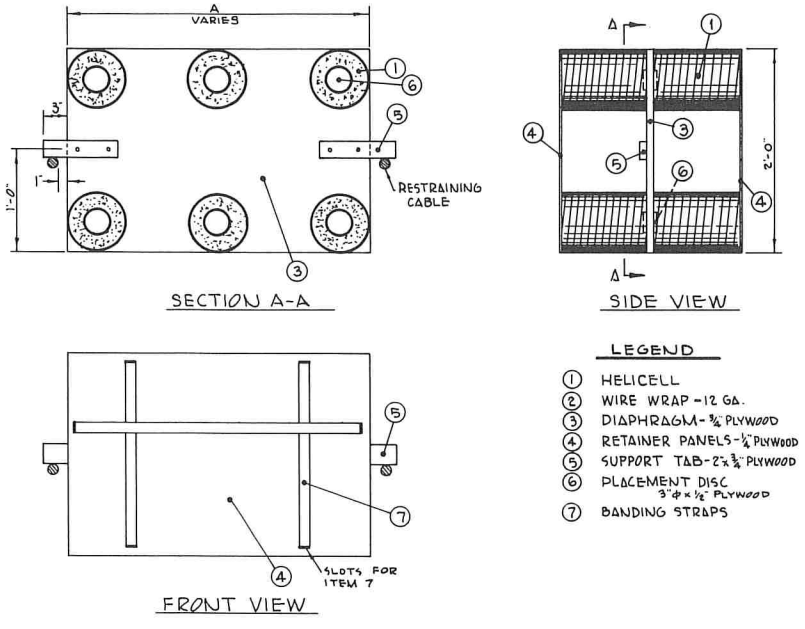

Figure 4. Helicell.

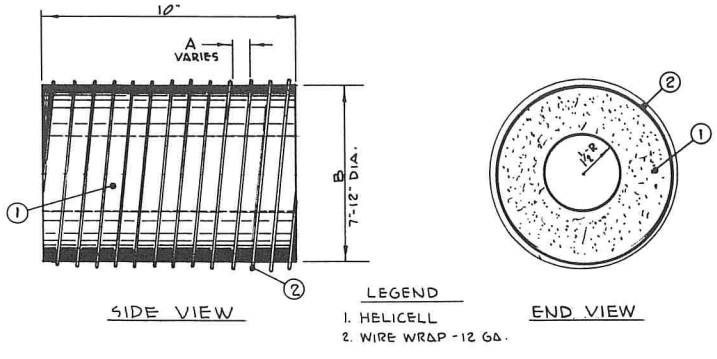

Figure 5. Cartridge mounting in unit.

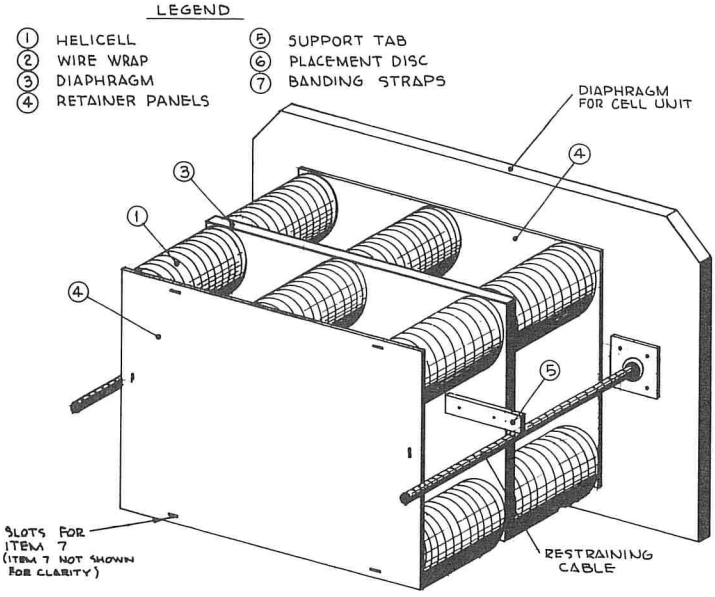

Figure 6. Nose treatment.

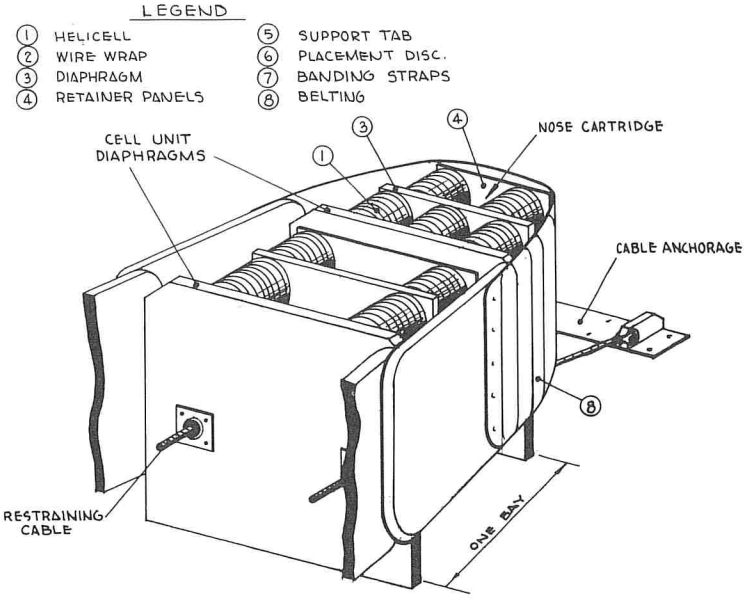

hicle impact speed was measured by trip-wire timers. Vehicle accelerations were measured by a biaxial strain-gauge accelerometer pack mounted on vehicle occupant compartment floor, between the front and rear seats, with hardline umbilicals leading to a direct-writing light beam oscillograph mounted in a chase vehicle. Electronic data were compared for internal consistency and were checked qualitatively against photometrics to determine overall agreement.

Dynamic stopping distance was measured by using photometric records. Most of the tests reported here were run with human drivers; three tests were run at speeds of between 50 and 56 mph.

To make an orderly, safe transition from known to new performance, we decided to gradually replace the water in the cell sandwich system, starting at the nose and working through the entire system, at speeds between 45 and 50 mph. This was accomplished in a series of 7 tests that were performed safely using human drivers. The drivers were restrained with aircraft-type lap belts and double shoulder harnesses, plus an additional restraint that was attached to the rear of the driver's safety helmet to limit head motion.

Both drivers who participated in the program reported minimal belt loads for all but the last test. Because of their report, we decided to continue testing the vermiculite system, which was designed for 60 mph, into the mid-50-mph speed range. During the last test (at 56 mph), a firm belt load was reported on the shoulder harness, and moderate load was reported on the lap belt. Drivers reported no physical discomfort from the loads applied during the tests.

TEST RESULTS

Pertinent test results are shown in Figure 7 and given in Table 1. The vehicles used were 1956-62 model lightweight standard sedans (Fig. 8), some of which were used in more than one crash test. In Test 1-2 a heavy, reinforced moving-barrier-type vehicle was used.

Square-Wave Response

The substitution of lightweight concrete cartridges for water cells has significantly flattened the acceleration response. This is attributed primarily to the removal of significant mass elements from the system. The initial peaks that characterize the performance of the water system (Test 1-2, Fig. 7, and 3, 4, 5) are significantly moderated as the vermiculite crush mechanism is substituted for the momentum-exchange mechanism of energy attenuation. The improvement is apparent when one compares the results shown in Figure 7. One can see a gradual flattening of the pulse form. It should be noted that the speeds represented in the lower portion of the figure are generally higher.

The advantages of one wave form versus another in terms of occupant protection presupposes some form of occupant restraint system. It is unlikely that any of the reported vehicle wave forms would offer clearly superior occupant protection, and none of them would clearly prevent injury to an unrestrained or lap-belt restrained occupant. Hence, the relative survivability benefits of these vehicle pulse forms are unknown. On the other hand, the cost of the barrier system is directly related to the space it occupies in the roadway. The combined effects shown in Figure 7 of the lower peak g and more nearly uniform square-wave response suggest a more efficient utilization of space.

An important fact that is not apparent in the figure is that the overall length of the barrier was actually shortened during this progression, from 19.2 ft in Test 1-2 to 17.2 ft in Test 1-20.

Velocity Sensitivity

Figure 9 shows the results of impact tests on individual cells. The data used to construct this figure are all derived from vehicle tests of helicell arrangements. Where more than one cluster was involved in a test, photometric data were used to calculate the dynamic loads on single cells within the cluster. Although the data are somewhat

Figure 7. Acceleration trace comparisons.

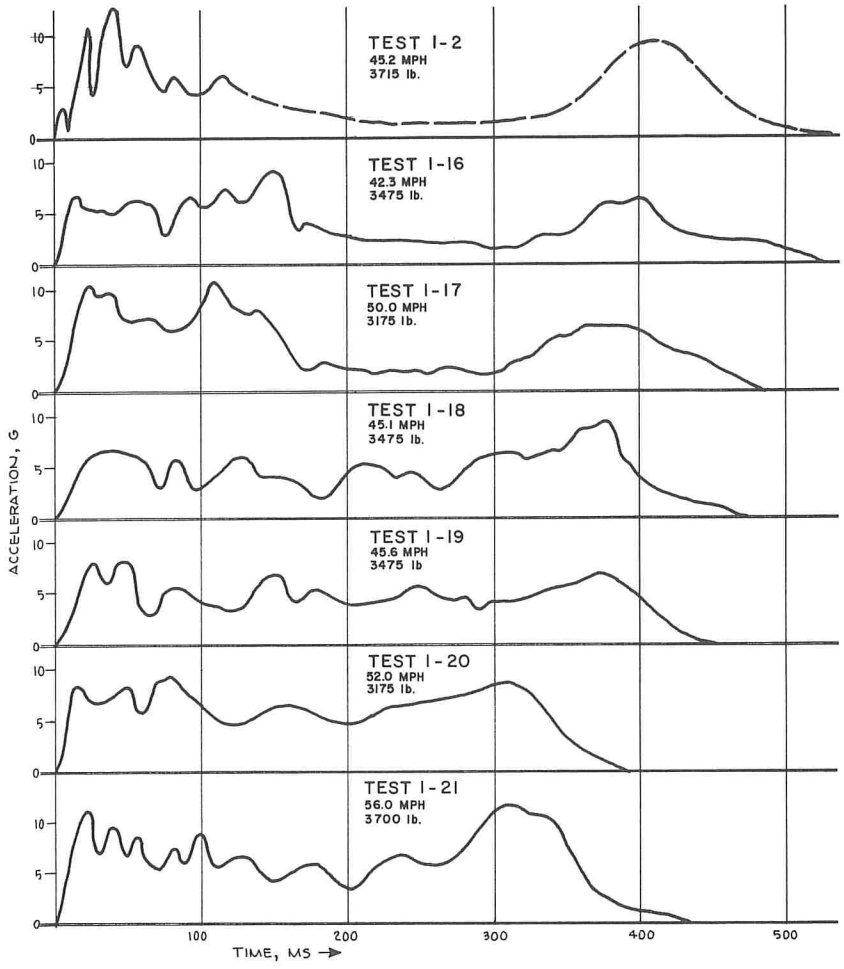

Table 1. Test data summary.

Test No.	Vehicle	Total Vehicle Weight (lb)	Impact Speed (mph)	Crush on Vehicle (in.)	Stopping Distance (ft)	Maximum g	Average g	No. of Bays (water)	No. of Bays (vermiculite)	Weight Reduction (lb)	Total Length (ft)
1-2	Test truck	3,715	45.2	0	13	14.5	5.25	8	1	135	19.2
1-16	1956 Studebaker Champ, 4-dr.	3,475	42.3	2	12.7	9	4.7	6	3	450	19.2
1-17	1959 Studebaker Lark, 4-dr.	3,175	50.0	8	13	11	6.4	6	3	450	19.2
1-18	1956 Studebaker Champ, 4-dr.	3,475	45.1	8	14.5	9.5	4.7	3	6	900	18.0
1-19	1956 Studebaker Champ, 4-dr.	3,475	45.6	0	13.5	8.0	5.1	0	9	1,400	17.2
1-20	1959 Studebaker Lark, 4-dr.	3,175	52	0	13.7	9.5	6.6	0	9	1,400	17.2
1-21	1962 Rambler, 4-dr.	3,700	56	10	14.5	11.5	7.2	0	10	1,550	18.3

Figure 8. Test vehicle before and after 53-mph impact.

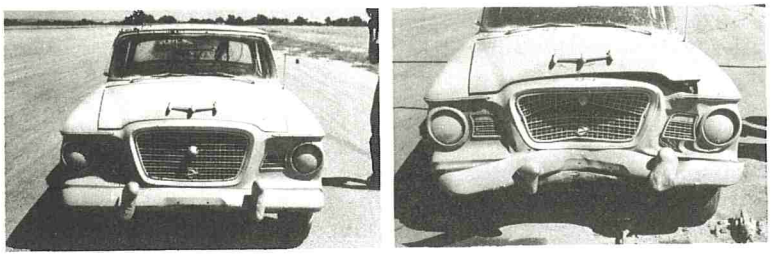

Figure 9. Vermiculite concrete cell velocity sensitivity.

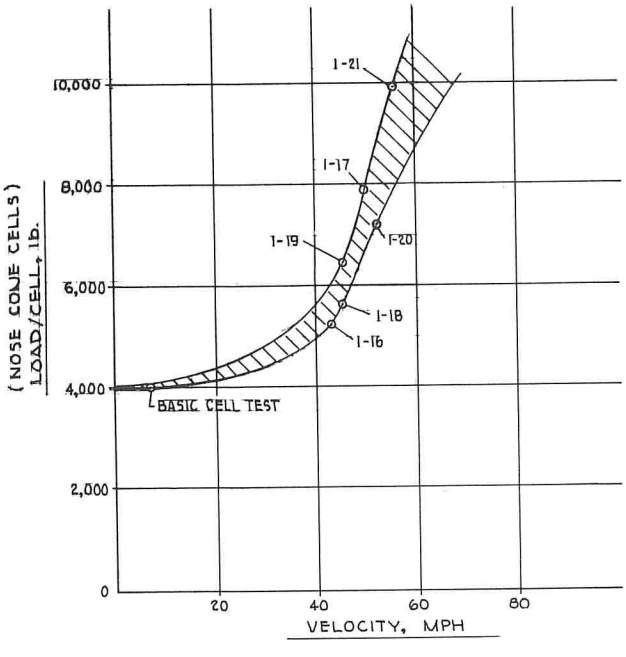

Figure 10. Peak g reduction at 45 mph with increasing use of vermiculite cartridges.

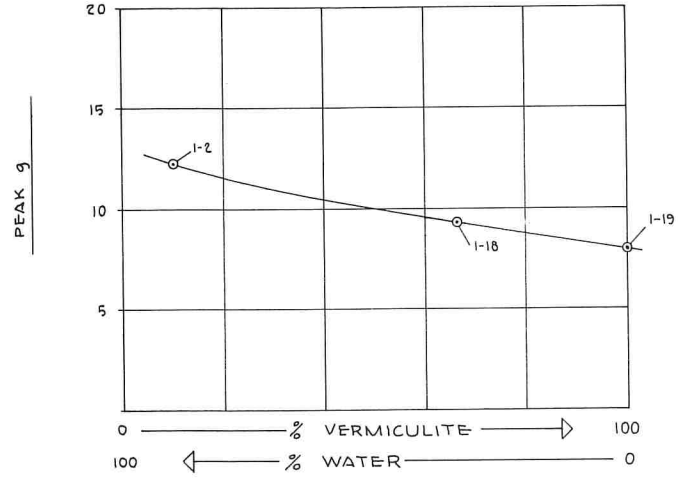

scattered, it is clear that some velocity sensitivity exists. It is not clear exactly what relation the total unit force bears to velocity; however, the potential clearly exists for the design of a unit whose response matches the velocity and mass of the arrested vehicle, similar in overall response to the water-filled plastic system (5).

Mass Matching

The moderation of the initial peak is thought to be especially significant for impacts involving compact and subcompact class vehicles. Further tests are planned to investigate this more specifically, i. e., 2,000-lb, 60-mph impacts.

The capability of the lightweight concrete system for mass and velocity matching is demonstrated in the stopping distance column of Table. 1.

Water Versus Rise

The effect of substitution of lightweight concrete cartridges for water cartridges is shown in Figure 10. Peak deceleration decreases with increasing use of concrete cartridges, particularly near the nose of the unit. This saving is primarily a result of mass reduction in the nose, with corresponding stiffness increase. The use of the lighter material has a lesser effect near the rear of the unit because dynamic effects are smaller in that region.

Vehicle Rise

One concept that was explored in the later tests was the control of vehicle rise by raising the center of pressure in the force path through the cushion. This was done by inserting stiffer helicells into the upper part of each cartridge and by using slotted cable grommets in the forward diaphragms. An improvement in vehicle stability was seen in film records of crash tests in which the force center angled gently upward, starting from a point on the unit nose that is above the vehicle center of gravity. Further test work is planned to investigate this benefit.

Weatherability

Exposure of the helicell units in service to moisture and freezing temperatures suggests that some steps should be taken to prevent intrusion of moisture. The most promising approach that has been attempted involves coating the helicell with asphalt roofing compound and enclosing the treated helicell in an aluminum foil skin. This inexpensive weatherproofing appears to offer adequate protection for all environments to which exposure is likely. Treated cells have been submerged in water for periods of days, frozen in 0-deg environments, thawed, and resoaked, without noticeable change in weight or characteristics occurring. The foil skin also serves to trap and hold most of the debris that is formed upon impact, which simplifies cleanup.

Refurbishment Advantages

The use of lightweight concrete cartridges makes possible a considerable reduction in overall cushion weight compared to the water system; cartridges sufficient for total refurbishment weigh less than 500 lb. Use of these cartridges greatly simplifies refurbishing because of the following:

1. A crew of two men is adequate;
2. A ½-ton pickup can easily carry men, material, and equipment to and from the site;
3. The materials for refurbishment can easily be stored near the crash site;
4. The refurbishment time is reduced by as much as 50 percent, thereby improving freeway usage and decreasing probability of secondary accidents;
5. Where practicable, user agencies can recycle cartridge components by simply replacing the vermiculite concrete cells; and
6. The cost of all cartridges needed to refurbish a typical 60-mph unit is estimated to be roughly $500.

CONCLUSIONS

This preliminary series of tests indicates a head-on crash performance that is about equivalent to the water cushion barrier with notable improvements in pulse-form flatness and initial peak deceleration.

The more nearly rectangular pulse form provided by the helicell barrier allows more efficient utilization of limited roadside space.

The helicell cartridges can be easily weatherproofed to allow use in all temperate-zone climates. Low component costs and modular construction reduce materials and labor costs for refurbishment.

Further tests are needed to verify the performance of this system in three areas: (a) low-to-moderate speed crashes with full-sized sedans, (b) several tests with compact cars, and (c) instrumented full-scale tests at oblique impacts. These tests will be completed in the near future.

REFERENCES

1. Warner, C. Y., and Walker, G. W. Crash Test Performance of a Prototype Lightweight Concrete Energy-Absorbing Guardrail System. Highway Research Record 343, 1971, pp. 13-18.
2. Warner, C. Y. Hydraulic-Plastic Cushions for Attenuation of Roadside Barrier Impacts. Highway Research Record 259, 1969, pp. 24-34.
3. Hayes, G. G., Ivey, D. L., and Hirsch T. J. Performance of the Hi-Dro Cushion Cell Barrier Vehicle-Impact Attenuator. Highway Research Record 343, 1971, pp. 93-99.
4. Nordlin, E. F., Woodstrom, J. H., and Doty, R. N. Dynamic Tests of an Energy-Absorbing Barrier Employing Water-Filled Cells. Highway Research Record 343, 1971, pp. 100-122.
5. Warner, C. Y., and Free, J. C. Water-Plastic Crash Attenuation System: Test Performance and Model Prediction. Highway Research Record 343, 1971, pp. 83-92.
6. Tamanini, F. J. Designing Fail-Safe Structures for Highway Safety. Transportation Engineering Jour., Proc. ASCE, Vol. 97, No. TE2, Proc. Paper 8150, May 1971.
7. Ivey, D. L., Buth, E., and Hirsch, T. J. Feasibility of Lightweight Cellular Concrete for Vehicle Crash Cushions. Highway Research Record 306, 1970, pp. 50-57.

DYNAMIC TESTS OF AN ENERGY-ABSORBING BARRIER EMPLOYING SAND-FILLED PLASTIC BARRELS

Eric F. Nordlin, J. Robert Stoker, and Robert N. Doty,
California Division of Highways

The results of three full-scale tests of vehicles impacting energy-absorbing barriers employing sand-filled frangible plastic barrels are reported. The barriers were designed for placement in front of fixed objects located in freeway gores. They were composed of an array of 15 to 17 barrels 36 in. in diameter by 30 and 36 in. high. The barriers were 21 and 25 ft long and tapered from a 9-ft width at the rear to a 3-ft width at the nose. The barrels were not attached to the ground. Sedans weighing approximately 4,700 lb impacted the nose of the barrier head on at a speed of approximately 60 mph and at a 15-deg angle. A small sedan weighting about 1,900 lb also impacted the nose of the barrier head on at 59 mph. The barrier was judged acceptable in the areas of cost, ease of construction and maintenance, aesthetics, simplicity, and versatility and is recommended for use in operational trial installations.

•DURING 1967 and 1968, approximately 25 percent of all California freeway fatalities occurred when vehicles ran off the road and collided with fixed objects. Consequently, the California Division of Highways is endeavoring to provide a 30-ft-wide recovery area, clear of fixed objects, adjacent to the traveled lanes. Wherever possible, fixed objects that cannot be removed from this recovery area are modified and made "breakaway." However, one of the most difficult problem areas has been the gores of freeway off-ramps that contain large signposts, bridge rail end posts, and other rigid structures. Various types of energy-absorbing barriers have been proposed for installation in front of or around these fixed objects to cushion vehicular impacts. The California Division of Highways has previously conducted full-scale crash tests of two of these barriers, one composed of water-filled plastic cells and the other composed of empty, 55-gallon steel oil drums (1, 2).

This report discusses three recent dynamic tests of a third barrier composed of an array of sand-filled frangible plastic barrels placed between the traveled way and the fixed object. The barrier was developed by John Fitch and is manufactured by Fibco, Inc., of Hartford, Connecticut. During 1967, more than 30 crash tests were conducted of impact attenuators that utilize sand supported by various types of material. This series of tests was supported by a few interested firms, and engineering assistance was provided by the New York State Department of Transportation. The tests proved the feasibility of using the concept of momentum transfer from the impacting vehicle to the sand but the need for a more sophisticated system for containing the sand became evident. A weatherproof, cylindrical, plastic barrel was developed that would provide lateral support for the sand but would shatter relatively easily when struck by a vehicle. The barrel was made of a high-density polyethylene produced by using a structural foam process.

In April 1969, Fitch conducted another series of six tests. This phase of his testing was supported by Connecticut under the auspices of a National Highway Safety Board project grant. The tests were conducted at speeds of 40 to 50 mph using vehicles weigh-

Sponsored by Committee on Traffic Safety Barriers and Sign, Signal and Lighting Supports.

ing 1,700, 3,000, 3,500, and 3,900 lb. The test barriers were 14½ to 25 ft long. A human driver was used in two tests. The barrels were placed in an open area with no fixed object behind the barrier. In all of the tests, except those using a 1,700-lb car, the stopping distance exceeded the barrier length. Reports of the tests indicated that the test vehicles were decelerated in an effective, stable manner; however, there was no instrumentation to measure peak g on the vehicle. The amount of debris that was generated as the barrier decelerated an impacting vehicle was unsatisfactory.

Subsequent to these tests, Fitch barriers had been installed at locations in several states. A few collisions with these barriers had been recorded with generally favorable performance. Thus, the sand inertial barrier concept appeared promising because of its apparent effectiveness in adequately decelerating impacting vehicles, adaptability to varied site conditions, simplicity, and relatively low first cost. However, due to the limited number of formally documented tests that had been conducted, a series of 60-mph tests using instrumented, relatively heavy and light vehicles was deemed necessary to more acurately evaluate the barrier's effectiveness.

OBJECTIVE

The objective of this research was to conduct instrumented vehicular impact tests of energy-absorbing barriers composed of sand-filled plastic barrels and, based on the results of these tests, determine the degree to which these barriers would minimize the hazards created by gore separation structures and other fixed objects. The following criteria were used to evaluate the barrier design:

1. The impact severity for the occupants of errant vehicles involved in head-on collisions into fixed objects located in gores must be reduced to a survivable level at impact velocities of 60 mph and less;
2. The barrier components should not be susceptible to dislodgement or ejection onto the traveled way when an impact occurs;
3. First cost and maintenance costs should be economically feasible; and
4. On-site repair time should be minimal because of the safety hazards to maintenance personnel and adjacent traffic when field repairs are in progress.

TEST PROCEDURE

All three tests were conducted on a section of runway at the Lincoln Municipal Airport located near Lincoln, California.

Test Vehicles

The full-sized vehicles used in these tests were 1968 Dodge sedans that, including the dummies and instrumentation, weighed approximately 4,700 lb. The vehicles were controlled by a remote operator following 200 ft behind the test vehicle in a control car equipped with a tone transmission system. A trip line in the path of the test car was used to cut off its ignition 10 ft prior to impact. The brakes were not applied before or during impact. A more complete description of the remote-control equipment is contained elsewhere (4).

A 1957 Volkswagen (VW) was steered and braked by remote control from a follow car as in the other two tests; however, because it was incapable of accelerating to 60 mph under its own power within the confines of the test site, a cable tow system was devised to pull the VW into the barrier. A detailed description of this system is included in the original report (5).

Test Dummies

Two anthropometric dummies were placed in the vehicle. A 165-lb dummy (50th percentile male) occupied the driver's seat and was secured by a conventional lap belt. A 210-lb dummy (95th percentile male) occupied the passenger side of the front seat for one of the tests (Appendix, Fig. 20).

Photographic Coverage

All of the tests were recorded with high-speed (250 to 400 frames per second) Photosonic motor-driven cameras that were manually actuated from a central control console. These cameras were located on the ground on both sides of the barrier, on a 30-ft-high light standard positioned directly above the barrier, and in the rear of the test vehicle. A motor-driven Hulcher camera with a speed of approximately 20 frames per second was located on scaffolding and provided documentary coverage of the tests. A ground-mounted high-speed camera and a normal-speed camera were hand panned through impact. Still photos, slides, and documentary movies were also taken.

Data Acquisition and Processing

Four accelerometers were mounted on both the driver dummy and the vehicle, and one seat-belt transducer was used on the driver dummy's lap belt. The accelerometers were all of the unbonded linear strain-gauge type (Appendix, Fig. 20). Signals from three strain gauges on the bridge approach guardrail were also transmitted by cable to the tape recorder for Test 241 (Appendix, Fig. 21).

For Test 241, a Krohn-Hite filter was used to obtain data filtered at a rate of 100 Hz. These filtered traces were easier to compare and to use for data reduction than were the unfiltered traces. They also gave a better overall record of the motion of the dummy and vehicle. The high-frequency spikes on the unfiltered records were assumed to be relatively insignificant as related to the overall motion of the vehicle.

After the data from Test 241 had been filtered, there was a malfunction of the Krohn-Hite filter. A Brush brown dot galvanometer with a frequency response of 22 Hz was used instead to obtain an effective filtration rate of 176 Hz for Tests 242 and 243. However, this filtration rate proved to be too unwieldy for numerical work, and a "hand-filtered" line was superimposed on it. This eliminated the high-frequency spikes and permitted the computation of the maximum deceleration values given in the test results. Copies of the filtered records of impact data for all the tests are contained elsewhere (5).

DESCRIPTION OF TEST BARRIER

The test barrier for Test 241 was composed of an array of frangible plastic barrels containing varied amounts of sand and was placed in front of a California Type 8 Bridge Approach Guardrail (BAGR) (Fig. 1 and Appendix, Figs. 22 and 23). Deceleration of the impacting vehicle was obtained through a transfer of momentum from the vehicle to the sand. The foamed plastic used for the barrels was frangible so that the sand was relatively unconfined when the modules were subjected to an impact-type load. Thus the barrier design was based on the conservation of momentum with adjustments so that standard barrel sizes could be used. The overall barrier length for the first test was approximately 21 ft. An additional 1-ft gap was left between the rear of the barrier and the nose of the BAGR to provide some additional deceleration distance and to minimize the accumulation of sand against the BAGR (which might provide a ramp for the vehicle).

Barrier Module

Several components were used to construct each barrel (Fig. 2). Frangible, high-density polyethylene plastic was used as the barrel material and a thin flexible plastic was used for the lids. A round plastic disc was available to place at the bottom of the barrel on soft ground; however, it was unnecessary for the barriers at this test site. An interlocking group of seven polystyrene (plastic) boards served as a core to support the sand at the proper height in the barrel. The core was covered with a thin, hard, circular, high-impact polystyrene disc. A flexible clear-plastic circular seal with upturned edges was seated on top of the disc to prevent the sand from spilling down to the ground. The sand was poured into the barrel to obtain the desired weight, and then a lid was riveted to the barrel in three or four places. Core heights available from the manufacturer permitted nominal sand weights (based on a sand density of 100 pcf) of 200, 400, 700, and 1,400 lb; a full barrel (with no core) contained 2,100 lb of sand. The barrels holding 1,400 and 2,100 lb of sand were 3 ft in diameter and 3 ft high; all other barrels were 3 ft in diameter and $2\frac{1}{2}$ ft high.

Barrier Design

The initial barrier (Test 241) was constructed using barrels containing 400 lb of sand at the nose and 2,100 lb of sand at the rear (Figs. 3 and 4 and Appendix, Fig. 22). This mass distribution was designed to obtain a relatively uniform rate of deceleration during impacts. The tapered barrier was 3 ft wide (one barrel) at the nose and 9 ft wide (three barrels) at the rear.

Simulated shoulder lines were placed 10 ft from the left side of the barrier and 4 ft from the right side as measured at the last row of barrels. These dimensions represented a four-lane freeway with a two-lane off-ramp as per the California Division of Highways' planning manual. The simulated gore area was 23 ft wide at this point. Instructions and observations on the installation and assembly of the test barriers are given elsewhere (5).

TEST RESULTS

Test 241

Test Vehicle—A 1968 Dodge sedan weighing 4,690 lb (including dummies) was used in this test. A 165-lb dummy occupied the driver's seat, and a 210-lb dummy occupied the passenger side of the front seat. Both dummies were secured by lap belts. The left front door and the gas tank were removed prior to the test.

Vehicle Behavior and Damage—The test vehicle, traveling at a speed of 58 mph, impacted the barrier head on and plowed through the entire barrier (Figs. 5 and 6). The vehicle axis was 1 ft to the left of the barrier axis at the time of impact. About 3 to 4 ft in front of the bridge railing, the vehicle ramped up on barrier debris and came to rest on the bridge rail just in front of the camera tower 24 ft behind the nose of the barrier. As the vehicle came to rest, it tilted sharply in a counterclockwise direction, because the left front wheel was not supported by the bridge rail, and almost turned over (Fig. 7) before returning to its final position.

Vehicle damage was confined mainly to the front end. Maximum significant crush at the center of the vehicle forestructure was 1⅔ ft. The crush was fairly uniform across the front of the vehicle but slightly less on the left side (Fig. 8 and Appendix, Fig. 24). The lower frame member, bumper, and front fenders were all severely buckled, and the radiator was shoved back against the engine. On the passenger side, the front windshield was cracked where the sun visor came down and was struck by the dummy's head. No crimp in the roof over the doorpost was observed. The doorpost on the driver's side was torn loose from its roof connection and displaced back ½ in. Immediately after impact, the hood flew open; however, it sustained no damage because the level of the hood was higher than the 2½-ft-high barrels at the nose of the barrier. The steering wheel deformation was 2½ in.; the collapsible steering column was foreshortened 0.7 in. when hit by the dummy. (See Fig. 25 in the Appendix for a summary of these results.)

Barrier Damage—Most of the broken foam plastic core pieces stayed under the vehicle. Although none of the lids was broken, all of them were detached from the barrels and several were displaced a considerable distance. Broken-barrel fragments did not travel far; four barrels along the right side of the barrier were left mostly intact. They had been shoved sideways and had tipped over, spilling sand out rather than "exploding." It appeared that most of the barrier resistance came from the left two-thirds of the barrier. Other than lids, little debris flew outside the "edge of pavement" lines except for some sand that extended 4 to 6 ft into traffic lanes on each side and beside the original barrier location on the right side and 10 to 15 ft beyond it on the left side (Appendix, Fig. 26). The last one or two rows of barrels did not shatter but leaned and compressed against the bridge rail and then fractured. These barrel pieces, plus the sand that was intermixed, piled up in front of the bridge rail and provided a ramp for the car. The broken plastic core pieces were small and mixed into the sand; hence, the sand did not appear suitable for reuse without sifting. Most of these fragments remained in the debris under the vehicle; however, many pieces on top of the pile were scattered quickly by the wind. This condition could pose a psychological hazard to drivers on an adjacent traveled way as they tried to dodge these pieces and other litter near the gore area.

Figure 1.

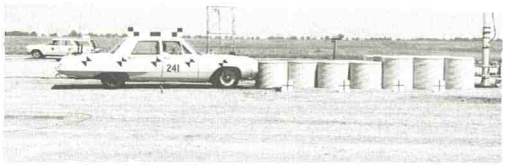

Figure 2.

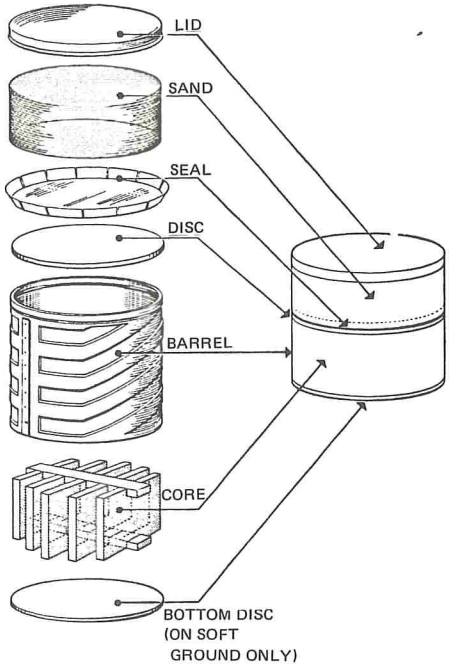

Figure 3.

Figure 4.

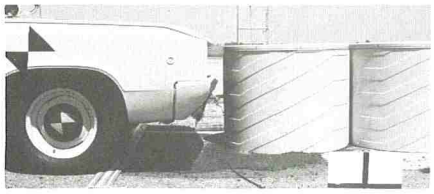

Figure 5.

Figure 6.

Figure 7.

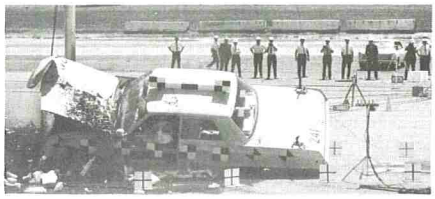

Figure 8.

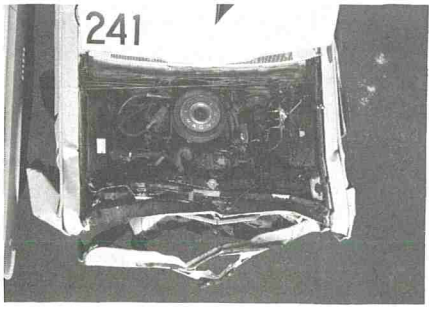

Figure 9.

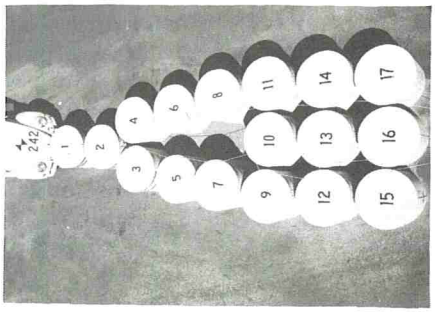

Instrumentation Results—The accelerometer records were cut off about 200 msec after impact on some of the channels when equipment in the test vehicle broke loose. It appeared, however, that in many cases the main pulse of the deceleration was recorded before the interruption. Visicorder traces filtered at 100 Hz were used to derive the highest average values of deceleration. The highest 50-msec average vehicle deceleration (longitudinal) was 10.7 g (longitudinal accelerometer, Location E, Appendix, Fig. 20). The highest 50-msec average dummy (head) deceleration was 25.2 g (longitudinal and vertical accelerometers, Location A, Appendix, Fig. 20).

A maximum lap-belt load of 990 lb was recorded with the seat-belt-force transducer. Thus, the total load on the dummy was well below the 5,000-lb maximum permitted by federal standards (6). The tubular steel bridge approach guardrails sustained stresses of 3,240, 3,620, and 6,120 psi—not excessive values. Records from the longitudinal and lateral accelerometers placed at the center of gravity of the vehicle (Location A, Appendix, Fig. 20) were cut off just before the main peak—about 200 msec after impact.

The Gadd Severity Index was computed using longitudinal and vertical deceleration components of motion from accelerometers in the head of the driver dummy. For the highest 50 msec, the number was computed to be 185. This is well below the critical value of 1,000.

Test 242

Barrier Description—The test barrier consisted of 17 plastic barrels filled with varied amounts of sand ranging from 200 lb at the nose of the barrier to 1,400 lb at the rear (Appendix, Fig. 22, and Figs. 9 and 10). The black tape on the barrels shows the bottom level of sand in the rear barrels and top and bottom levels in the front barrels. The preceding weights are nominal for an assumed sand density of 100 pcf. Because it had been determined that the actual (moist) sand density for Test 241 was only 80 pcf, sand that had been run through a dryer just prior to delivery was used for Test 242. This sand had a higher density of 88 pcf (moisture content of 0.4 percent). The plastic barrel components were all identical to those used in Test 241.

The barrier was lengthened from 21 ft (Test 241) to 24 ft (nominal), and the barrel weights were decreased at the nose to provide a softer impact. Also, the rear barrels were changed from 2,100 to 1,400 lb, and the void space at the rear increased from 1 to 2 ft in an attempt to lessen the accumulation of sand and debris against the fixed object that had caused ramping in Test 241. A section of New Jersey concrete median barrier was used as the fixed object instead of the bridge rail because of the location of the ground anchors for the cable tow system used in this test.

A cotton sash cord was threaded continuously through all of the lids and was tied to the camera tower to prevent the lids from sailing onto the traveled way after impact, as had occurred during Test 241.

Test Vehicle—A 1,940-lb 1957 Volkswagen sedan was used in this test. Vehicle weight included a 165-lb dummy that was secured in the driver's seat by a lap belt, a water-filled gas tank, a spare tire (in front), and all the radio control equipment. The left door was replaced with a small steel channel brace so that the action of the dummy could be recorded by the cameras.

Vehicle Behavior and Damage—The VW hit the barrier nose head on with its axis about 9 in. to the left of the barrier centerline. The impact velocity was 59 mph. The vehicle came to rest 19 ft beyond the nose of the barrier with all its wheels on the ground (Figs. 11 and 12). During impact there was a 16-in. rise at the rear of the vehicle (measured at a target on the right rear fender). (See Fig. 27 in the Appendix for a summary of the test results.)

The front truck lid remained closed and was moderately buckled, as were the front fenders. Maximum crush at the forestructure of the VW was only 8 in. (Appendix, Fig. 24, and Fig. 13). The impact from the dummy's head caused the entire windshield to pop out. The substitution of a pulley for the standard VW steering wheel (required for radio control of the VW) prevented measurement of any steering wheel deformation.

Barrier Damage—Figure 28 in the Appendix shows the location of the barrier debris. A small number of barrel core pieces were found under the VW, but there was no other

Figure 10.

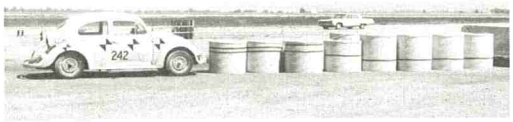

Figure 11.

Figure 12.

Figure 13.

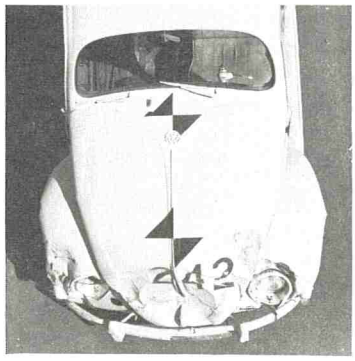

Figure 14.

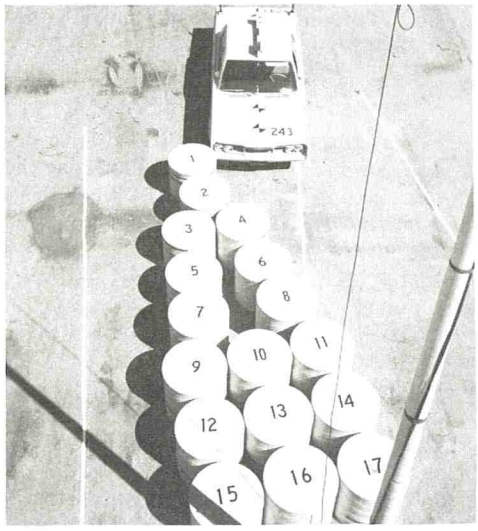

Figure 15.

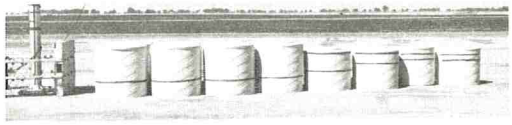

Figure 16.

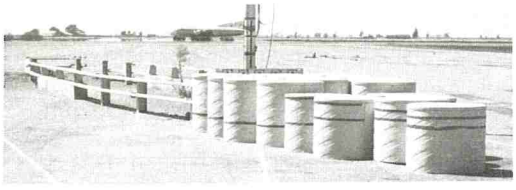

Figure 17.

Figure 18.

Figure 19.

debris either under or behind it. There was no debris outside the 10-ft shoulder line, but a small amount extended 9 ft beyond the 4-ft shoulder line. There was no sand covering the front of the VW. Very little debris was found beyond the back of the barrier. The lids all remained attached to the cotton rope and were clustered near the rear of the barrier. At least nine of the barrels were totally destroyed. Four or five barrels were compressed but unbroken and could have been reused; however, some of their inner foam plastic cores were crushed. Three barrels were undamaged and undisturbed. The compressed barrels had moved forward during impact; it is not known whether they could have been dragged on the ground and repositioned without breaking the plastic barrels and cores or spilling the sand.

Instrumentation Results—Visicorder traces were used to derive the highest average values of deceleration. The highest 50-msec average vehicle deceleration (longitudinal) was 8.7 g (longitudinal and lateral accelerometers). The highest 50-msec average dummy (head) deceleration was 44.0 g (longitudinal, lateral, and vertical accelerometers).

Vehicular lateral decelerations (two accelerometers) were about 2 g maximum for 5 msec with 1-msec ringing spikes of 8 to 10 g. The seat-belt force transducer was inoperable. The Gadd Severity Index for the driver dummy's head was computed to be 1,280, significantly greater than the critical value of 1,000.

Test 243

Barrier Description—The barrier for this test had the same size, number, and configuration of barrels as was used for Test 242 (Figs. 14 through 16). As in Test 242, the sand was dried prior to delivery. It had a density of 89.2 pcf and a moisture content of 0.8 percent.

Lids were attached to the barrels with four equidistant pop-rivets according to the manufacturer's directions. Three extra rivets were added in a short row next to one of these four rivets. This row of rivets was randomly located and was not on the same side of all the barrels. It was hoped that these extra rivets would provide a hinge effect and minimize the wide scattering of lids that occurred during Test 241.

Test Vehicle—A 4,770-lb 1968 Dodge sedan was used in this test. Vehicle weight included a 165-lb dummy secured in the driver's seat by a lap belt, a water-filled gas tank, and all the radio control equipment.

Vehicle Behavior and Damage—The crash vehicle hit the nose of the barrier about a foot to the right of the planned point of impact at a speed of 57 mph and an angle of 15 deg with the barrier axis. It ramped up midway into the barrier, continued on through it, narrowly missed the right corner of the Type 8 bridge approach guardrail nose, and stopped with the rear of the vehicle even with the last row of barrels in the barrier. It came to rest with all wheels on the ground on a thin layer of sand (Figs. 17 and 18). (See Fig. 29 in the Appendix for a summary of the test results.)

Damage to the vehicle forestructure was quite severe (Fig. 19). The front end, including fenders, was uniformly crushed back against the engine. The maximum crush was 21 in. (Appendix, Fig. 24). The engine was not displaced. The lower longitudinal front frame members and the bumper were sharply buckled down to the ground and back against the front wheels. The hood was undamaged because of the relatively low height (30 in.) of the first four rows of barrels. A crimp in the roof was observed on the driver's side above the doorpost. The rest of the car was undamaged. Maximum deformation of the steering wheel was $2\frac{3}{4}$ in. The collapsible steering column was foreshortened $\frac{3}{4}$ in. by the dummy's impact.

Barrier Damage—Four barrels remained standing at the rear corner of the barrier. Of these, only two were undamaged. Large amounts of debris were scattered to the front and right front of the crash vehicle, some of which extended about 20 ft to the right of the 4-ft shoulder line and across the traffic lane (Appendix, Fig. 30). The right front corner of the vehicle projected about 3 ft into the traffic lane; the right rear was about 1 ft inside the shoulder line.

The barrel lids were thrown far ahead of the vehicle, as much as 67 to 70 ft beyond the back of the barrier; however, only 3 or 4 lids landed in the traffic lanes. One lid

landed 26 ft to the left of the 10-ft shoulder line. The extra rivets on the lids did not appear to have any beneficial effect. This may have been due, in part, to the lack of a washer on the rivet inside the barrel.

A large number of broken foam core pieces were found under the crash vehicle, and many other pieces were thrown beyond the vehicle. These latter pieces were immediately blown freely about by a moderate wind and could have posed a psychological hazard if they had been blown across traffic lanes.

Instrumentation Results—The highest 50-msec average vehicle deceleration (longitudinal) was 7.9 g. The highest 50-msec dummy (head) deceleration was 34.0 g (longitudinal, lateral, and vertical accelerometers).

The seat-belt force transducer had a maximum reading of 600 lb. Vehicular lateral decelerations (two accelerometers) were about 3 g maximum for 5 msec with 1-msec spikes up to 10 g. The Gadd Severity Index was 580.

DISCUSSION

Vehicular Deceleration

The records of vehicular longitudinal deceleration for Test 242 contained four distinct pulses spaced about 50 msec apart. All were in the 10-g range with valleys of about 5 g. This pulsing occurred as the vehicle went from one row of barrels to the next. The overall shape of the deceleration data indicated that this barrier configuration (Test 242) was better than that used for Test 241 (two 700-lb barrels with three 1,400-lb barrels in the midsection of the barrier). This abrupt change in barrier mass for Test 241 coincided with a 15-g 5-msec vehicular deceleration that occurred as the vehicle passed the midsection of the barrier. For Test 242, the midsection of the barrier contained two 700-lb barrels followed by two 1,400-lb barrels and then by three 1,400-lb barrels—a smoother transition of mass that was reflected in the deceleration data.

The vehicular longitudinal decelerations for Test 243 were fairly constant at 7 to 9 g with several main pulses and were similar in magnitude and shape to those for Test 242, thus showing that the barrier configuration, which was identical for both tests, had a similar effect on cars with different weights. The deceleration pulse was decaying as the vehicle passed through the last two rows of 1,400-lb barrels; thus it appeared that these last rows had already been set in motion by the time the vehicle passed through them and, therefore, had a low decelerative effect. The vehicle had a velocity of about 14 mph as it penetrated the last row of barrels; hence, the barrier did not have enough mass and/or width to stop a 4,770-lb vehicle impacting near the nose at an angle of 15 deg and a speed of 57 mph.

The highest 50-msec average longitudinal vehicular passenger compartment decelerations measured during each test are as follows:

1. Test 241, one accelerometer, 10.7 g;
2. Test 242, two accelerometers, 8.7 g; and
3. Test 243, two accelerometers, 7.9 g.

The severity of these decelerations can be interpreted by comparing them with the recommended 200-msec deceleration tolerance limits proposed by Cornell (8). The Cornell limits, which were 5, 10, and 25 g for unrestrained, lap-belted, and fully restrained occupants, define what would be, in the opinion of the researchers, a survivable environment under almost all circumstances when applied to a 50-msec time interval. Thus the vehicular passenger compartment decelerations in the longitudinal direction were judged acceptable for restrained passengers. Only in Test 241 did the computed value slightly exceed the maximum value of 10 g for lap-belted passengers. The vehicular decelerations were also under the value of 12 g for the highest 40-msec period, another criterion that has sometimes been used to evaluate collision severity (7).

Computed values of the Gadd Severity Index indicate that in Test 242 the dummy driver might have suffered fatal head injuries. Therefore, acceptable vehicular decelerations, based on the criteria previously described, do not automatically eliminate the possibility of fatal injuries.

Gadd Severity Index

Longitudinal, lateral, and vertical components of deceleration from the dummy's head were vectorially combined at identical times after impact (at successive 0.0025-sec increments) to obtain resultant values of deceleration. Then the Gadd Severity Index (9),

$$\left(\int_{t_1}^{t_2} a^{2.5}\, dt \right)$$

was computed over the 50-msec period with the highest average resultant values of head deceleration using 20 successive time intervals with dt = 0.0025 sec. The following Gadd Severity Index values (based on 1- to 50-msec pulse duration) were calculated for the test series.

1. Test 241, 185;
2. Test 242, 1,280; and
3. Test 243, 580.

The Gadd Severity Index of 1,280 in Test 242 indicated that even a lap-belted passenger probably would have suffered fatal head injuries if his head struck the windshield frame as violently as did the head of the dummy. This high number was not surprising in that the head of the dummy broke the windshield and forced it entirely out of the car and then dented a section near the small radius edge of the unpadded stiff metal dashboard. The steering wheel had been removed to accommodate the remote steering apparatus. If it had been in place, it might have minimized the impact severity when the dummy struck the dash; however, a front-seat passenger with no steering wheel in front of him might normally impact the dash as the dummy driver did. This reinforces the idea that the injuries sustained by the vehicle occupants in a 60-mph collision with an energy-absorbing barrier are dependent on the impact protection provided by the vehicle interior surfaces if ejection does not occur and both a lap belt and a shoulder harness are not in use. A discussion of this severity index and the tolerance of the human head to deceleration is given elsewhere (5).

Debris

In all of the tests, the foam plastic core material that supported the sand in the barrels was broken into small pieces. This material did not land in the traveled way initially, except after the angular impact in Test 243; however, the pieces were so light that the slightest breeze blew them all over the test site. If this material is used in operational barrier installations, it could pose a litter and maintenance problem after barrier impacts. In addition, this material could create a psychological hazard to nearby motorists even though it is lightweight and harmless.

The barrel lids were another source of debris. After impact, they sailed through the air for distances up to 100 ft. Most of them stayed in the gore area during the head-on impacts, but the few that landed in the traveled way posed a potential psychological hazard for nearby motorists. In Test 242, the cotton sash cord was threaded continuously through all of the lids and anchored at the rear of the barrier, which proved to be an effective method of keeping all the lids in the gore area. However, the cord gave the barrier a slightly less desirable appearance.

Broken barrel pieces and sand were mostly contained in the gore area except during the angular impact of Test 243. In Tests 241 and 243 the impact vehicles tended to ramp over the debris, especially in Test 241 where the rear of the barrier was only 12 in. from the bridge approach guardrail. The VW did not ramp up because of the sloping forestructure of the vehicle, which tended to nose under the sand in the front barrels of the barrier. The debris scattered, in the traveled way after an angular impact such as Test 243, appears to be one currently unsolved drawback of this barrier.

Barrier Dimensions

The test barriers were close to the minimum length required to provide reasonable safety for restrained passengers in vehicles impacting at a speed of 60 mph. The barrier could be increased in length to provide a softer impact; however, this would reduce possible recovery area. Site conditions would partially govern the decision regarding optimum barrier length; initial installation and long-term maintenance costs would vary with the length of the barrier.

Redirection

In all the tests, including Test 243, that involved an angular impact, the vehicle was not redirected but continued on a straight course after impacting the barrier.

Sand Density

The sand used in the barrels was sampled during barrier construction. Subsequent test results indicated that the density of the sand was significantly lower than the nominal 100-pcf unit weight assumed by the manufacturer, as can be seen in the following:

1. Test 241, 80 pcf, water content 6.7 percent;
2. Test 242, 88 pcf, water content 0.4 percent (sand had been run through a dryer just prior to delivery); and
3. Test 243, 89 pcf, water content 0.8 percent (sand had been run through a dryer just prior to delivery).

The general range of unit weights for dry, loose sand is 90 to 100 pcf, and for damp, loose sand it is 85 to 95 pcf (10). Thus, the sand used for the barriers tested fell just below the lower end of the normal weight range. Graphs that show how sand volume increases by 15 to 35 percent (maximum) for coarse to fine sand respectively and how moisture contents range from 0 to 20 percent are given elsewhere (11).

It was concluded that it would probably be too bothersome and expensive to have sand dried for operational barriers. The added weight of the dried sand would not change the effectiveness of the barrier significantly; however, it is well to realize that sand density is a variable factor and that, if sand with a density of 100 pcf was used in a barrier, the performance could differ somewhat from that reported here.

Aesthetics

This barrier presents a low, relatively uniform shape. The barrels can be ordered in bright or dark colors. Care should be taken to provide a level site so that the barrels will not lean at random angles. For these who do object to the imposition of bright cylindrical shapes on the streamlined highway profile, a cover for the entire barrier might be desirable. Any cover selected should be a weather-resistant, taut, flexible material and should not inhibit the free movement of the sand during impacts. Material wrapped around the sides would be preferable to a complete cover until full-scale tests of barriers with covered tops are conducted.

Accident Experience

Accident reports from Connecticut indicate that 15 in-service barriers were impacted 16 times (3). In 13 cases, the vehicle was driven away before accident information could be gathered. Several of these impacts were nuisance hits. However, it was reported that the barrier may have prevented an impending collision with a fixed object in many of these cases. The three remaining reported accidents were all serious, yet in all cases the drivers received only minor injuries and it was clear that the barrier had prevented serious injuries or deaths.

The manufacturer reported that as of May 1, 1971, there were 135 barrier installations in 20 states and two foreign countries (12). There had been 81 impacts of the barrier at speeds of up to 65 mph with only one injury. In 80 percent of these impacts, the vehicle was driven away and the accident was not reported.

Design Considerations

Barrier size and configuration must be selected for each site. The barrier configuration will depend on (a) the width of the fixed object to be shielded, (b) the predicted speed and angle of the impacting vehicles, and (c) the available space in the gore, shoulders, and traffic lanes. The presence of curbs and guardrails may also affect the design. A curb immediately in front of the barrier nose could adversely affect barrier performance because the vehicle may vault over the curb, thus preventing the vehicle from impacting the modules at the optimum height for vehicle stability and uniform deceleration. Such a curb should be removed.

The width of the back row of modules should always be greater than the width of the fixed object. This will soften the impacts of those vehicles striking the rear portion of the barrier at an angle and provide some deceleration prior to striking the corners, if any, of the fixed object. The barrier modules should be set back from the traffic lanes to minimize the number of casual vehicular contacts with the barrier and the amount of debris thrown into the traveled way when an impact does occur. Also, space should be left behind the last row of modules so that sand and debris will not be confined and increase the ramping effect of the vehicle.

The lower foot of sand in the 2,100-lb modules provides additional mass as a backup for the front of the barrier. However, the velocity of the vehicle at the time it makes direct contact with the back row of the barrier is not sufficient to explosively displace this sand. Consequently, it is displaced very little and thus tends to form a ramp. The use of 1,400-lb modules in place of 2,100-lb modules in the last row would therefore appear desirable to eliminate this relatively ineffective lower foot of sand.

A recent report (3) stated that some nonimpact failures of these cores had occurred when they were placed on sloped gore areas. The failures occurred only when the strong axis of the core material was perpendicular to the cross slope and consisted of collapse of the core. To prevent this, one should place the strong axis of the form plastic core blocks parallel to the cross slope to prevent collapse of the core due to barrel movement down the cross slope that is induced by traffic vibrations. Also, the manufacturer is studying new core block configurations and new core materials. It might prove advisable to enclose cores made of light, crushable foam plastic with a flexible fine-mesh bag to limit their scatter after a barrier impact.

If placed in climates subject to temperatures below 32 F, the addition of at least 5 percent road salt to the sand should be specified to preclude solidification of the moist sand.

A thin wire or rope may be threaded continuously through all module lids and anchored to the ground at the rear of the barrier to minimize dispersal of lids during impact (Test 242).

A recommended minimum optimum barrier length is 21 to 24 ft. This length provides survivable deceleration levels for 60-mph impacts without taking away excessive recovery area for errant vehicles.

CONCLUSIONS

The results of the three full-scale tests reported here indicate that the hazards presented by many existing gore separation structures and other fixed objects can be significantly reduced by providing protection with energy-absorbing barriers that incorporate sand-filled plastic barrels.

Electronically measured vehicular and dummy decelerations, confirmed by analysis of the photographic data, indicate that occupants of full-sized vehicles (4,700 lb including occupants) that impact these barriers at a speed of 60 mph will, in most cases, sustain little or no injury if they wear a lap belt and shoulder harness, minor injuries if they wear only a lap belt, and moderate injuries if they are unrestrained. However, occupants of smaller vehicles, such as a 2,000-lb VW, may sustain serious injuries even if they are restrained by a lap belt. Because this barrier will provide no significant vehicular redirection, the lateral decelerations sustained during collisions with the barrier will be minimal.

Confinement of the sand will result in a tendency for an impacting vehicle to rise. Thus, the modules placed near the rear of the barrier should not be full (eliminate the

relatively ineffective lower foot of sand), and a 2-ft-wide void should be provided between the rear of the barrier and the face of the fixed object to minimize the accumulation of barrier debris and the associated formation of a ramp adjacent to the fixed object.

A considerable amount of debris will be generated during a 60-mph collision with this barrier. However, most of this debris will be propelled straight ahead of the impacting vehicle. Thus, this debris will present a hazard for adjacent motorists only when high-speed, oblique-angle impacts occur unless the debris is scattered by wind. Tying the lids together and encasing the core material will improve this debris problem somewhat.

The reported first cost of approximately 20 installations of this barrier in Connecticut ranged from $1,500 to $3,300 each (3). Each barrel used for the test barriers costs $130. Thus, the material cost for the test barriers was approximately $2,000 because the test barriers contained 15 and 17 modules each. Although little or no routine maintenance should be required, even relatively mild impacts will almost always require replacement of at least several barrels. However, the simplicity of the barrier's construction will permit minimal on-site repair time once debris-removal operations are complete.

ACKNOWLEDGMENT

This work was accomplished in cooperation with the U. S. Department of Transportation, Federal Highway Administration, as Item D-4-69 of Work Program HPR-PR-1 (8), Part 2, Research. The opinions, findings, and conclusions expressed in this publication are those of the authors and not necessarily those of the Federal Highway Administration.

REFERENCES

1. Nordlin, E. F., Woodstrom, J. H., and Doty, R. N. Dynamic Tests of an Energy Absorbing Barrier Employing Water-Filled Cells, Series XXI. California Division of Highways, Nov. 1970; also Highway Research Record 343, 1971, pp. 100-122.
2. Nordlin, E. F., Woodstrom, J. H., and Doty, R. N. Dynamic Tests of an Energy Absorbing Barrier Employing Steel Drums, Series XXII. California Division of Highways, Oct. 1970; also Highway Research Record 343, 1971, pp. 123-141.
3. Kudzia, W. J., Schwegler, L. T., and Hough, M. The Fitch Inertial Barrier and Its Performance in Connecticut.
4. Nordlin, E. F., Woodstrom, J. H., and Hackett, R. P. Dynamic Tests of the California Type 20 Bridge Barrier Rail, Series XXIII. California Division of Highways, Oct. 1970; also Highway Research Record 343, 1971, pp. 57-74.
5. Nordlin, E. F., Stoker, J. R., and Doty, R. N. Dynamic Tests of an Energy Absorbing Barrier Employing Sand-Filled Frangible Plastic Barrels, Series XXIV. California Division of Highways, July 1971.
6. Federal Motor Vehicle Safety Standards. National Highway Safety Bureau, U. S. Department of Transportation, with amendments and interpretations through Aug. 6, 1968.
7. Development of a Hydraulic-Plastic Barrier for Impact-Energy Absorption. BPR-DOT Contract No. FH-11-6909 Final Report, Department of Mechanical Engineering, Brigham Young University.
8. Highway Barrier Analysis and Test Program. Summary Report for period July 1960 to July 1961, Cornell Aeronautical Laboratory Rept. VJ-1472-V3, July 1969.
9. Gadd, C. W. Use of a Weighted-Impulse Criterion for Estimating Injury Hazard. Proc., 10th Stapp Car Crash Conf., SAE, Nov. 1966.
10. Nahum, A. M., Siegel, A. W., and Trachentburg, S. B. Causes of Significant Injuries in Nonfatal Traffic Accidents. Proc., 10th Stapp Car Crash Conf., SAE, Nov. 1966.
11. Troxell and Davis. Concrete. McGraw-Hill Engineering Series, 1956.
12. Fibco, Inc. Fitch Barriers Save Lives. 15 Lewis Street, Hartford, Connecticut, May 1, 1971.

APPENDIX

DETAILS OF BARRIER DESIGN AND PERFORMANCE

Figure 20.

VEHICLE INSTRUMENTATION

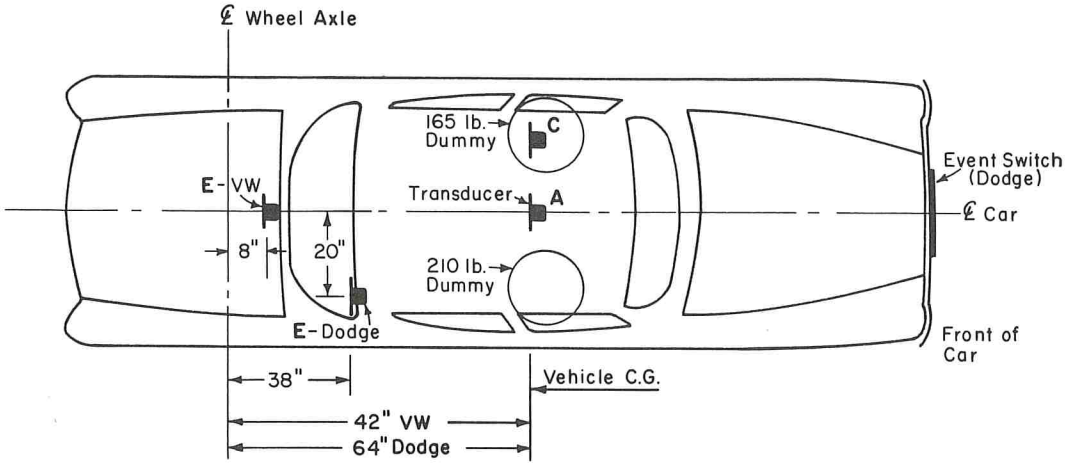

Tests 241 & 243
(Dodge)

CHANNEL NO.	LOCATION[1]	DESCRIPTION
1	C	Longitudinal accelerometer - head.
2	C	Lateral accelerometer - head.
3	C	Vertical accelerometer - head.
4	C	Longitudinal accelerometer - chest.
5	A	Longitudinal accelerometer.
6	A	Lateral accelerometer.
7	E	Longitudinal accelerometer.
8	E	Lateral accelerometer.
9	C	Seat belt transducer - lap belt.
13	L	Event switch mounted across front bumper.
	E	Impact-O-Graph with mechanical stylus.

Test 242
(Volkswagen)

1	C	Longitudinal accelerometer - head.
2	C	Vertical accelerometer - head.
3	C	Lateral accelerometer - head.
4	C	Longitudinal accelerometer - chest.
5	A	Longitudinal accelerometer.
6	E	Longitudinal accelerometer.
7	A	Lateral accelerometer.
8	E	Lateral accelerometer.
9	C	Seat belt transducer - lap belt.

Note:

[1] A and E on vehicle floor; C on back of dummy's chest cavity and back of dummy's head cavity.

Figure 21.

BARRIER INSTRUMENTATION

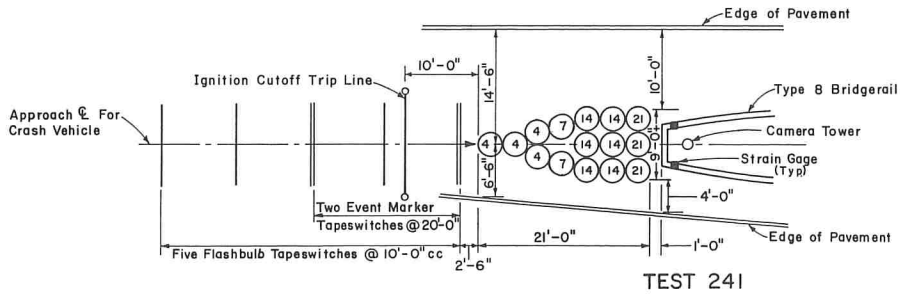

TEST 241

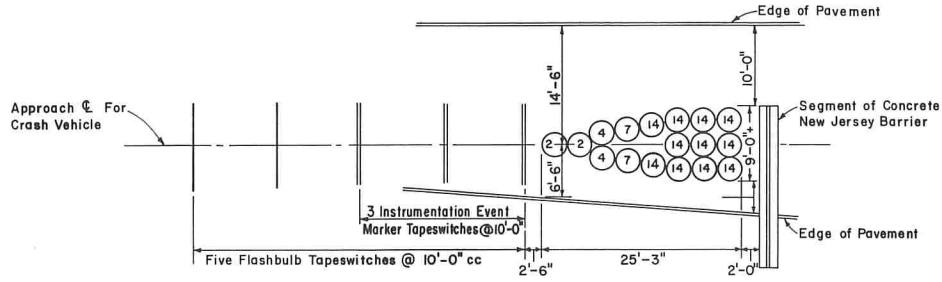

TEST 242

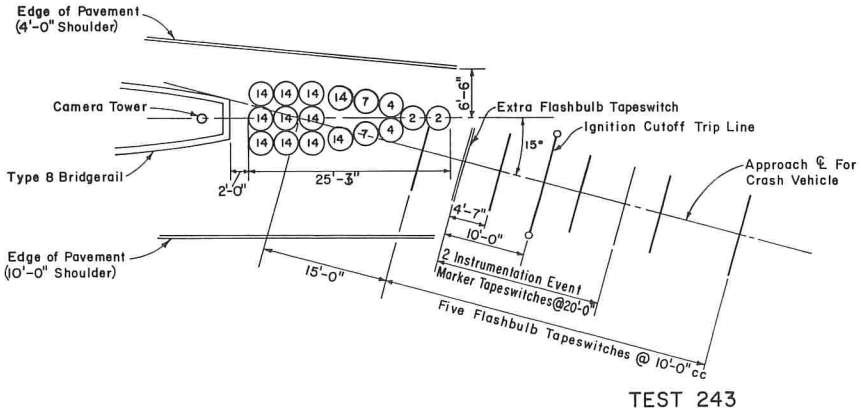

TEST 243

LEGEND

■ – Strain gage on top surface of upper and lower rails, 8 in. behind nose of bridgerail – total 3

(14) – Barrels with nominal wt. of sand in hundreds of pounds.

Figure 22.

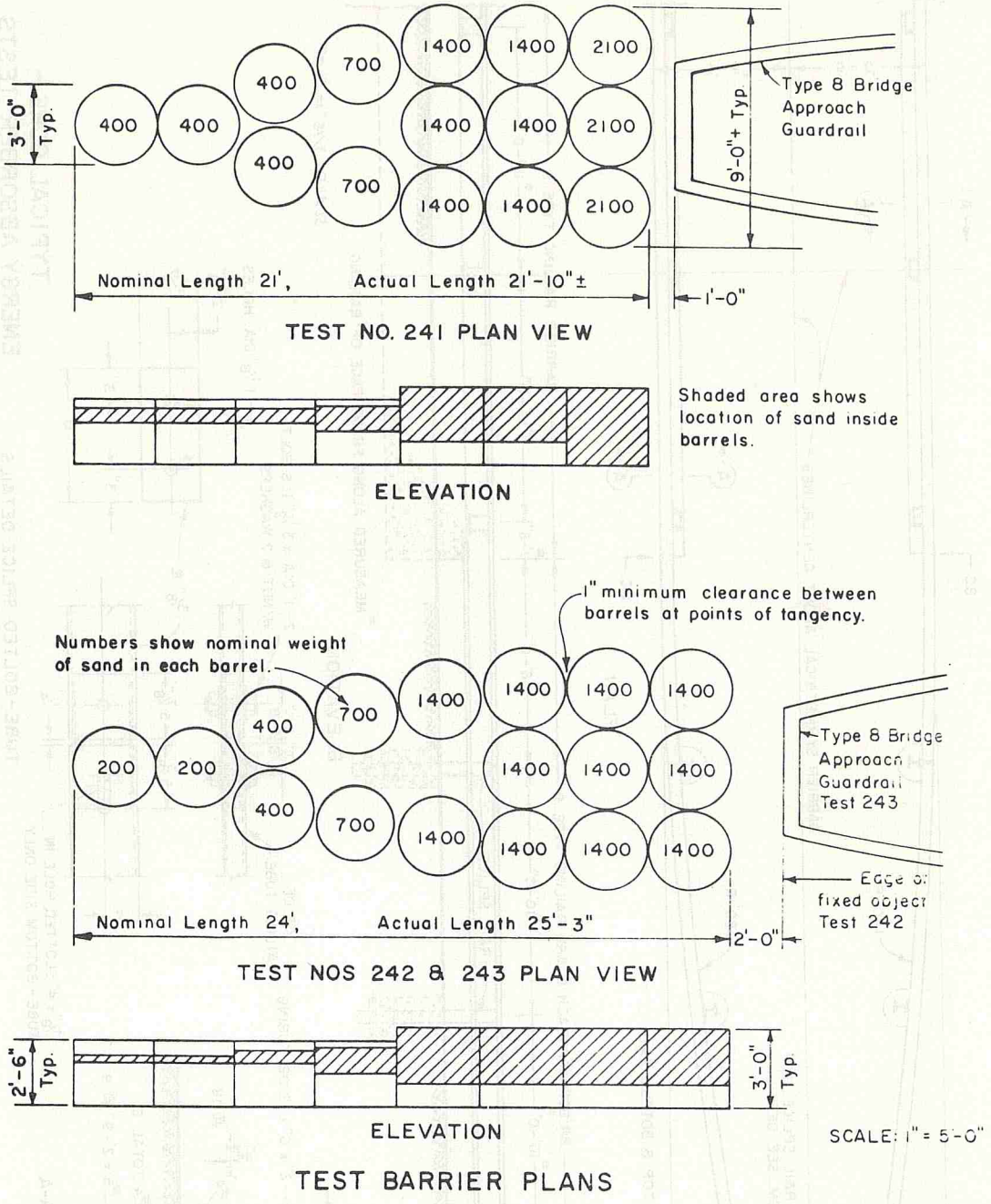
3'-0" Typ.
400
400
400
400
700
700
1400
1400
1400
1400
1400
1400
2100
2100
2100
9'-0"+ Typ.
Type 8 Bridge Approach Guardrail
Nominal Length 21', Actual Length 21'-10"±
1'-0"
TEST NO. 241 PLAN VIEW
Shaded area shows location of sand inside barrels.
ELEVATION
1" minimum clearance between barrels at points of tangency.
Numbers show nominal weight of sand in each barrel.
200
200
400
400
700
700
1400
1400
1400
1400
1400
1400
1400
1400
1400
Type 8 Bridge Approach Guardrail Test 243
Edge of fixed object Test 242
Nominal Length 24', Actual Length 25'-3"
2'-0"
TEST NOS 242 & 243 PLAN VIEW
2'-6" Typ.
3'-0" Typ.
ELEVATION
SCALE: 1" = 5'-0"
TEST BARRIER PLANS

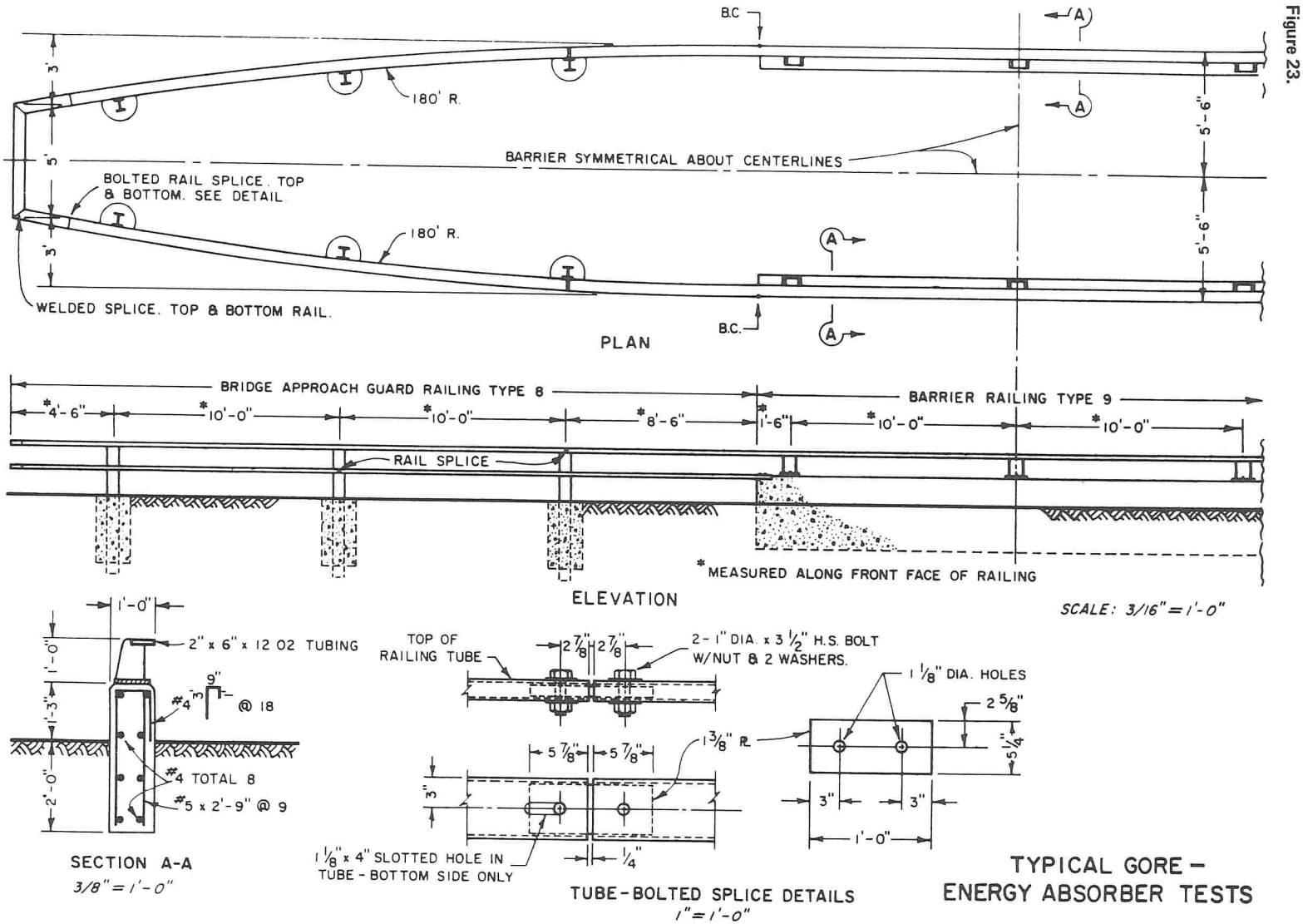
B.C
A
180' R.
BARRIER SYMMETRICAL ABOUT CENTERLINES
BOLTED RAIL SPLICE. TOP & BOTTOM. SEE DETAIL.
WELDED SPLICE. TOP & BOTTOM RAIL.
5'-9"
PLAN
BRIDGE APPROACH GUARD RAILING TYPE 8
BARRIER RAILING TYPE 9
*4'-6"
*10'-0"
*8'-6"
*1'-6"
RAIL SPLICE
* MEASURED ALONG FRONT FACE OF RAILING
ELEVATION
SCALE: 3/16" = 1'-0"
2" x 6" x 12 02 TUBING
#4 TOTAL 8
#5 x 2'-9" @ 9
SECTION A-A
3/8" = 1'-0"
TOP OF RAILING TUBE
2 - 1" DIA. x 3 1/2" H.S. BOLT W/NUT & 2 WASHERS.
1 1/8" DIA. HOLES
1 1/8" x 4" SLOTTED HOLE IN TUBE - BOTTOM SIDE ONLY
TUBE-BOLTED SPLICE DETAILS
1" = 1'-0"
TYPICAL GORE - ENERGY ABSORBER TESTS

Figure 23.

Figure 24.

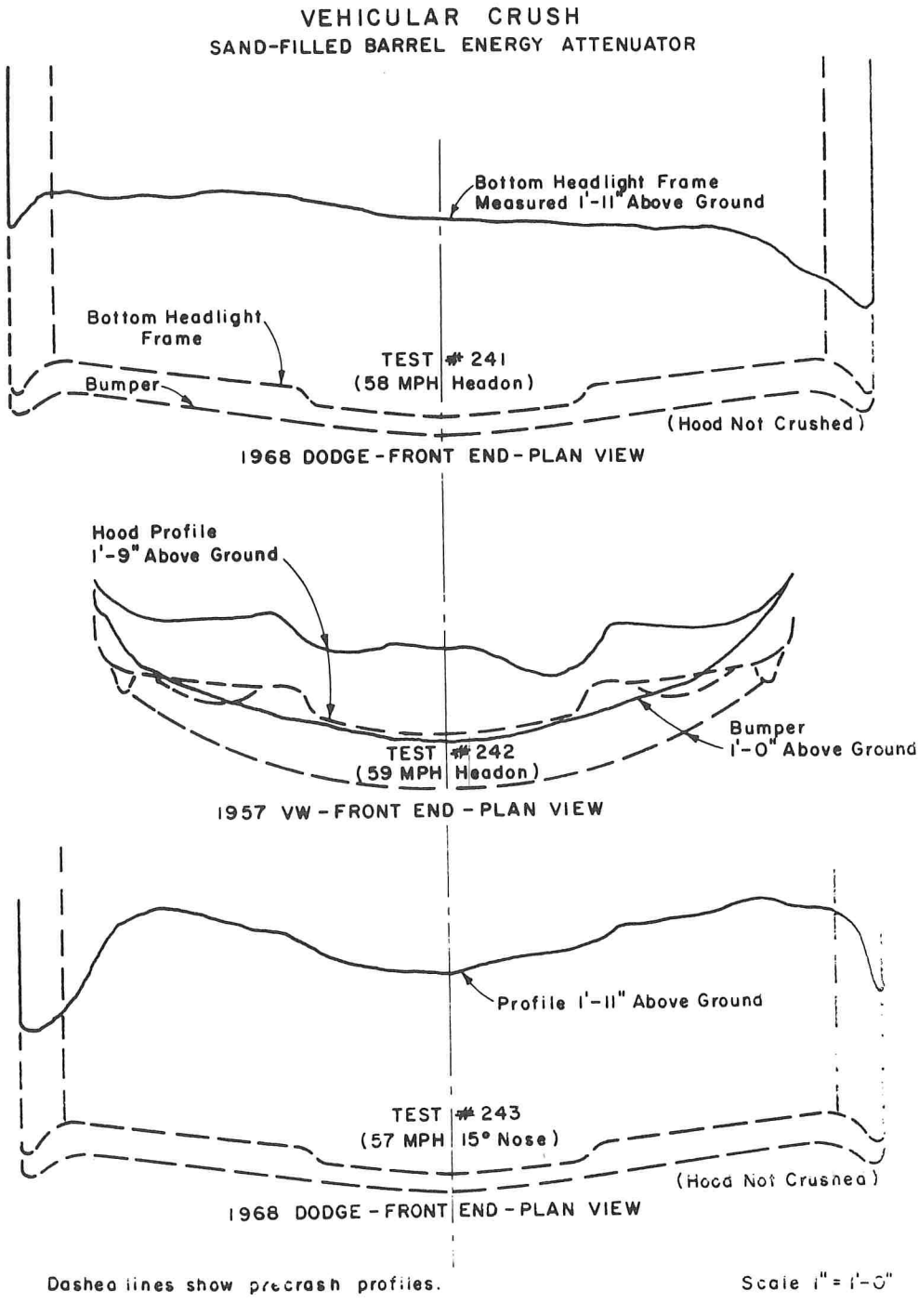
VEHICULAR CRUSH
SAND-FILLED BARREL ENERGY ATTENUATOR
Bottom Headlight Frame
Measured 1'-11" Above Ground
Bottom Headlight Frame
Bumper
TEST # 241
(58 MPH Headon)
(Hood Not Crushed)
1968 DODGE - FRONT END - PLAN VIEW
Hood Profile
1'-9" Above Ground
Bumper
1'-0" Above Ground
TEST # 242
(59 MPH Headon)
1957 VW - FRONT END - PLAN VIEW
Profile 1'-11" Above Ground
TEST # 243
(57 MPH 15° Nose)
(Hood Not Crushed)
1968 DODGE - FRONT END - PLAN VIEW
Dashed lines show precrash profiles.
Scale 1" = 1'-0"

Figure 25.

Impact + 0.027 Sec.

Impact + 0.231 Sec.

Impact + 0.435 Sec.

Impact + 2.373 Sec.

Test No.	241
Date of Test	May 21, 1970
Vehicle	1968 Dodge
Vehicle Weight (w/dummies and Instrumentation)	4690 lb.
Impact Velocity (V_o)	58.0 mph
Impact Angle	Head-on
Dummy Restraint	Lap Belt
Barrier Depth	21'-10"
No. of Plastic Barrels	15
Deceleration Distance of Passenger Compartment	24'-0"
Maximum Vehicular Deformation at Forestructure	1'-8"
Passenger Compartment Deceleration - Highest 50 ms. avg. - accelerometer record, 100 Hertz	10.7 G's
Vehicular Deceleration - Avg. value based on $V_o^2 = 2as$ where s = 24.0' (stopping distance)	4.7 G's
Gadd Severity Index (Dummy's head)	185

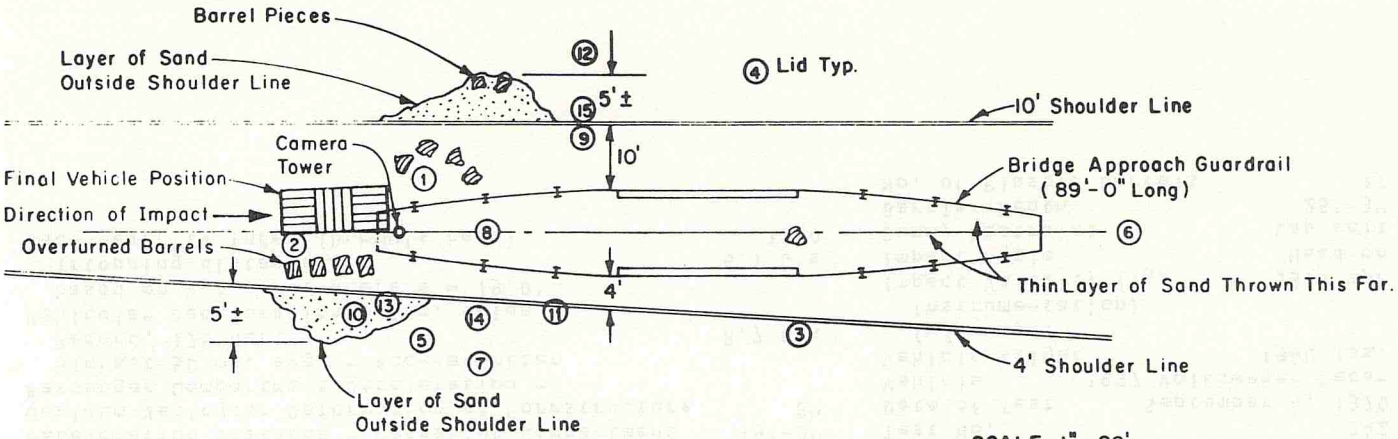

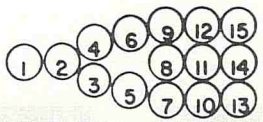

ORIGINAL BARREL CONFIGURATION & NUMBERS

DEBRIS LOCATION DIAGRAM
TEST 241

Figure 26.

Figure 27.

Impact + 0.022 Sec.

Impact + 0.163 Sec.

Impact + 0.586 Sec.

Impact + 4.536 Sec.

Deceleration Distance - Passenger Compartment	19'-0"
Maximum Vehicular Deformation at Forestructure	8"
Passenger Compartment Deceleration -	
Highest 50 ms. avg. - Accelerometer	8.7 G's
Record, 176 Hertz	
Vehicular Deceleration = Avg. value	
based on $V_o^2 = 2as$ where s = 19.0'	
(stopping distance)	6.1 G's
Gadd Severity Index (Dummy's head)	1280

Test No.	242
Date of Test	September 4, 1970
Vehicle	1957 Volkswagen Sedan
Vehicle Weight	1940 lbs.
(w/dummy &	
Instrumentation)	
Impact Velocity (V_o)	59.0 mph
Impact Angle	Head-on
Dummy Restraint	Lap belt
Barrier Depth	25'-3"
No. of Plastic Barrels	17

Figure 28.

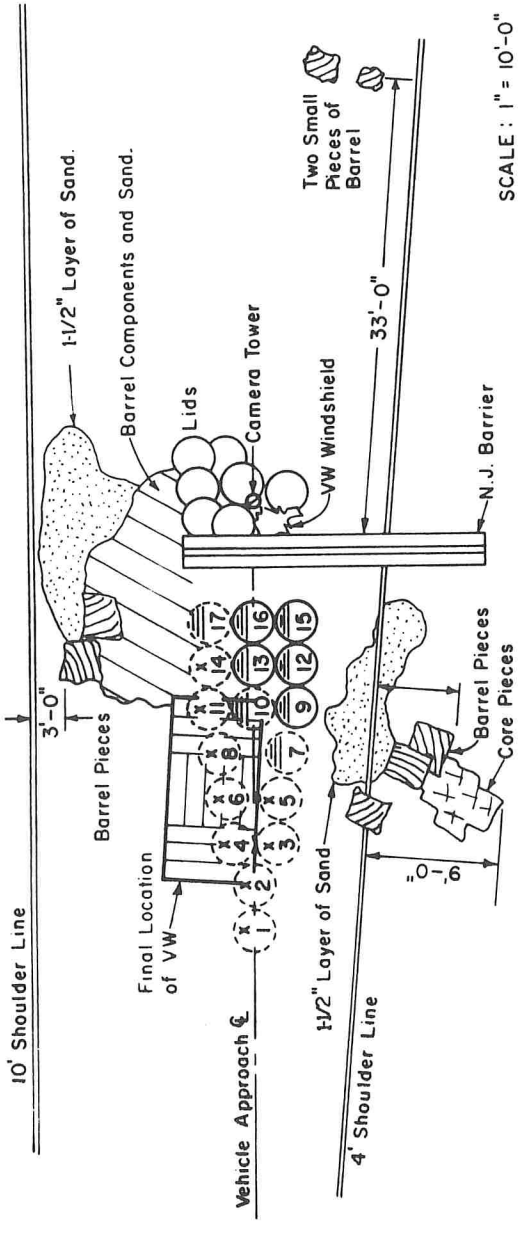

NOTES:

1. Barrels 9, 12, 13, 15, & 16 were all intact with lids on; two were slightly compressed. No. 16 was 9" from N.J. Barrier.
2. Barrels with an (π) were broken and thrown out of position.
3. All lids remained tied together.
4. Small number of core pieces under car.
5. All 4 wheels of VW on ground.
6. Barrels 7 & 10 were compressed but unbroken, lids were off.
7. Barrel 17 was compressed, unbroken, lid off, leaning against N.J. Barrier.

DEBRIS LOCATION DIAGRAM
TEST 242

Figure 29.

Impact + 0.012 Sec.

Impact + 0.180 Sec.

Impact + 0.348 Sec.

Impact + 8.880 Sec.

Deceleration Distance - Passenger Compartment	39'-0"	Test No.	243
Maximum Vehicular Deformation at Forestructure	1'-9"	Date of Test	September 24, 1970
Passenger Compartment Deceleration -		Vehicle	1968 Dodge
Highest 50 ms. avg. - accelerometer		Vehicle Weight	4770 lbs.
record, 176 Hertz	7.9 G's	(w/dummy &	
Vehicular Deceleration - Avg. value based		Instrumentation)	
on $V_o^2 = 2as$ where $s = 39'-0"$		Impact Velocity (V_o)	57 mph
(stopping distance)	2.8 G's	Impact Angle	15° nose
Gadd Severity Index (Dummy's head)	580	Dummy Restraint	Lap belt
		Barrier Depth	25'-3"
		No. of Plastic Barrels	17

Figure 30.

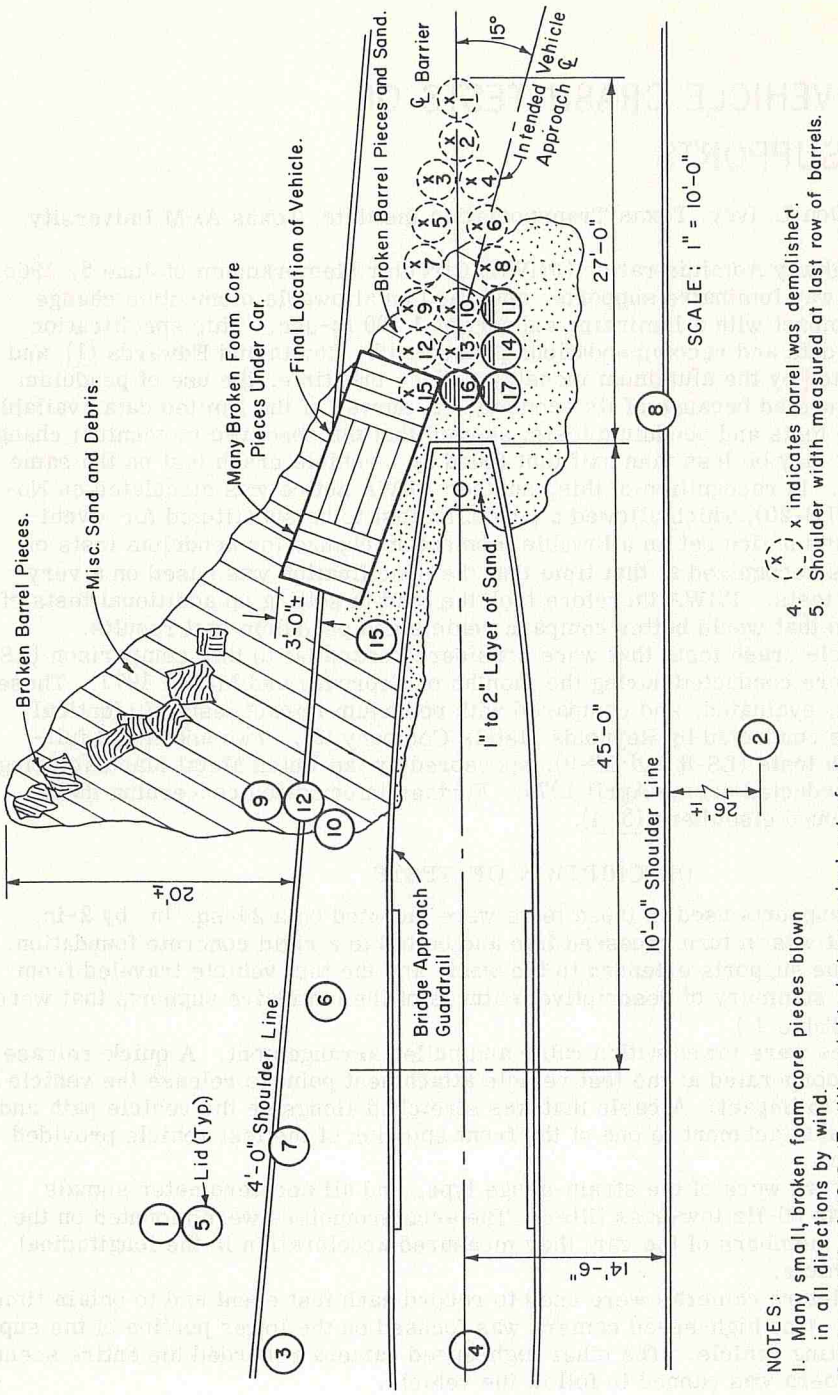

DEBRIS LOCATION DIAGRAM
TEST 243

FULL-SCALE VEHICLE CRASH TESTS OF LUMINAIRE SUPPORTS

Eugene Buth and Don L. Ivey, Texas Transportation Institute, Texas A&M University

•THE Federal Highway Administration (FHWA) Circular Memorandum of June 5, 1968, concerning breakaway luminaire supports, specified an allowable momentum change during a vehicle impact with a luminaire support of 1,100 lb-sec. This specification was derived from data and recommendations presented by Rowan and Edwards (1) and from tests conducted by the aluminum industry. Since that time, the use of pendulum tests has been requested because of its economy. A survey of the limited data available, comparing vehicle tests and pendulum tests, showed that the observed momentum change in a pendulum test may be less than half that found by a vehicle crash test on the same luminaire support. In recognition of this, another FHWA notice was circulated on November 16, 1970 (TO-20), which allowed a pendulum test to be substituted for a vehicle crash test. This notice set an allowable momentum change for pendulum tests of 400 lb-sec. It was recognized at that time that the specification was based on a very limited number of tests. FHWA therefore took the lead in setting up additional tests of luminaire supports that would better compare vehicle and pendulum test results.

The seven vehicle crash tests that were considered essential to this comparison (LS-1 through LS-7) were conducted during the months of February and March 1971. These tests are reported, evaluated, and compared with pendulum impact tests of identical luminaire supports conducted by Reynolds Metals Company (2). Two additional full-scale vehicle crash tests (LS-8 and LS-9), sponsored by the Union Metal Manufacturing Company, were conducted during April 1971. Further information concerning these nine tests can be found elsewhere (3, 4).

DESCRIPTION OF TESTS

The luminaire supports used in these tests were mounted on a 24-sq. in. by 2-in. thick baseplate that was in turn recessed into and bolted to a rigid concrete foundation. The mast arm of the supports extended to the west, and the test vehicle traveled from south to north. (A summary of descriptive features of the luminaire supports that were tested is given in Table 1.)

The test vehicles were towed with a cable and pulley arrangement. A quick-release mechanism was incorporated at the test vehicle attachment point to release the vehicle immediately prior to impact. A cable that was stretched alongside the vehicle path and threaded through an attachment to one of the front spindles of the test vehicle provided directional guidance.

All accelerometers were of the strain-gauge type, and all accelerometer signals were run through an 80-Hz low-pass filter. The accelerometers were mounted on the longitudinal frame members of the car; they measured acceleration in the longitudinal direction of the vehicle.

Three motion picture cameras were used to record each test event and to obtain time-displacement data. One high-speed camera was focused on the lower portion of the support and the impacting vehicle. The other high-speed camera recorded the entire scene. A documentary camera was panned to follow the vehicle.

Sponsored by Committee on Traffic Safety Barriers and Sign, Signal and Lighting Supports.

Table 1. Luminaire support characteristics.

Test No.	NEMA Test No.[a]	Pole Manufacturer	Aluminum Alloy and Temper		Support Height (ft)	Shaft Length (ft)	Shaft Wall Thickness (in.)	Shaft Base Diameter (in.)	Shaft Cap Diameter (in.)	Height Above Ground of Handhole Center[b] (ft)	Shoe Base Height (in.)
			Shaft	Base							
LS-1	3	Kerrigan	6063-T6	356-T6	35	32	0.250	8	4.5	1.2	3.5
LS-2	10	HAPCO	6063-T6	356-T6	40	37.2	0.250	10	6	1.5	5
LS-3	9	P&K	6063-T6	356-F	40	37.7	0.250	10	5.5	1.0	5
LS-4	10	HAPCO	6063-T6	356-T6	40	37.2	0.250	10	6	1.5	5
LS-5	4	P&K	6063-T6	356-F	40	37.7	0.188	10	5.5	1.0	5.5
LS-6	—	Kerrigan (HAPCO base)	6063-T6	356-T6	50.25	45.25	0.250	10	6	1.7	4[c]
LS-7	10	HAPCO	6063-T6	356-T6	40	37.2	0.250	10	6	1.5	5
LS-8	—	Union Metal	6063-T6		50	47.5	0.250	12	6.6	—	6
LS-9	—	Union Metal	Steel	Steel	45	38	11 gauge	9	5.1	—	—

[a]Ref. 2.
[b]Measurement was approximate; handhole was oriented opposite the impacted side of the pole.
[c]Four-inch shoe base was bolted to 6-in. pedestals.

Table 2. Test data.

Test No.	Vehicle	Vehicle Weight (lb)	Vehicle Residual Deformation (ft)	Film				Change in Momentum		Accelerometer Data		
				Initial Speed		Final Speed		High-Speed Film (lb-sec)	Accelerometer (lb-sec)	Maximum Deceleration (g)	Average Deceleration and Time	
				fps	mph	fps	mph				g	msec
LS-1	1963 Plymouth	3,600	1.6	58.5	39.9	49.6	33.8	990	960	10.3	3.8	70
LS-2	1963 Plymouth	3,550	1.5	58.1	39.6	47.3	32.2	1,190	1,280	13.4	5.0	72
LS-3	1963 Plymouth	3,750	1.8	59.4	40.5	46.9	32.0	1,420	1,390	10.4	5.6	68
LS-4	1963 Plymouth	3,590	1.3	61.6	42.0	52.0	35.5	1,070	1,070	9.8	4.4	68
LS-5	1963 Plymouth	3,650	1.3	60.1	41.0	54.9	37.5	590	680	6.4	2.0	92
LS-6	1963 Plymouth	3,620	1.3	59.6	40.6	52.3	35.7	820	710	5.0	2.6	75
LS-7	1957 Cadillac	5,050	1.2	60.9	41.5	51.9	35.4	1,410	1,330	9.8	4.4	60
LS-8	1963 Chevrolet	3,650	1.7	56.8	38.7	36.5	24.9	2,300	2,165	18.8	7.6	90
LS-9	1963 Chevrolet	3,710	0.3	59.0	40.2	55.5	37.8	405	425	5.4	1.9	42

1963 Plymouths were used in Tests LS-1 through LS-6, a 1957 Cadillac in Test LS-7, and 1963 Chevrolets in Tests LS-8 and LS-9. These vehicles were instrumented with accelerometers on the longitudinal frame members. A dummy, restrained by a strain-gauged seat belt to determine seat-belt forces, occupied the driver's seat in all of the tests except LS-8 and LS-9.

Eight of the luminaire supports tested were made of Alloy 6063-T6 aluminum with Alloy 356 cast aluminum shoe bases welded on. In Test LS-6, the support and base were mounted on 6-in. tall frangible pedestals. A 9-in. diameter steel luminaire support with a unidirectional slip base was tested in Test LS-9. This base incorporated three anchor bolt slots that were equally spaced on a $7\frac{5}{8}$-in. radius bolt circle and oriented in the same direction. The upper horizontal surface of the baseplate was sloped on a 1 to 6 slope in the area around each slot, and a matching wedge washer was used on each bolt. This arrangement allowed relief of the anchor bolt clamping force once the base began to slip. Each support was a single mast arm unit with an attached 50-lb weight to simulate the weight of a luminaire.

EXPERIMENTAL TEST RESULTS

A brief summary of the experimental data for each of the tests is given in Table 2. The behavior exhibited by each of the luminaire supports is as follows:

Test LS-1 (Figs. 1 and 2): The welds connecting the base to the pole fractured, and the entire pole was pulled from the base. The pole was completely fractured at the handhole, and the fragment from the lower end (about 18 in. long) was severely deformed. This failure mode differs from that exhibited in the NEMA pendulum test (2) of an identical support. In the pendulum test, the corners of the base were broken off, and the welds did not fail.

Test LS-2 (Figs. 3 and 4): The cast aluminum base as well as the pole itself were significantly damaged. The lower end of the pole below the handhole was broken off and dragged under the vehicle. Portions of the base remained attached to the pole segment. This mode of failure was very similar to the one in the NEMA pendulum test except that in the pendulum test the pole was not completely fractured at the handhole.

Test LS-3 (Figs. 5 and 6): The pole in this test was severely damaged although it was not completely fractured. The four corners of the base were broken off; the back two anchor bolts were bent, but the front two were not damaged. The pole scraped along the left side of the roof of the vehicle, which caused a minor deformation in the left rear area of the roof and broke the rear window. The failure modes in the vehicle crash test and NEMA pendulum test compare more closely for this support than for any other support tested.

Test LS-4 (Figs. 7 and 8): The luminaire support used in this test was identical to that used in Test LS-2, and the failure mode of the lower end of the support was very similar. However, in Test LS-4 the mast arm suffered significantly more damage than did the one in Test LS-2.

Test LS-5 (Figs. 9 and 10): No damage to the base resulted in this test. The pole was sheared adjacent to the top weld connecting it to the base. On the high-speed film, this shear failure was observed to be a progressive failure. The mast arm broke loose from the pole almost immediately, thereby reducing the mass of the portion of the luminaire support that was in contact with the vehicle. This failure mode differed significantly from that reported for the NEMA pendulum test. The pendulum test of this support resulted in a failure mode very similar to the vehicle in Test LS-3.

Test LS-6 (Figs. 11 and 12): The two pedestals on the approach side of the base failed at the manufactured "weak link" failure plane as anticipated, without causing bolt damage. Neither of the remaining two pedestals failed at the manufactured failure plane, and the anchor bolts on this side of the base were severely damaged. The base of the support contacted the right rear edge of the roof of the vehicle and slid down and along the right upper edge of the trunk compartment. This did not cause any glass breakage. No pendulum test results for a support using pedestals were available for comparison.

Figure 1. Luminaire support and vehicle after Test LS-1.

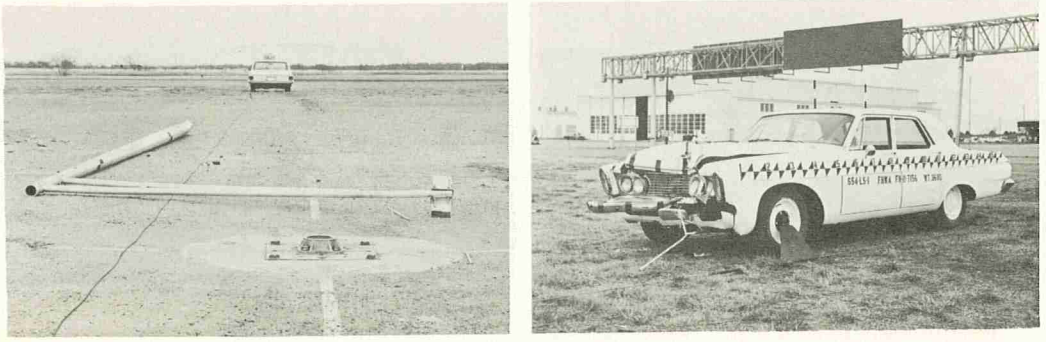

Figure 2. Final position of and damage to luminaire support, Test LS-1.

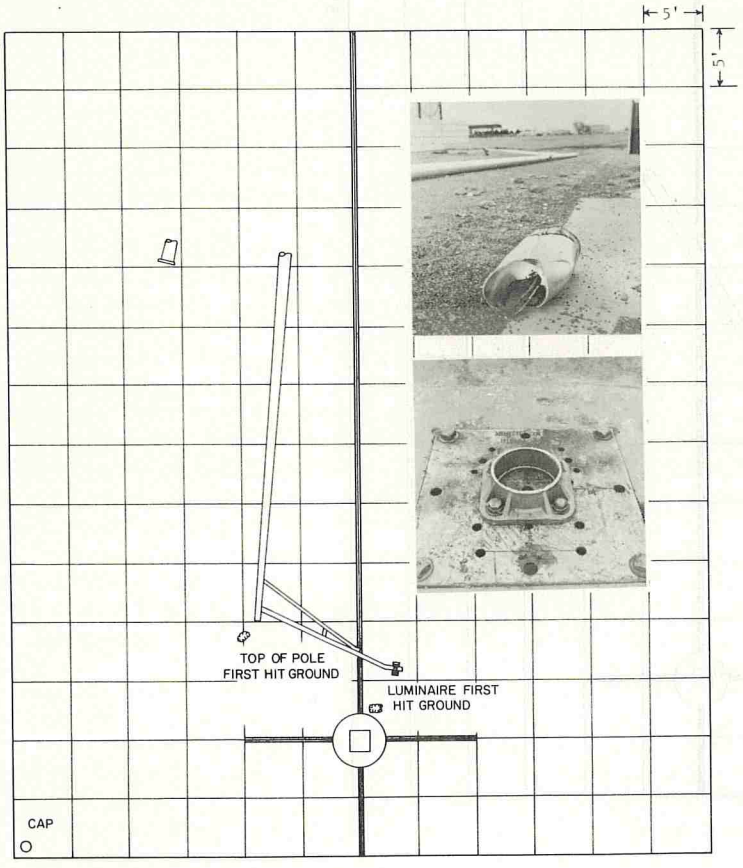

Figure 3. Luminaire support and vehicle after Test LS-2.

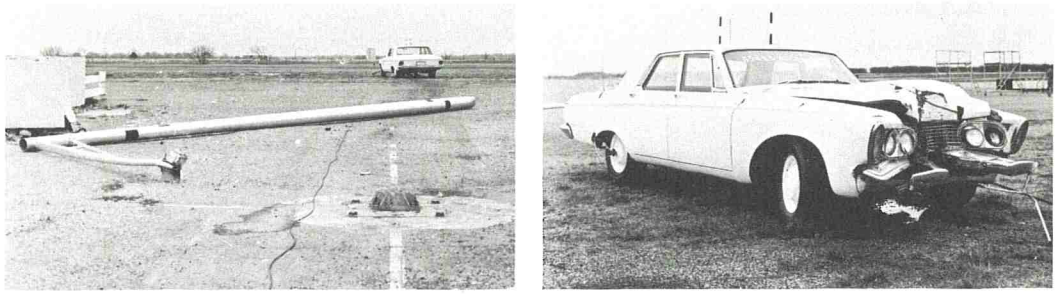

Figure 4. Final position of and damage to luminaire support, Test LS-2.

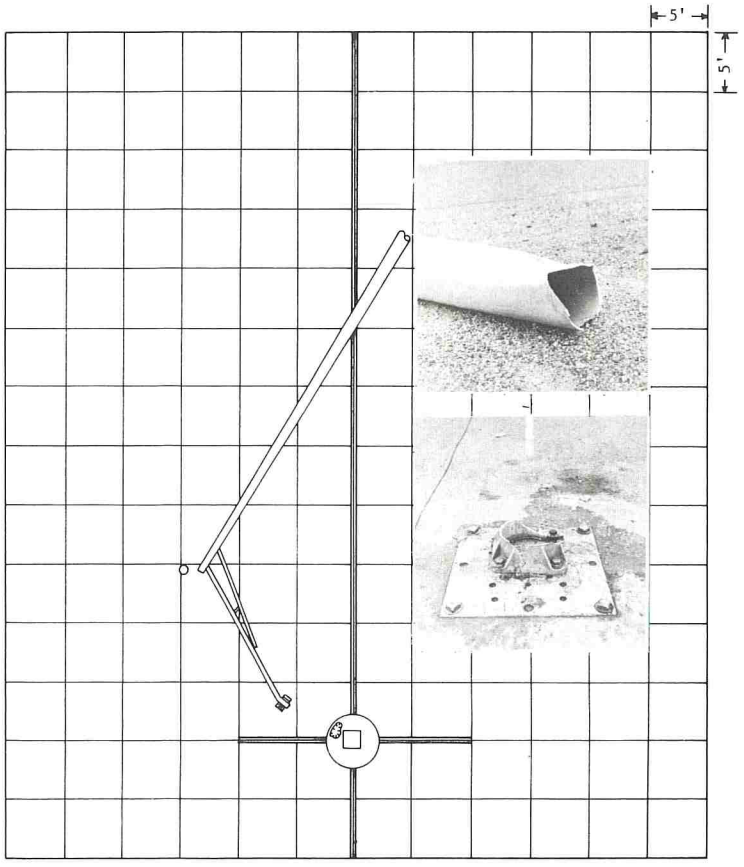

Figure 5. Luminaire support and vehicle after Test LS-3

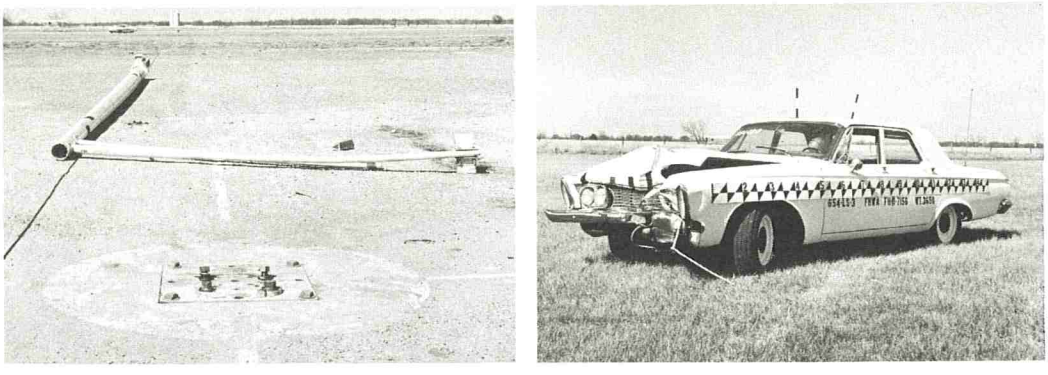

Figure 6. Final position of and damage to luminaire support, Test LS-3.

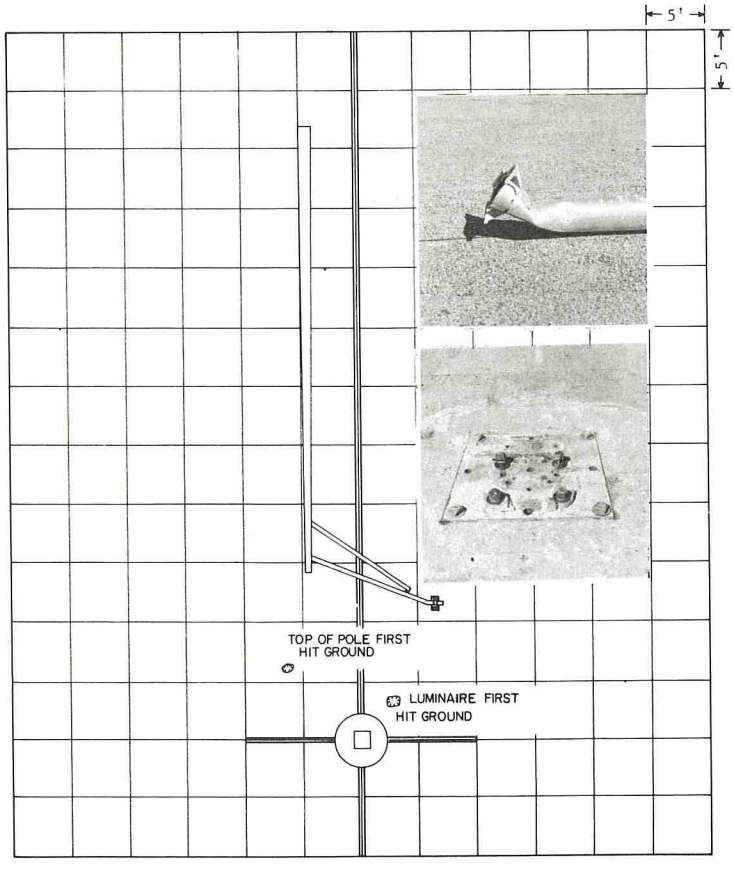

Figure 7. Luminaire support and vehicle after Test LS-4.

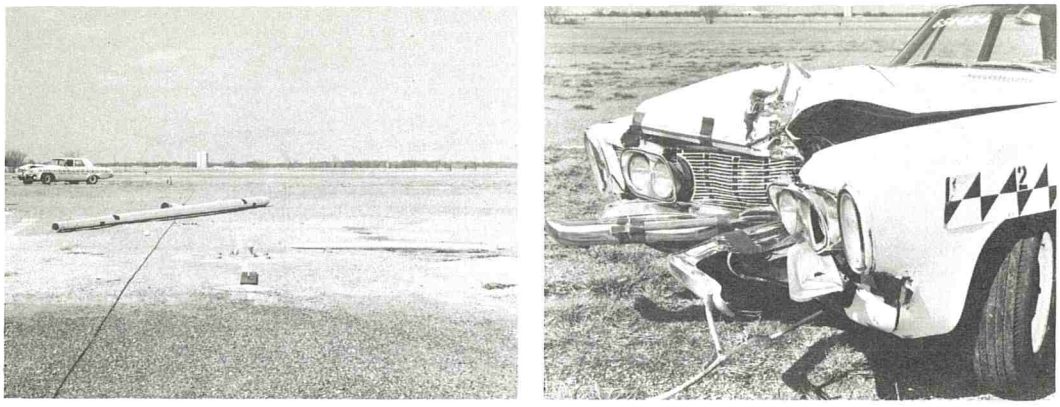

Figure 8. Final position of and damage to luminaire support, Test LS-4.

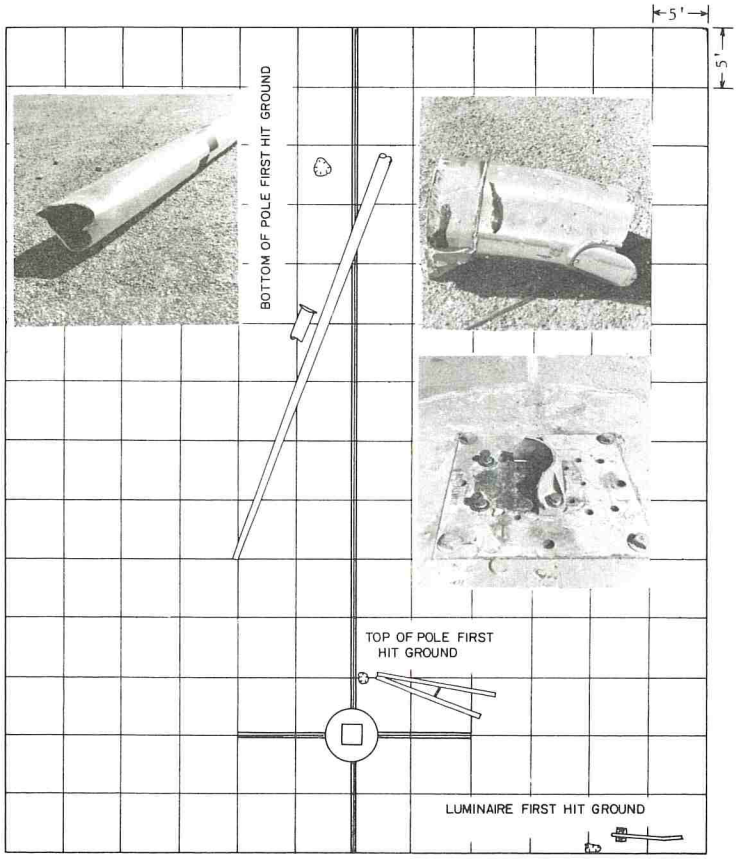

Figure 9. Luminaire support and vehicle after Test LS-5.

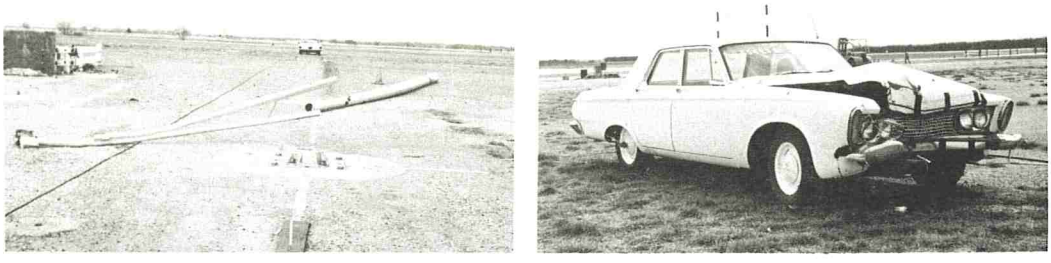

Figure 10. Final position of and damage to luminaire support, Test LS-5.

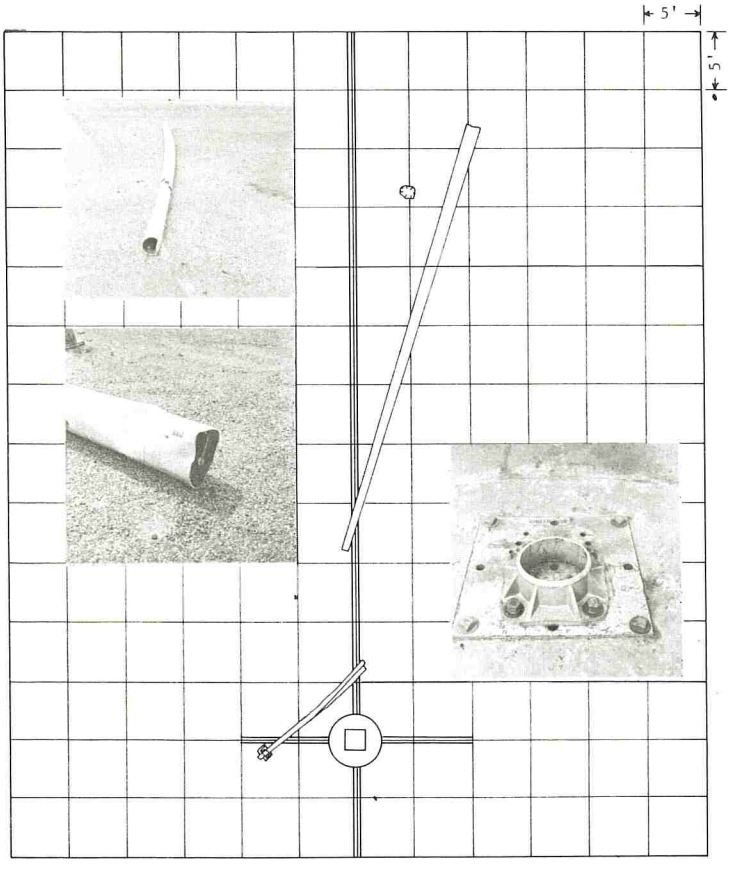

Figure 11. Luminaire support and vehicle after Test LS-6.

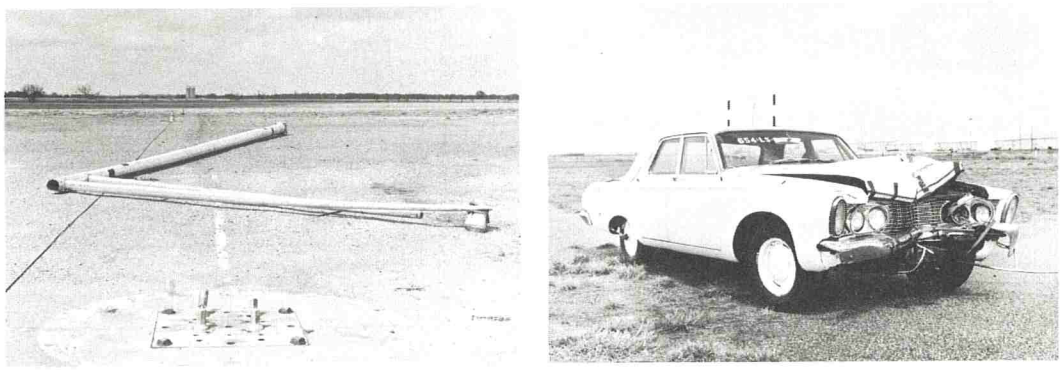

Figure 12. Final position of and damage to luminaire support, Test LS-6.

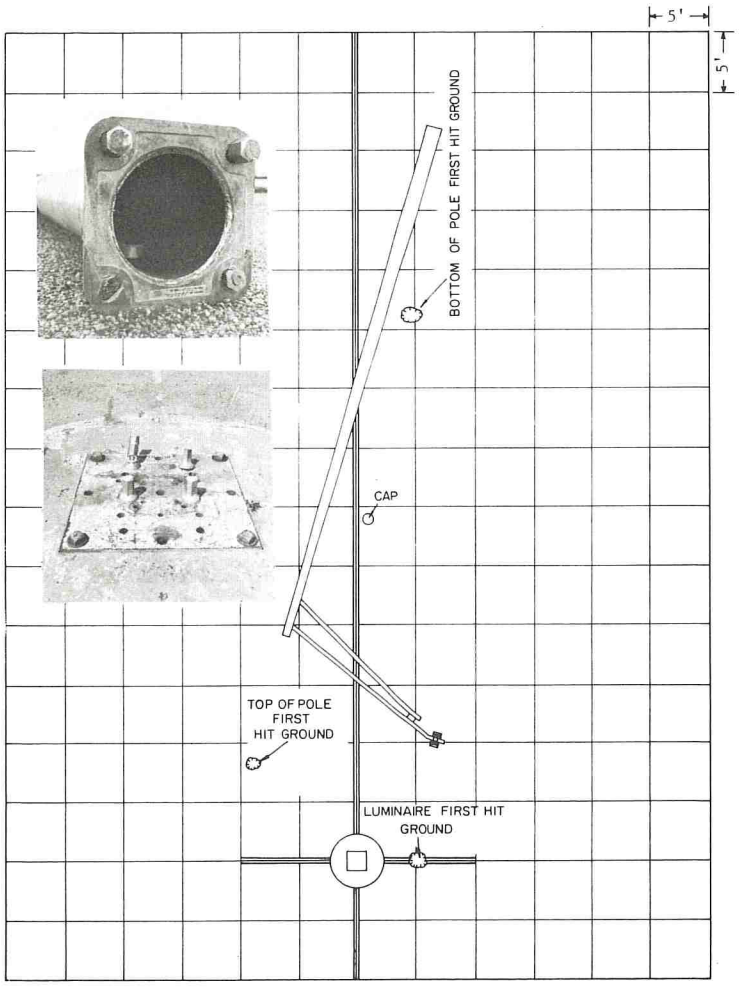

Test LS-7 (Figs. 13 and 14): A support identical to those used in Tests LS-2 and LS-4 was used in this test with a heavier vehicle. The failure mode exhibited here was not significantly different from the other two. A slightly larger portion of the base remained intact on the foundation and slightly more weld failure occurred.

Test LS-8 (Figs. 15 and 16): Pieces of the two front corners of the base were left in place, and a portion of the rear of the base remained on the pole. The remainder of the base was fragmented. The sides of the shoe base were forced through the space between the two rear bolts, which caused the rear bolts to bend both back and outward. The pole did not rotate and completely lose contact with the vehicle. It did reach a point at which it was only in contact with the deformed vehicle hood; then it hit the roof, cracked the front windshield, and shattered the rear window before disengaging the vehicle.

Test LS-9 (Figs. 17 and 18): The slip base on this pole became disengaged quickly, and the pole rotated up, which allowed the vehicle to pass under it with a relatively small change in speed. The slight vehicle damage and the momentum and speed change data attest to the "crashworthiness" of this support under the particular test conditions.

ANALYSIS OF TEST DATA

The values of momentum change that are given in Table 2 were calculated from high-speed film and accelerometer data. The close-up camera data were used to determine initial and final speed. Initial speed of the vehicle was calculated over a distance of about 4 ft prior to contact with the luminaire support. Final speed was calculated over a similar distance immediately after the vehicle lost contact with the luminaire support

Both the close-up and the overall views were used to estimate loss of contact. If the pole could still be seen on the close-up view at loss of contact, this view was used. Where the pole was not in view during close-up the overall view was used to determine loss of contact. By subtracting the "lost-contact" speed from the contact speed, we derived the change of speed during impact. The momentum change was found by multiplying the vehicle mass by this change in speed.

Momentum loss was also calculated by determining the speed change from the accelerometer traces. Integration of these accelerometer traces gives change in speed, which is again multiplied by vehicle mass to give change in momentum during the collision. Reasonable agreement was found between the two methods of determining change of momentum; but there is sufficient variation between the two methods that it is possible that in future testing some poles may pass a given specification by one data-analysis procedure and fail by the other. It would appear that tolerances, based on expected test variations, should be applied to the determination of specification compliance. However, the tests reported, the values obtained for momentum change using the two methods were either both below or both above the 1,100 lb-sec criterion. The maximum variation between the two momentum changes for a particular test was 125 lb-sec found in Test LS-8. The average difference in the two methods of analyzing the nine tests was 64 lb-sec, with seven of the nine showing a difference of 90 lb-sec or less.

SUMMARY OF RESULTS

A comparison of change in momentum values for the full-scale vehicle crash tests and the NEMA pendulum tests is shown in Figure 19. Change in momentum values for the Ohio, Illinois, and Maryland emergency call boxes (5) tested in an earlier phase of this study are also included in the figure. The ratio of pendulum-to-vehicle momentum changes of 400 to 1,100 lb-sec, which was implied in FHWA (TO-20), appears to be justified in four of the six tests compared, especially considering the natural variation to be expected in tests of this type. Tests LS-3 and LS-5 show the problems inherent in a specification that allows more than one test method. Test LS-3 was outside the FHWA criterion for both vehicle and pendulum tests as contrasted with Test LS-5, which was well below the criterion for vehicle tests and above the criterion for pendulum tests. Test LS-4 also was within the FHWA criterion for vehicle tests and outside it for pendulum tests.

Figure 13. Luminaire support and vehicle after Test LS-7.

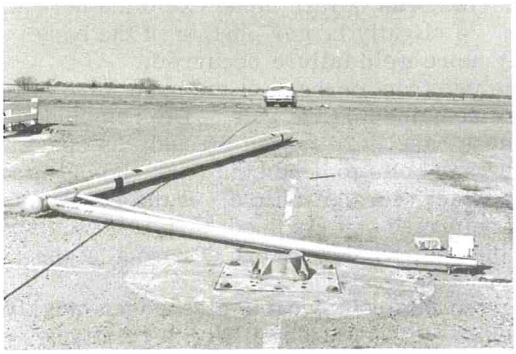

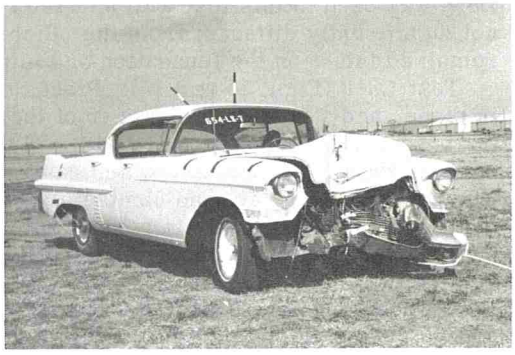

Figure 14. Final position of and damage to luminaire support, Test LS-7.

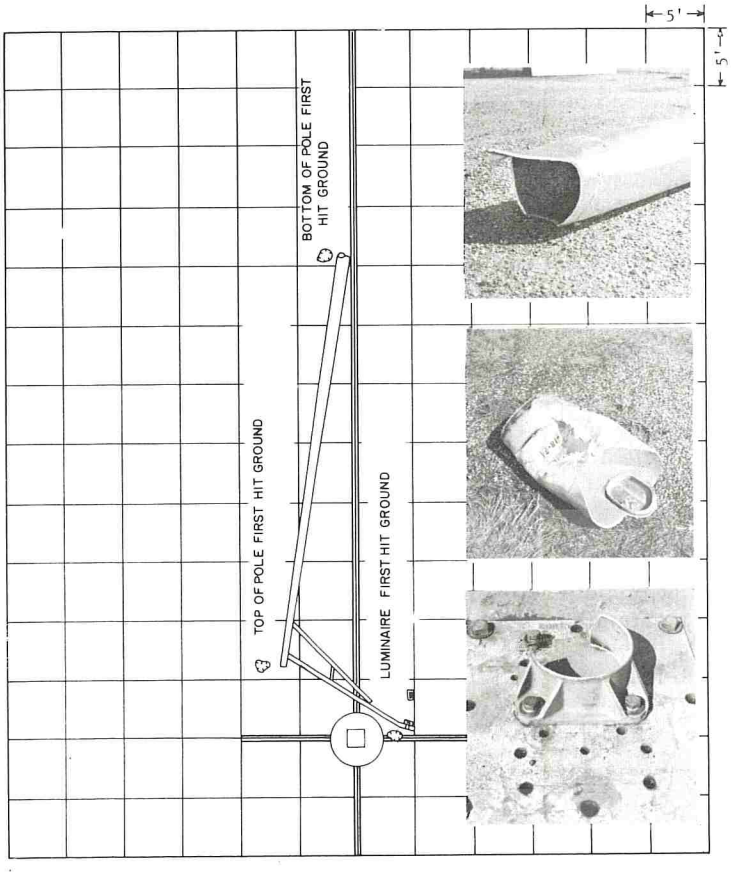

Figure 15. Luminaire support and vehicle test after Test LS-8.

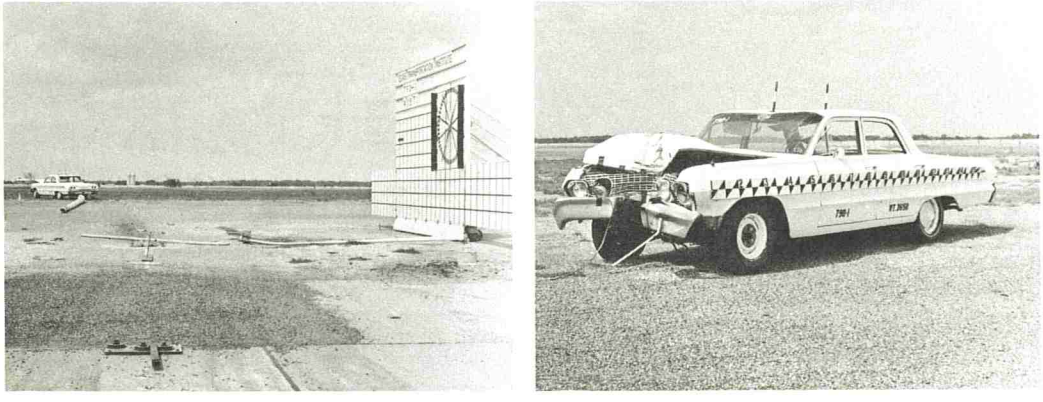

Figure 16. Final position of and damage to luminaire support, Test LS-8.

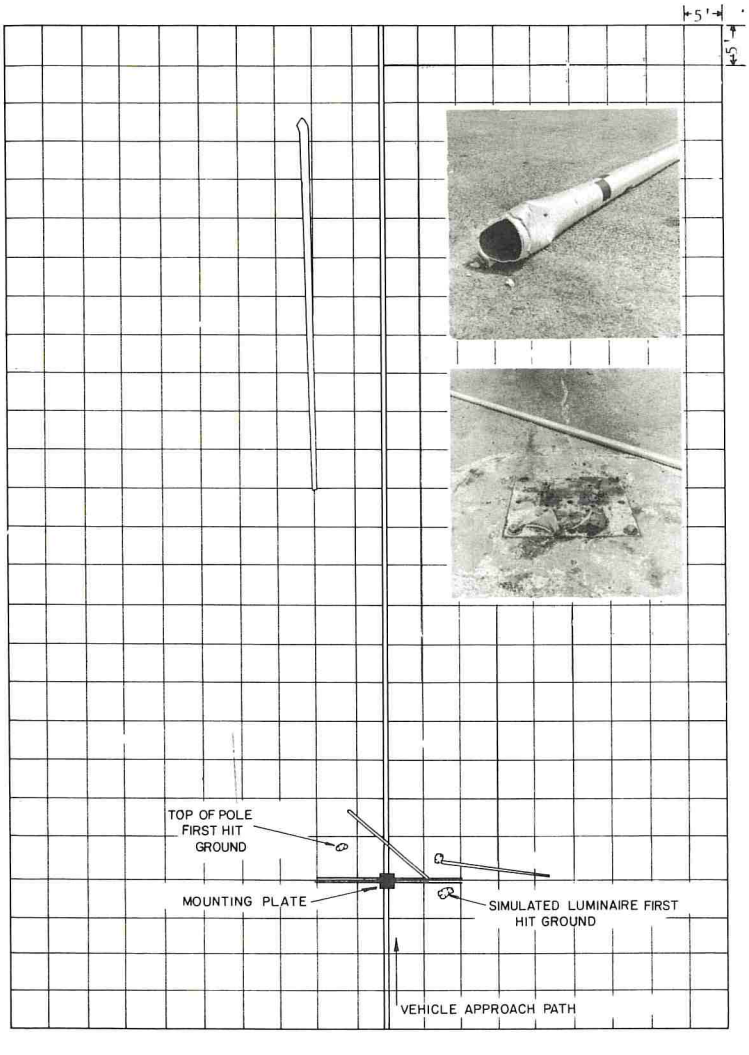

Figure 17. Luminaire support and vehicle after Test LS-9.

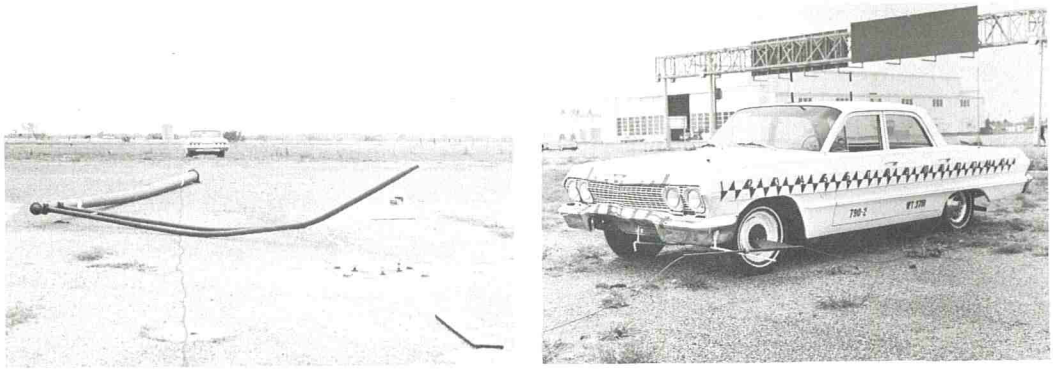

Figure 18. Final position of and damage to luminaire support, Test LS-9.

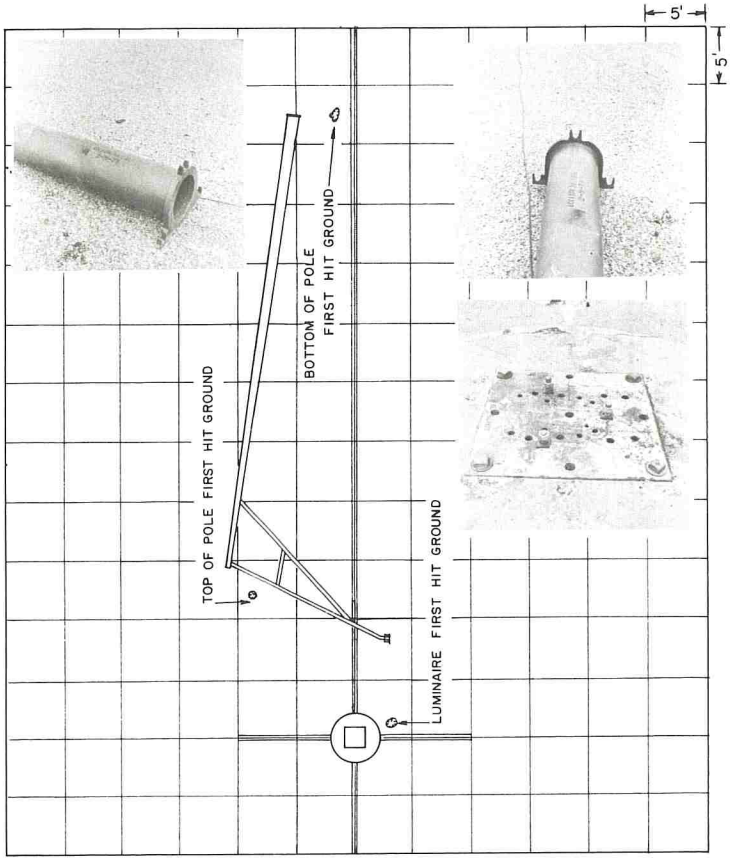

Figure 19. Comparison of momentum change in pendulum tests and full-scale vehicle tests.

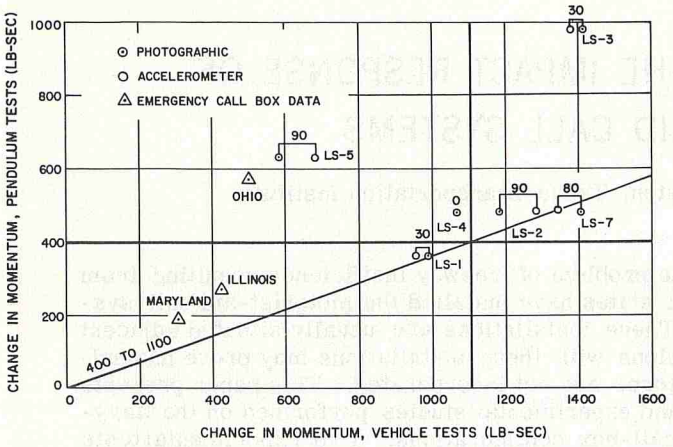

In an effort to give a gross indication of test-to-test variability, we conducted Tests LS-2, LS-4, and LS-7. The vehicles used in Tests LS-2 and LS-4 were the same make and model and resulted in differences in momentum changes of 120 lb-sec when using the photographic data reduction method and 210 lb-sec when using the accelerometer method. The impact speeds of these two tests differed by 2.4 mph. The significance of this variation in speed is unknown. Test LS-7 was conducted on the same luminaire support design, but a different make and model vehicle was used. The maximum difference (340 lb-sec), using the photographic data-reduction method, was between Tests LS-4 and LS-7. It is likely that this is a significant variation considering the magnitude of variations between tests of the same make vehicle. However, several replications would be necessary to make this a definite conclusion.

Because duplicate tests were not performed in the NEMA study by Hart (2), test-to-test variations under pendulum test conditions were not indicated. Because of the scatter of data, a definitive relationship between the results of the two tests does not appear probable. Different energy levels and velocities of the impacting mass would be expected to present the possibility of different failure modes and different values of change in momentum. Different failure modes between pendulum and vehicle tests were rather pronounced for the support used in Test LS-5. Probably the most influential complicating factor is the difference in crushability of contemporary vehicles and the pendulums in current use.

REFERENCES

1. Rowan, N.J., and Edwards, T.C. Impact Behavior of Luminaire Supports. Highway Research Record 222, 1968, pp. 20-41.
2. Hart, C.J. NEMA Impact Tests. Reynolds Metals Company, Project No. 49-805-8007, October 1969.
3. Buth, E., and Ivey, D.L. Full-Scale Vehicle Crash Tests of Luminaire Supports. Texas Transportation Institute, Texas A&M University, Technical Memorandum 654-4, April 1971.
4. Hayes, G.G. Vehicle Crash Tests of Luminaire Supports. Texas Transportation Institute, Texas A&M University, Technical Report 790, May 1971.
5. Martinez, J.E., and Buth, E. Safety Evaluation of Illinois, Ohio, and Maryland Emergency Call Boxes. Texas Transportation Institute, Texas A&M University, Technical Memorandums 654-1, 2, and 3, August 1971.

AN EVALUATION OF THE IMPACT RESPONSE OF VARIOUS MOTORIST-AID CALL SYSTEMS

J. E. Martinez and D. E. Hairston, Texas Transportation Institute, Texas A&M University

In an effort to alleviate the problem of freeway inefficiency resulting from disabled vehicles, several states have installed the motorist-aid call system on urban freeways. These installations are usually situated adjacent to the roadway, and collisions with these installations may prove hazardous if adequate safety features are not incorporated. This paper presents the findings of analytical and experimental studies performed on the Maryland, Illinois, and Ohio call-box configurations. Two experimental tests were conducted for each: a pendulum test and a full-scale crash test. A parameter study was carried out with the aid of a mathematical model verified by the full-scale crash tests. The study employed vehicle weights varying from 2,000 to 5,000 lb and impacting velocities ranging from 20 to 60 mph. The most significant findings of the study may be summarized as follows: (a) The vehicle velocity and momentum changes due to the collision were considerably less than the established tolerable limits to 11 mph and 1,100 lb-sec; (b) vehicle damage was minor; (c) call-box damage is usually severe, and the unit generally has to be completely replaced after a collision; and (d) detachment of call-box assembly components during a collision may produce a hazardous condition.

•THE motorist-aid call system has been installed on some urban freeways in an effort to aid the problem of freeway inefficiency resulting from disabled vehicles and also to serve as a convenience to distressed motorists. Typical installations have the call boxes spaced at approximately ¼-mile intervals on each shoulder and in each direction of travel so that a motorist is not required to cross main lane traffic to place a call.

Because these installations are usually situated next to the roadway, collisions with these installations may be hazardous to the motorist if adequate safety features are not incorporated in the call system design. For example, a nonfrangible base attachment could cause large vehicular deceleration rates and possible injury to the occupants. Also, a call box improperly secured to the support post could come loose after impact and go through the windshield of the impacting vehicle. In addition, the dynamic characteristics of the call box may be such that, upon impact, the entire system rotates and strikes the vehicle compartment in the area of the windshield. Besides the safety considerations, aesthetics and initial and replacement costs of the installation must be duly considered.

This paper presents the results of three full-scale vehicle crash tests, pendulum impact tests, and parameter studies conducted with the aid of a mathematical model. The findings are for call-box installations proposed for use by Illinois, Maryland, and Ohio.

Sponsored by Committee on Traffic Safety Barriers and Sign, Signal and Lighting Supports.

DESCRIPTIONS OF INSTALLATIONS

Illinois System

The Illinois installation consists of a support post made of 5-in. diameter aluminum tubing with ¼-in. thick walls. Two aluminum signs, 3 ft square and 0.08 in. thick each, are bolted to the top as shown in Figure 1, and the cast aluminum base is welded to the support post. The terminal enclosure, also made of cast aluminum, is clamped to the support with steel bands. The entire assembly is approximately 13 ft high (Fig. 1).

Maryland System

The Maryland installation consists of a support post made from 3-in. diameter aluminum tubing with ¼-in. thick walls. The base of the post is composed of a 10-in. square aluminum plate with a thickness of 1 in. and gusseted with 4⅜-in. thick plates. The terminal enclosure (call box) is clamped to the support post by means of two bolts and a steel band, and the antenna is connected to the top of the support post by a friction joint. The structure is more than 18 ft high (Fig. 2).

Ohio System

The Ohio installation consists of a hollow rectangular support post made of steel that has a cast metal base. The terminal enclosure is fixed to the top of the support post, and the assembly is bolted to a concrete foundation by means of four anchor bolts. The structure is approximately 5½ ft high (Fig. 3).

COMPUTER SIMULATION

Each call-box assembly was idealized as a rigid body possessing three degrees of freedom: two translational and one angular. The assumptions are that the call-box assembly undergoes rigid-body planar motion after being struck by a vehicle, and that the vehicle behaves as a single-degree-of-freedom spring-mass system. This type of vehicular representation has produced satisfactory results in the analysis of roadside signs (1), luminaire supports (2), and overhead sign bridge structures (3). It is recognized that the planar motion assumption is not correct for off-center collisions on the structures under consideration; however, the analysis presented here is directed to central impacts and small vehicular approach angles. Under these circumstances the model should yield a satisfactory phenomenological behavior for the dynamic response of the structure and the vehicle.

The computer program established for the structural and vehicular response solved the equations of motion numerically and required knowledge of the structural geometric and inertia properties and the vehicular mass and geometry. Further, the base resistive-force variation for the structure was required and was obtained from the pendulum test data.

The output information from the computer program consists of the vehicular displacements and velocities and displacements of selected points of the call-box assembly. These values are printed at specified time intervals and also when (a) the base is fractured, (b) the support post loses contact with the vehicle, or (c) the call-box assembly either strikes the ground or recontacts the vehicle. The program automatically terminates when the third condition is met.

EXPERIMENTAL EVALUATION

Pendulum Tests

The pendulum tests were conducted to provide information for the computer simulation. The pendulum consisted of a 1,000-lb concrete-filled cylinder supported by four cables as shown in Figure 4a. These cables supported the ram in such a manner that upon release the ram swung as a pendulum from a height of approximately 15 ft and contacted the call-box support at a distance approximately 1½ ft from the bottom, the

Figure 1. Illinois call-box assembly.

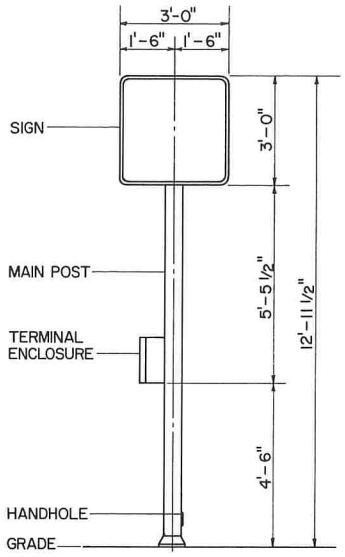

Figure 2. Maryland call-box assembly.

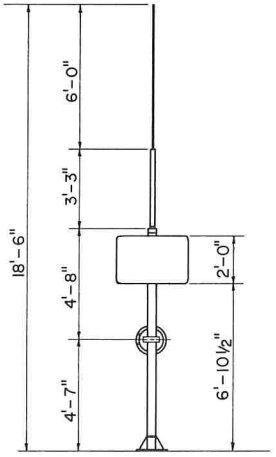

Figure 3. Ohio call-box assembly.

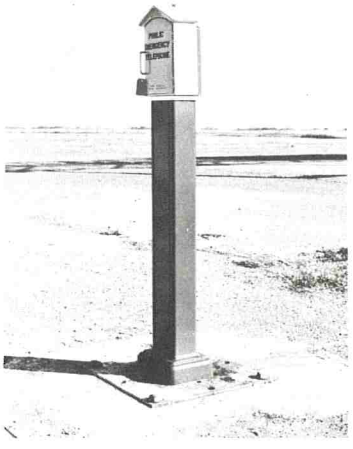

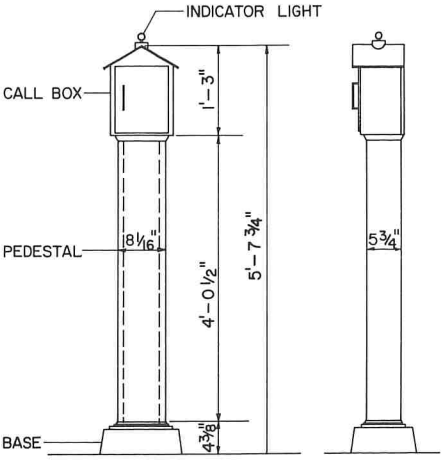

Figure 4. Maryland call-box assembly pendulum test.

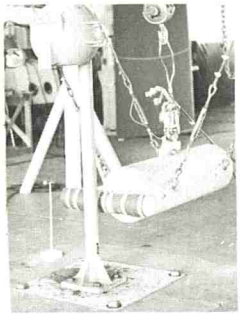

a. Impacting Ram

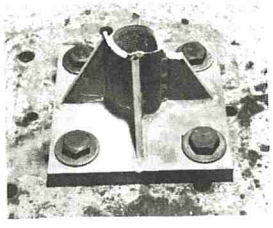

b. Results of test

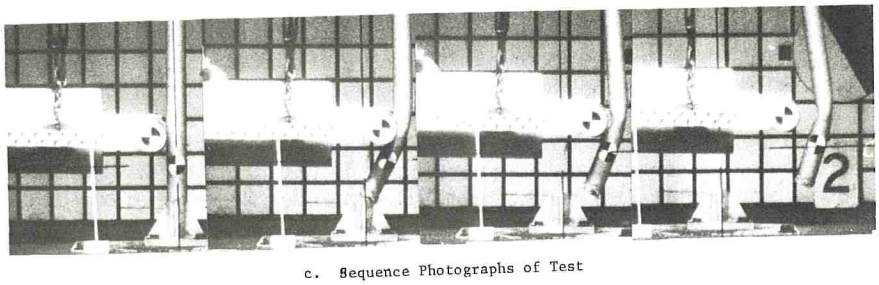

c. Sequence Photographs of Test

Table 1. Comparison of model and crash test results.

Test	Vehicle Weight (lb)	Velocity (mph) Initial	Change	Time to Fracture Base (sec)	Post Contact With Vehicle Roof: Time (sec)	Vehicle Translation (ft)	Post Rotation (deg)	Comment
Maryland Crash	2,870	43.2	2.3	0.039	0.192	11.6	81	Post contacts roof above windshield with point 10.8 ft from top of assembly.
Model	2,870	43.2	2.4	0.029	0.191	11.5	78	Post contacts roof above windshield with point 10.5 ft from top of assembly.
Illinois Crash	2,870	41.2	3.2	0.038	0.363			Post contacts left rear edge of roof as shown in Figure 5 after 0.363 sec.
Model	2,870	41.2	3.6	0.042	0.289			Post contacts roof 2.5 ft forward of rear window after 0.289 sec.
Ohio Crash	2,840	41.1	3.90	0.059				
Model	2,840	41.1	3.83	0.057				Post rides front end of vehicle rotating slightly toward the vehicle, then drops and hits ground in front of vehicle.

normal bumper height for most vehicles. The purpose of the tests was to supply base force-deformation data that could be used to simulate a vehicle crash test.

The instrumentation employed to obtain the test data consisted of an accelerometer attached to the back end of the impacting ram and a high-speed camera that photographed the test from a direction perpendicular to the plan of ram travel. Selected sequential photographs obtained with this camera for the test of the Maryland system are shown in Figure 4c. Figure 4b shows the results of the test and clearly indicates the mode of failure of the base. The pendulum tests have always provided valuable information concerning the force-deformation characteristics of a structure.

Vehicle Crash Tests

To evaluate the computer simulation, we conducted full-scale vehicle crash tests for each call-box assembly. The impact on each support was head on, and contact was made at the center of the front end of the vehicle. Figure 5 shows sequence photographs of the crash tests, and Table 1 gives a summary of model and crash test results.

Each vehicle was instrumented with two strain-gauge accelerometers, one on each longitudinal frame member, to measure longitudinal decelerations. In addition, a mechanical impact-o-graph was mounted in the vehicle trunk as a secondary source of acceleration data. An Alderson anthropometric dummy secured by a seat belt simulated the driver. The seat-belt assembly included a load cell that measured the seat-belt force. Two high-speed cameras, aligned perpendicular to the direction of vehicle travel, were used to obtain the photographic data. Documentary low-speed cameras provided additional test coverage.

Illinois Call-Box Crash Test

Figure 5a shows sequence photographs of the crash test that indicates that the motion of the assembly was not planar because the assembly rotated not only about an axis perpendicular to the vertical plane containing the path of the vehicle but also about its own longitudinal axis. This phenomenon permits the assembly to remain in the air longer and moves the point of secondary impact toward the rear of the vehicle. From this figure it can also be noted that the component parts of the assembly did not become detached during the collision; however, it should be emphasized that the collision occurred at a speed of 40 mph. At higher speeds some of the component parts can become detached if they are not properly secured.

Figure 6a shows the remains of the base after the crash test and clearly indicates that three of the anchor bolts were fractured. A similar failure mode was observed in the pendulum test. The shaft of the assembly was not severely bent. The vehicle damage was slight and the vehicular velocity, momentum, and deceleration changes encountered during the collision were quite low and should not prove hazardous to vehicle occupants experiencing a similar collision.

Maryland Call-Box Crash Test

Figure 5b shows that the call-box door was detached as a result of the impact but did not strike the windshield area of the vehicle. Figure 6b shows the base after the test and indicates its mode of failure. The anchor bolts, in this case, were not damaged. A similar failure mode had been observed in the pendulum test.

The vehicle damage was minor and the vehicular velocity, momentum, and deceleration changes encountered during the collision were again quite low. Individual parts of the assembly could become detached during a collision, which would create a hazard for vehicle occupants.

Ohio Call-Box Crash Tests

Figure 5c shows that the call box became detached from the support post during the collision but did not strike the vehicle. The assembly translated in the direction of the impact and rotated away from the vehicle because of the relatively low center of mass of the assembly produced by the detachment of the call box. If the call box had not become detached, the assembly could have rotated toward the vehicle.

Figure 5. Sequence photographs of crash tests.

a. Illinois

b. Maryland

c. Ohio

Figure 6. Crash test results.

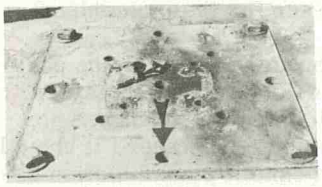

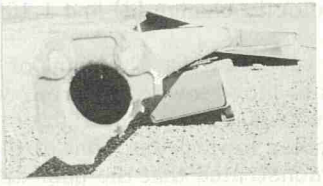

a. Illinois

b. Maryland

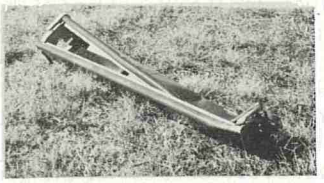

c. Ohio

The support post, in this case, was severly damaged. The four anchor bolts of the base were severely damaged and would require replacement or extensive repair work (Fig. 6c).

The vehicle damage was again minor and, as in the previous tests, the vehicular velocity, momentum, and deceleration changes were well within tolerable limits.

CORRELATION OF MATHEMATICAL MODEL AND CRASH TEST RESULTS

From the values given in Table 1, it is apparent that the agreement between the mathematical model and the crash tests is quite good. Although the tests revealed that the support post is deformed significantly even though the model precludes this effect, the overall behavior of the assembly is satisfactorily represented by the model.

The agreement in the vehicular velocity changes and deceleration rates was excellent considering the degree of approximation that was used in the vehicle idealization. Thus, based on these findings, the parameter study presented in the next section was performed with the aid of the mathematical model.

PARAMETER STUDY

Based on the mathematical model verified by the full-scale crash tests, a parameter study was conducted to obtain the response of the assemblies and the impacting vehicle for a variety of cases. The study employed vehicles weighing from 2,000 to 5,000 lb and considered impacting speeds of 20, 40, and 60 mph. The results obtained for 2,000- and 5,000-lb vehicles are shown in Figures 7 and 8.

The findings of the study reveal that, for all the cases considered, the vehicular velocity changes, deceleration rates, and momentum changes are quite low and always remain well below the limits that have been suggested as being tolerable. These limits are 11 mph for the vehicular velocity change (4) and 1,100 lb-sec for the momentum change (5).

The Illinois assembly study revealed that the point of secondary impact by the post on the roof of the vehicle tends to move toward the rear windshield area as the speed and weight of the vehicle are increased. For the lighter vehicles, the tendency is for the post to strike somewhat further toward the front of the vehicle. However, it should be noted that the crash test demonstrated that the post did not exhibit planar motion because a rotation about its longitudinal axis took place. If this occurs in all cases, the simulation would normally predict shorter secondary impact times and a secondary impact point that is closer to the front of the vehicle. Thus, for this assembly, it appears that unless the assembly strikes the rear windshield of the vehicle, the secondary impact will not create a hazardous situation.

Figures 7b and 8b indicate that the Maryland call-box assembly behaves similarly to the Illinois assembly (Figs. 7a and 8a). The point of secondary impact by the post on the top of the vehicle tends to move toward the rear windshield area as the speed of the heavier vehicle is increased and strikes above the front windshield area for most lightweight vehicles traveling at low and medium speeds. Thus, it appears that, for the vehicles and speeds considered, a collision with a Maryland call-box assembly does not create a hazardous situation. However, due regard must be given to the possibility of component parts of the assembly becoming detached during the collision and striking the windshield of the vehicle.

Two systems, one of which included the properties of the call box, were considered for the Ohio call-box configuration; this simulated the condition observed in the crash test. The two systems behaved in a very similar manner for all the cases considered. As shown in Figures 7c and 8c, the call-box system rides the vehicle front end, rotates slightly toward the vehicle, and then drops to the ground in front of the vehicle. The system that contains the effects of the mass of the call box shows a stronger tendency to rotate toward the vehicle; however, because of the geometric and inertia properties of the assembly, it does not appear that the trajectory would be appreciably changed under actual field conditions. Thus, based on the parameter study and observation of the crash test, it appears that a hazardous situation is not created unless component

Figure 7. Parameter study results for 2,000-lb vehicle.

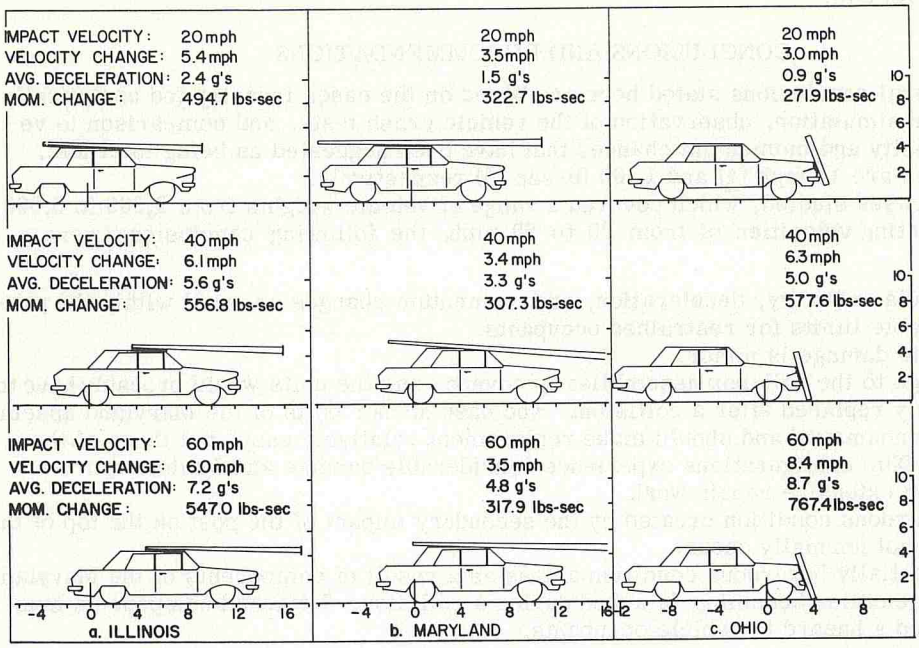

Figure 8. Parameter study results for 5,000-lb vehicle.

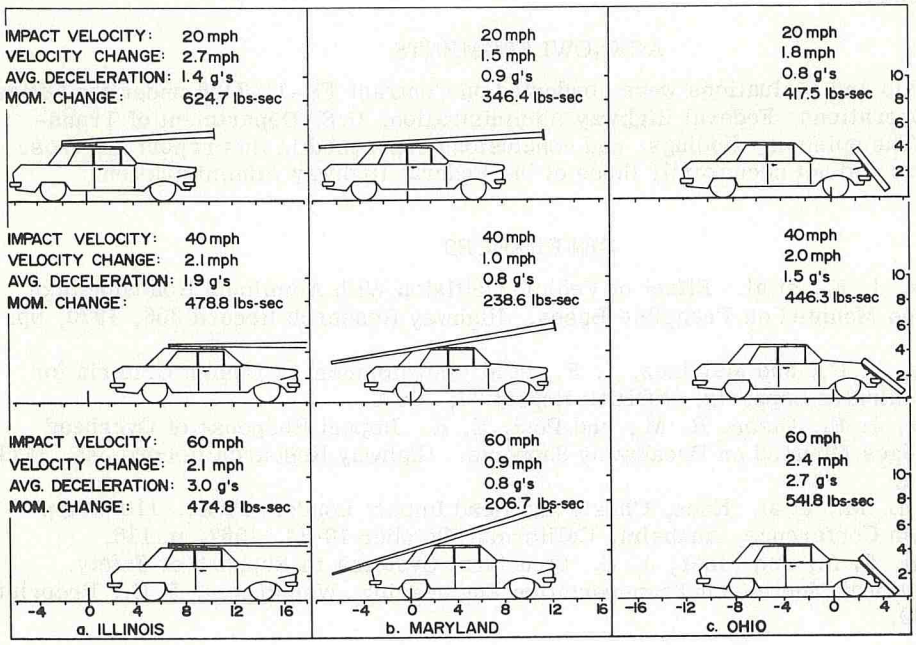

parts of this assembly become detached during the collision and strike the windshield area of the vehicle.

CONCLUSIONS AND RECOMMENDATIONS

The general conclusions stated here are based on the cases investigated analytically by computer simulation, observation of the vehicle crash tests, and comparison to vehicular velocity and momentum changes that have been suggested as being tolerable. These values are 11 mph (4) and 1,100 lb-sec (5) respectively.

For the cases studied, which covered a range of vehicle weights from 2,000 to 5,000 lb and impacting velocities of from 20 to 60 mph, the following conclusions were reached:

1. Vehicular velocity, deceleration, and momentum changes are well within the published tolerable limits for restrained occupants.
2. Vehicle damage is minor.
3. Damage to the call-box assemblies is severe, and the units would probably have to be completely replaced after a collision. The base anchor bolts of the Maryland assembly remain undamaged and should make replacement relatively easy, but those of the Illinois and Ohio configurations experience considerable damage and would require replacement or extensive repair work.
4. A hazardous condition created by the secondary impact of the post on the top of the vehicle will not normally occur.
5. A potentially hazardous condition arises as a result of components of the Maryland and Ohio assemblies becoming detached during a collision. Detached components must be considered a hazard to vehicle occupants.

It is recommended that the component parts of the call-box assemblies be adequately secured so that they will not become detached during a collision. In particular, the attachments of the call box to the support post and the hinges of the call-box door should be strengthened.

ACKNOWLEDGMENTS

These tests and evaluations were conducted on Contract FH-11-7156 under the Office of Traffic Operations, Federal Highway Administration, U.S. Department of Transportation. The opinions, findings, and conclusions expressed in this report are those of the authors and not necessarily those of the Federal Highway Administration.

REFERENCES

1. Martinez, J. E., et al. Effect of Vehicle Collision With Aluminum Roadside Sign Structures Mounted on Frangible Bases. Highway Research Record 306, 1970, pp. 58-70.
2. Edwards, T. C., and Martinez, J. E., et al. Development of Design Criteria for Safer Luminaire Supports. NCHRP Report 77, 1969.
3. Martinez, J. E., Olson, R. M., and Post, E. R. Impact Response of Overhead Sign Bridges Mounted on Breakaway Supports. Highway Research Record 346, 1971, pp. 23-34.
4. Patrick, L. M., et al. Knee, Chest, and Head Impact Loads. Proc., 11th Stapp Car Crash Conference, Anaheim, California, October 10-11, 1967, p. 116.
5. Tamanini, F. J., and Viner, J. G. Structural Systems in Support of Safety. ASCE National Meeting on Transportation Engineering, Washington, D.C., Preprint 930, 1969.

EVALUATION OF A NEW GUARDRAIL TERMINAL

M. E. Bronstad and J. D. Michie, Southwest Research Institute

ABRIDGMENT

•UPSTREAM guardrail terminals have been identified as roadside hazards. Ramped terminals have launched errant vehicles while beams terminated with straight sections have speared passenger compartments.

A promising guardrail terminal (Fig. 1) for the G4S or G4W (1) barrier was evaluated by full-scale crash tests. This terminal develops effective redirective properties of the barrier for angle impacts occurring downstream from the end span, yet it will safely break away for direct impact. Principal features of the concept are the (a) anchor-cable-to-end post detail and (b) beam end design. As shown in Figure 1, the cable, which develops adequate beam tensile strength, is attached through a hole in the end post, which is set in concrete. This hole, located near grade level, weakens the post in flexure and shear for forces applied above the hole. Hence, when a vehicle strikes the post, it breaks at the hole; this releases the cable and thus greatly diminishes spearing forces that can develop in the beam. In addition, the beam is ended by a special 11-in. radius bend that is stiffened with a steel diaphragm or lighweight concrete and that serves as a "load spreader" to further reduce the possibility of beam-spearing during direct-on hits. For downstream impacts, forces are introduced to the end post via the anchor cable. For these cases, the hole has no adverse effect on the post strength, and the cable forces are transmitted through the post to the foundation. Principles of the concept and component functions are summarized in Table 1.

In the test program, three full-scale crash tests were conducted. All guardrail installations were basically the G4W system anchored by the breakaway cable terminal. The test series is summarized in Table 2; sequential test events are shown in Figure 2.

Test results are compared to terminal design purpose and service requirements in Table 3. In general, the design was considered to be quite promising. Terminal performance for end-on impacts indicated a need for "softening" the longitudinal stiffness of the beam. With this single improvement, the breakaway cable terminal should prove to be a safe, economical solution to the W-beam guardrail terminal problem.

ACKNOWLEDGMENT

The work discussed in this report was sponsored by the American Association of State Highway Officials in cooperation with the Federal Highway Administration. The effort was conducted as a part of a National Cooperative Highway Research Program, which is administered by the Highway Research Board of the National Academy of Sciences-National Research Council. The opinions, findings, and conclusions expressed in this paper are those of the authors and not necessarily those of the sponsoring agencies.

REFERENCE

1. Michie, J. D., and Bronstad, M. E. Location, Selection, and Maintenance of Highway Traffic Barriers. NCHRP Rept. 118, 1971.

Sponsored by Committee on Traffic Safety Barriers and Sign, Signal and Lighting Supports.

Figure 1. Breakaway cable terminal details.

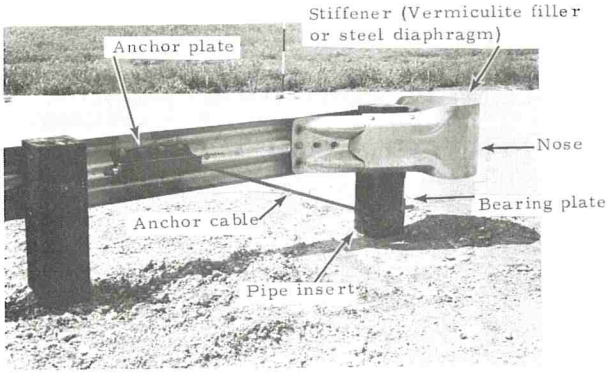

Figure 2. Test series sequence of events.

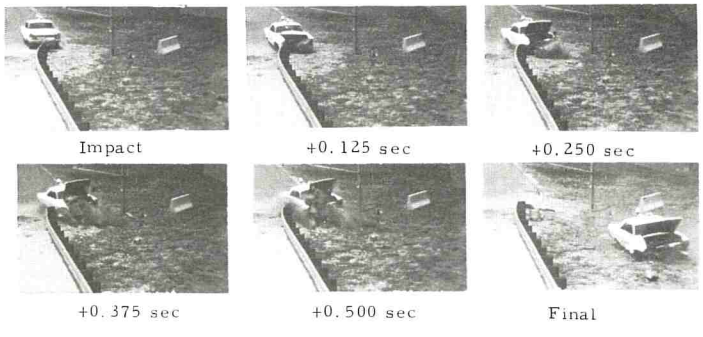

(a) Test 130

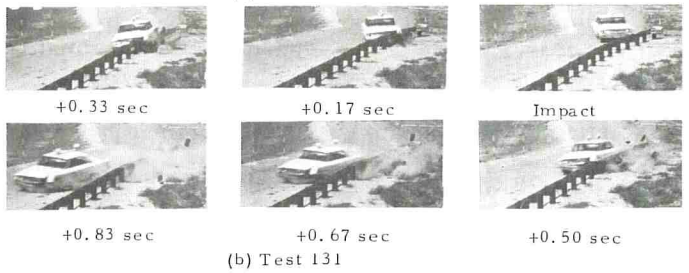

(b) Test 131

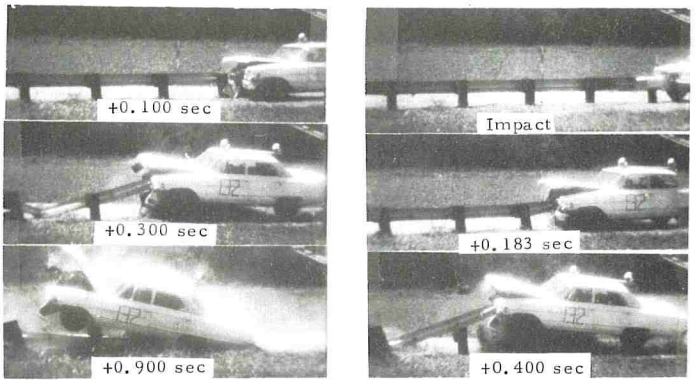

(c) Test 132

Table 1. Breakaway cable terminal.

Component	Design Function	
	End-On Impacts	Downstream Impacts
End post	Post breaks away at bored hole, releasing cable, thus minimizing spearing forces.	Post is designed to transfer breaking strength of cable to the concrete footing.
Pipe insert	No function.	Distributes forces due to vertical component of cable to the post. Size was determined from bearing strength of southern pine.
Bearing plate	No function.	Distributes horizontal forces from cable to post. Size was determined from bearing strength of southern pine.
End nose	Large nose is stiffened by vermiculite concrete (Tests 130 and 131) or steel diaphragms (Test 132) to distribute loads over a large area, thus reducing chances of rail penetration into passenger compartment.	No function.
Anchor cable	The cable does not perform for end-on impacts, but it is essential that it does not develop spearing forces in the W-beam.	Cable transfers tensile forces from beam to end post. Proper anchorage is essential for angle impacts downstream from the end.
Concrete footing	No function.	Distributes loads from end post to soil.
End flare	For Tests 130 and 131, a horizontal flare was installed to introduce eccentric loads for end-on impacts, thus bending beam away from car.	No function.

Table 2. Summary of guardrail terminal tests.

Test Number	Purpose	Vehicle Weight (lb)	Vehicle Speed (mph)	Impact Angle (deg)	Maximum Average Deceleration Longitudinal (g)	Maximum Average Deceleration Lateral (g)	Remarks
130	End-on impact (with flare)	4,138	61.0	0	10.8[a] 2.5[b]	1.7[a]	Vehicle was redirected behind the rail; vehicle stability was good throughout.
131	Test anchorage for downstream impact	4,000	59.4	15	4.6[a]	4.6[a]	Vehicle was redirected at large exit angle. No sign of anchorage failure.
132	End-on impact (without flare)	4,100	58.5	0	8.6[a] 3.4[b]	1.2[a]	Vehicle was redirected behind rail; considerable upward pitch of the vehicle noted.

[a]Highest 50-msec average. [b]Based on stopping distance.

Table 3. Critique of terminal performance.

Design Purpose and Service Requirements	Test Results
Develop structural effectiveness of "length-of-need" section.	Test 131 demonstrated anchor effectiveness.
Provide degree of protection for terminal section impacts consistent with "length-of-need" impacts.	Deceleration levels for end-on impacts were well within limits specified for crash cushions.
Develop tensile and/or flexural strength necessary to ensure desirable redirection performance of the "length-of-need" section.	Test 131 demonstrated the anchor effectiveness.
Either by redirection, containment, or controlled penetration, minimize vehicle and occupant decelerations for terminal section impacts. (In some cases end-on impacts can be eliminated, e.g., extending rail end into back slope.)	Vehicle was redirected for angular impact near the end (Test 131) and was redirected behind the rail for the two end-on tests (130 and 132). Decelerations were within limits specified for crash cushions.
Not launch, roll, or pocket an impacting vehicle.	Vehicle stability was good in Tests 130 and 131, with no pocketing for angular impact. Undesirable vehicle instability occurred in Test 132.
Be designed so that possible penetration of vehicle passenger compartment by system component is minimized.	No penetration of passenger compartment occurred in any of the tests.
Be economical in construction, damage repair, and maintenance.	Terminal construction costs are in-line with existing standards. Damage to terminal was not excessive for end-on tests. Several components were reusable.
Have a pleasing and functional appearance.	Terminal design fulfills this requirement.
Minimize vehicle damage.	Damage to the vehicle front end was severe for the end-on impacts; however, the passenger compartment integrity was not violated.

CRASH TEST EVALUATION OF STRONG-POST, ENERGY-ABSORBING GUARDRAIL USING A LAPPED W-BEAM FOR TRANSITIONS AND MEDIAN BARRIERS

Grant W. Walker, Dynamics Research Manufacturing, Inc.; and
Charles Y. Warner, Brigham Young University

Crash tests, including tests with human drivers, were performed to evaluate a lapped W-section strong-post guardrail designed for transition sections and median barriers. Energy-absorbing cartridges were used to limit the vehicle loads imposed while keeping rail deflection to a minimum. Results show that full-sized conventional vehicles can survive impacts at a speed of 60 mph and an angle of 10 deg without complete loss of steering control.

•ACCIDENTS frequently occur at transitions from wide to narrow roadways, particularly on high-density traffic roads. Many of these transitions exist because construction costs have restricted the width of bridge decks, which reduces the number and/or width of lanes and shoulders. Bridge deck transitions invariably involve rigid bridge railings. One approach that is frequently used to improve this situation is to install a W-4 type guardrail as a funnel section (1). Although this procedure is successful for some low-energy impacts, it is not very successful for high-speed impacts. Vehicles striking the guardrail near the end of the bridge can vault the guardrail and enter the hazardous area beyond, or they may be disabled by the guardrail contact and thrown into the high-density traffic flow on the bridge deck, and create a hazard for other vehicles.

Tests of the W-4 guardrail in applications where limited deflection is allowed have shown that it typically inflicts severe damage on vehicle suspension parts, thus rendering vehicles uncontrollable after they separate from the rail. Further, in W-4 guardrail crashes where limited lateral deflection is available, high lateral loads coupled with the concentration of loading along the rather narrow W-beam result in sizeable longitudinal impulses on the vehicle.

This paper presents a prototype guardrail system-bridge rail transition region. The system is compatible with the W-4 guardrail. It allows gradual stiffening of the rail to provide adequate redirection of the vehicle past the rigid bridge parapet while protecting vehicle components that are essential to regaining driver control.

The system combines the energy-absorbing effects of the vermiculite concrete guardrail with a strengthened face beam that prevents penetration of the vehicle components into the support posts. It is composed of hardware components already generally used for these applications (1).

BARRIER DESIGN OBJECTIVES

The prototype barrier described in this paper was designed especially for the transition section. The following performance objectives were established:

1. Provide protection for conventional automobiles weighing up to 5,000 lb that impact the guardrail at speeds of up to 60 mph and angles of up to 25 deg.

Sponsored by Committee on Traffic Safety Barriers and Sign, Signal and Lighting Supports.

2. Safely prevent the automobile from penetrating laterally more than 12 in. past the impacting surface of the rail by providing as much energy absorption as is practicable within the 12-in. space. This would eliminate the serious consequences of wheel contact with the support posts during a crash.
3. Avoid penetration or ramping in impacts by conventional 2,000-to 5,000-lb automobiles at entry speeds of up to 60 mph and angles of up to 25 deg.
4. Employ readily available hardware components insofar as is possible. The resulting system must be compatible with existing W-4 guardrail and rigid concrete bridge rails and should minimize maintenance and refurbishing costs.
5. In view of the relatively large lateral force impulses that must be applied to the vehicle to meet the first 2 objectives, the design should embody means to distribute the impact loads more broadly over the vehicle surfaces.
6. Apply loads in such a way as to minimize damage to critical safety items on the vehicle, such as steering and suspension systems, so that vehicle control can be regained as quickly as possible.

Attachment hardware that prevents snagging of vehicle parts was developed during the course of the project. This was in response to test experience that showed deleterious effects from contact of safety critical parts such as tires and wheels with such unobtrusive barrier system elements as $\frac{5}{8}$-in. carriage bolt heads. In some instances, such contact resulted in catastrophic damage to tires, steering, and suspension parts.

The broader distribution of forces over the vehicle structure was combined with shorter lateral stopping distances to increase the lateral acceleration loading on the vehicle. It was felt, however, that the net longitudinal loading would be reduced, because the net friction coefficient between vehicle and rail would be reduced, the tendency to pocket the rail would decrease, and the time in contact with the rail would decrease. It was felt that the sum of these four factors would improve survivability by reducing overall occupant impulses and by maintaining steering and suspension integrity.

TEST PROCEDURE

The system tested was built of common guardrail components coupled with vermiculite concrete attentuation cartridges (2). Figure 1 shows the system demonstrating the use of conventional steel W-beam sections, lapped and supported on closely spaced, heavily treated Douglas fir posts. The posts were set in compacted earth fill and buried to a depth of 3 ft. Energy-absorbing cartridges were constructed of helicell elements (Fig. 2) and held in place between rail and post by the hardware shown in Figure 3. The helicell unit is constructed of lightweight concrete that is restrained by a tightly wrapped wire coil. Upon longitudinal impact, the concrete material shatters and "flows" into the hollow center core of the cell and exits between the wire strands, which regulate the maximum size of debris particles. The spent cartridge is replaced, and new or straightened rails are fastened through the cartridges to the posts.

In the early tests in this series, fastening bolts were used to connect the W-beams, cartridges, and blocks as suggested by usual practices (Fig. 3, Detail A). It was noted, however, that in this attachment system the $\frac{5}{8}$-in. bolts snagged vehicle components. Similar snagging has been experienced in earlier tests with W-4 and modified W-4 sections. Wheel and tire damage is often inflicted by attachment bolts for the 6 ⌐ 8.2 rubbing rail in the W-4 configuration. In view of the sometimes catastrophic results of these snagging loads on steering and suspension performance, it was decided that an improved fastening system should be used. Tests were subsequently performed on a system that included fasteners (Fig. 3, Detail B).

This design was suggested by Bronstad and Burkett as a means of reducing shear strength of fasteners (3). The purpose here was not to reduce shear strength but to prevent bolt heads from deflecting into the path of vehicle components.

The tests in this series were conducted on an abandoned airport runway. A plan view of the test site is shown in Figure 4. Figure 5 shows the application that was simulated.

The data were collected in these tests by techniques similar to those used elsewhere (2). High-speed photometrics were obtained from four ground cameras. Vehicle

Figure 1. Guardrail treatment for bridge approach.

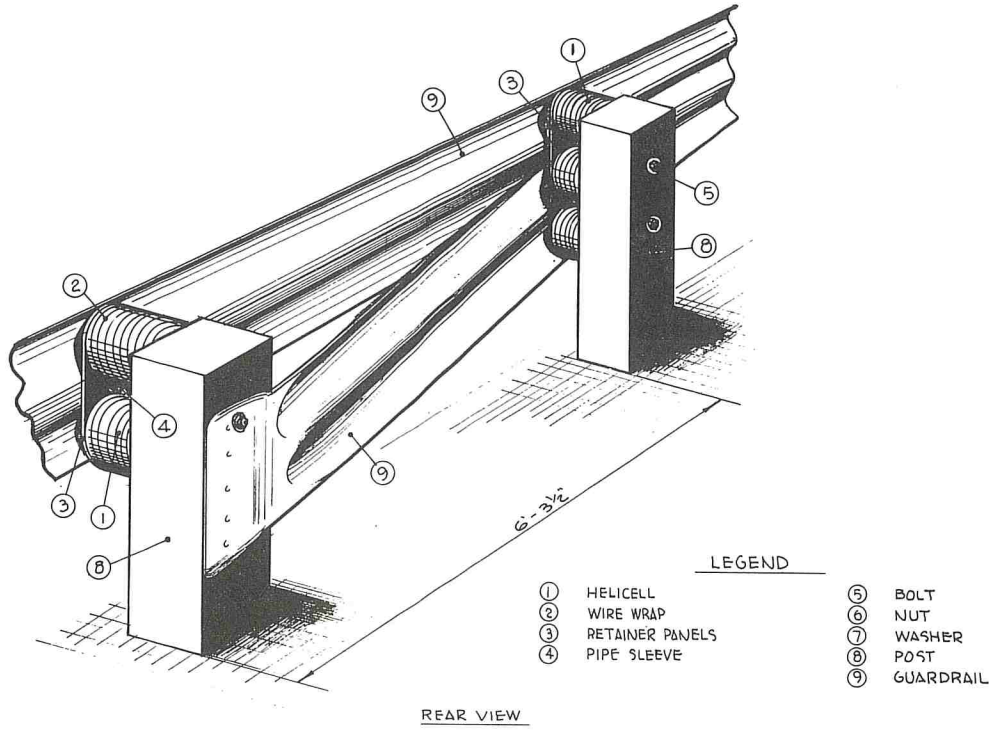

Figure 2. Helicell.

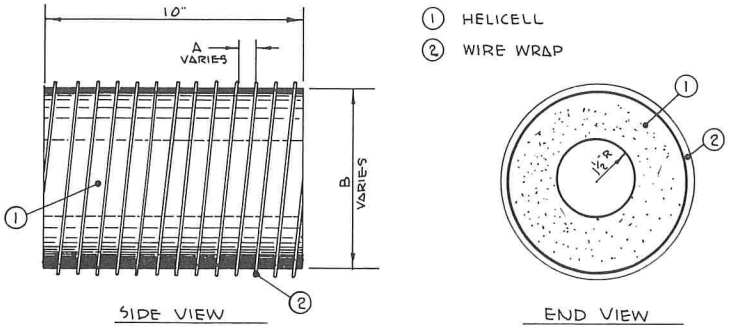

Figure 3. Fastening hardware.

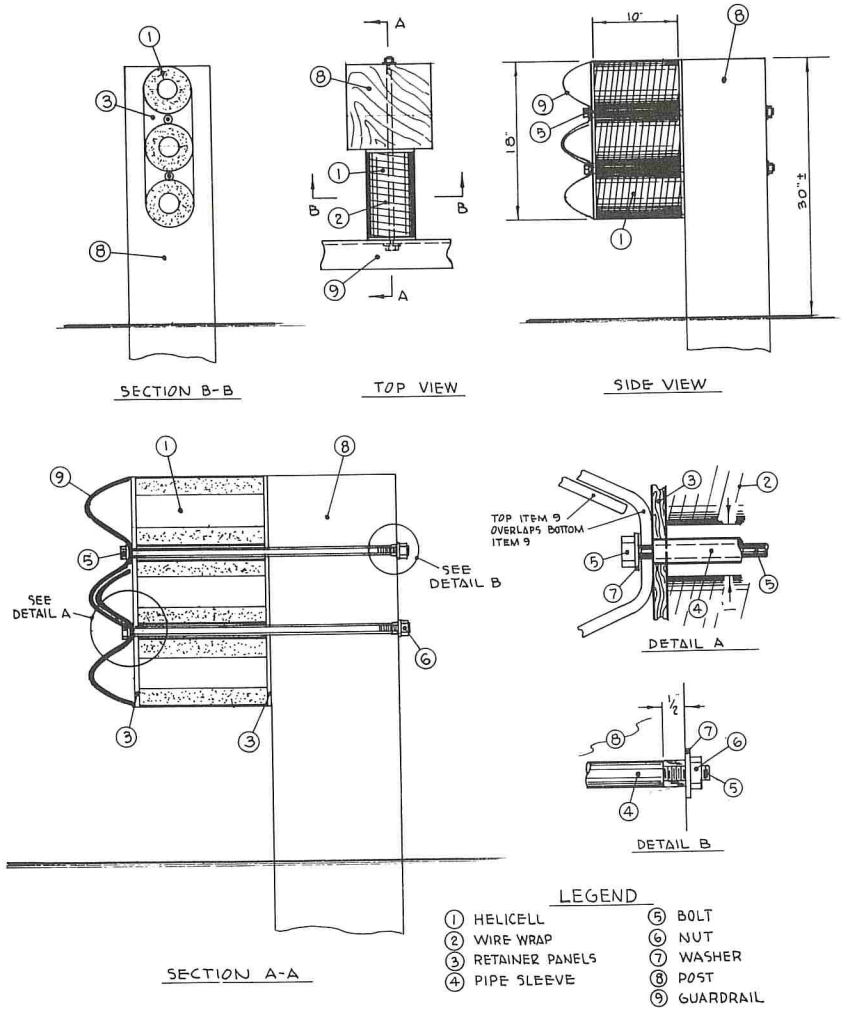

Figure 4. Test installation of simulated bridge approach.

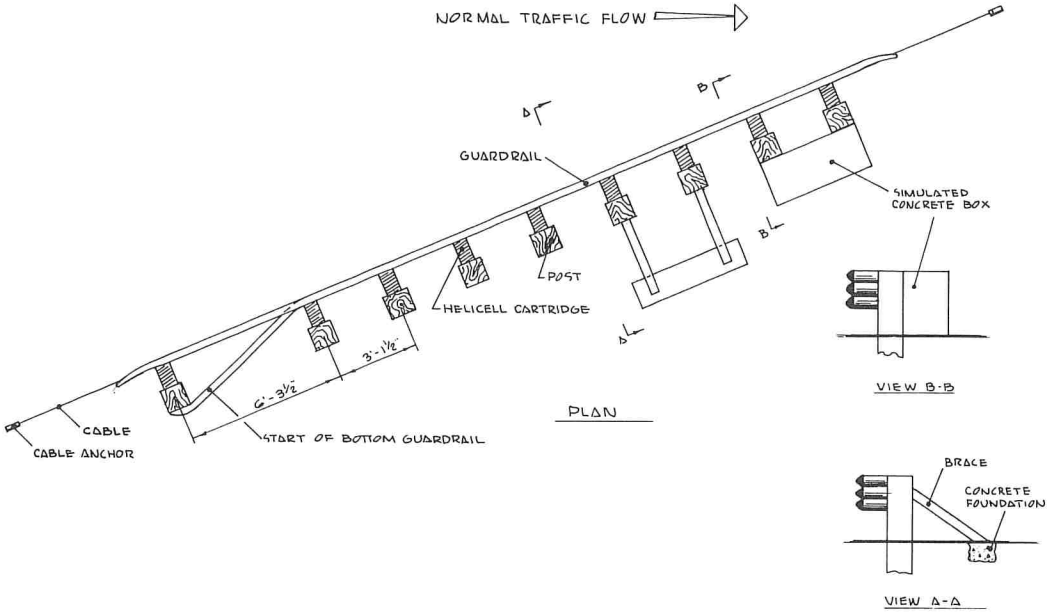

Figure 5. Guardrail protection at bridge approach using helicell cartridge backup.

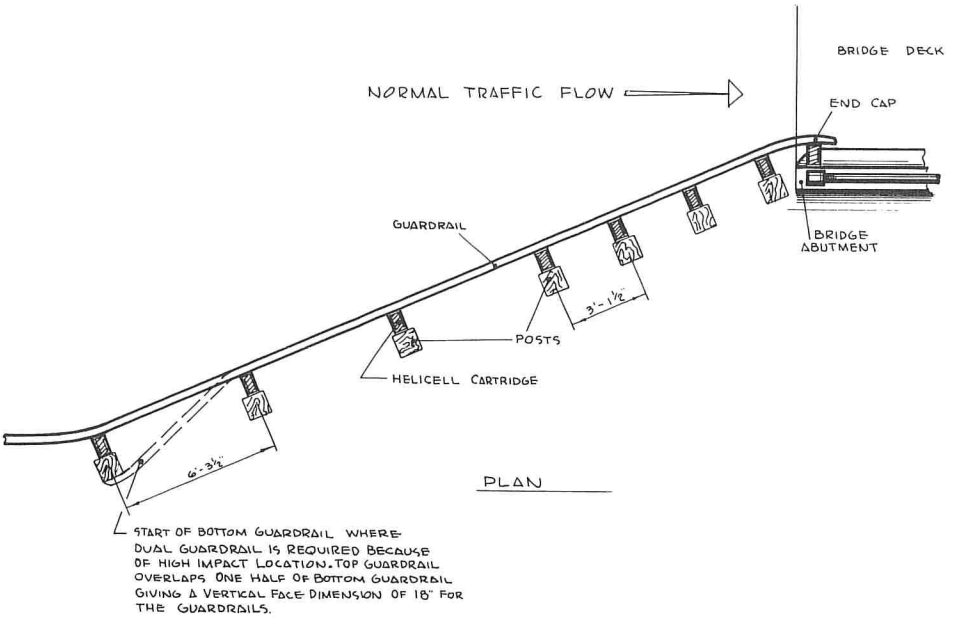

impact speed was measured by trip-wire timers. Vehicle accelerations were measured by a biaxial strain-gauge accelerometer that was pack-mounted on the left side of the vehicle compartment floor, between the front and rear seats, with hard-line umbilicals leading to a direct-writing light beam oscillograph mounted in a chase vehicle. Electronic data were compared for internal consistency and were checked qualitatively against photometrics to determine overall agreement. Dynamic contact distance was measured from the photometric records.

TEST RESULTS

Table 1 summarizes the important parameters and results for this series of tests. Figure 6 shows acceleration-time histories as measured on the floor pan of the test vehicles. Figures 7 and 8 show vehicle and guardrail damage after a 57-mph, 24-deg impact (Test 1-14). A description of each test follows.

Test 1-12

In this test, a 1959 Buick Electra convertible weighing 4,600 lb impacted the rail at a speed of 47 mph and an angle of 30 deg.

The vehicle left the rail at approximately a 10-deg angle and rolled on all four tires. Damage was limited to sheet metal and minor suspension bending; there was no discernible frame damage. The right front tire remained inflated throughout the post-test roll, and the car was steerable following impact.

Six vermiculite concrete cartridges were activated, but there was reserve energy absorption capability following impact, and the vehicle came to rest more than 100 yd from the point of impact. Maximum deflection of the rail was in excess of 7 in., with post deflection limited to less than 1 in. Both longitudinal and lateral average g loads were less than 3 g.

Six $\frac{5}{8}$-in. bolts holding the rail to the posts were bent during impact. This increased the longitudinal acceleration loading and the velocity change. (Later in the test series the fastening hardware was changed, which eliminated this problem.) The axle or structural parts of the car did not penetrate the posts.

Test 1-13

In this test, a 1952 Cheverolet station wagon weighing approximately 3,800 lb impacted the rail at a speed of 50 mph and an angle of 25 deg. The results were similar to those of Test 1-12 in that the exit angle was near 10 deg and the damage to the car was limited to sheet metal and minor suspension damage. There was no damage to the vehicle frame. Run-out distance was approximately 150 yd, the trajectory curving back toward the rail. Both lateral and longitudinal average g loads were less than 3 g.

The car was steerable following impact. There was no discernible barrier post deflection with the rail deflecting in excess of 7 in. Several bolts holding the rail to the posts were snagged and bent by the car. The axle or structural parts of the car did not penetrate or snag the post, as is common in impacts with W-4 guardrail design.

Test 1-14

In this test, a 1960 Oldsmobile hardtop convertible weighing 4,300 lb impacted the rail at a speed of 56 mph and an angle of 24 deg. Again, damage to the vehicle was limited to moderate suspension bending and sheet metal deformation, at both front and rear of the car, with no discernible frame damage. The vehicle left the rail at a 10-deg angle and rolled freely on all four tires. Six rail bolts were snagged during impact. Both longitudinal and lateral average g loads, were approximately 4 g during impact.

There was reserve energy absorption capacity in the activated cartridges even though the test was run near the upper limit of guardrail test velocities and angles.

Because of the lack of frame damage, repair of the car would have been justified if it had been a late model.

Table 1. Test results.

Test No.	Barrier Type	Overall Conditions of Test: Impact Speed (mph)	Total Vehicle Weight (lb)	Impact Angle (deg)	Total Kinetic Energy (ft-lb x 10^{-5})	Change in Kinetic Energy During Impact (ft-lb x 10^{-5})	Exit Speed (mph)	Test Results: Duration of Contact (sec)	Max. Dynamic Lateral Deflection: Top of Post (in.)	Max. Dynamic Lateral Deflection: Rail (in.)	Accelerations (g): Long. Peak	Accelerations (g): Long. Avg	Accelerations (g): Lateral Peak	Accelerations (g): Lateral Avg	Speed Change During Contact (mph)	Exit Angle (deg)	Run-out Distance (yd)
1-12	Strong post energy absorption	47	4,700	30	3.47	1.48	35	320	0	8+	5.0	2.7	5.0	3.0	12	10	100+
1-13	Guardrail with lapped W-section	49	3,800	25	3.00	1.08	39	360	0	6	5.0	2.5	6.0	2.6	10	10	150
1-14	Guardrail with lapped W-section	57	4,300	24	4.49	2.09	41	310	0	8+	7.5	4.0	6.0	4.5	15	10	80
1-15	Guardrail with lapped W-section	50	4,175	21	3.43	1.25	40.5	–	0	–	–	–	–	–	9.5	8	200
1-22	Guardrail with lapped W-section	60	3,200	21	3.84	0.51	55	290	0	5	5.0	2.5	9.0	6.0	5.0	12	90

Figure 6. Lateral and longitudinal load comparisons.

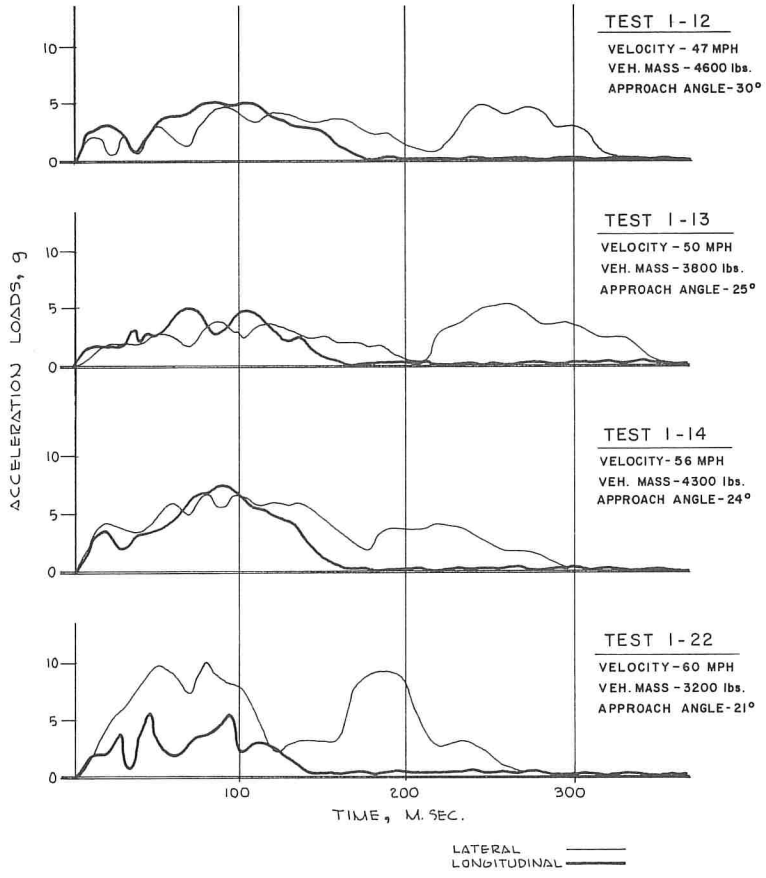

Figure 7. Test vehicle before and after impacts.

Figure 8. Guardrail before and after impacts.

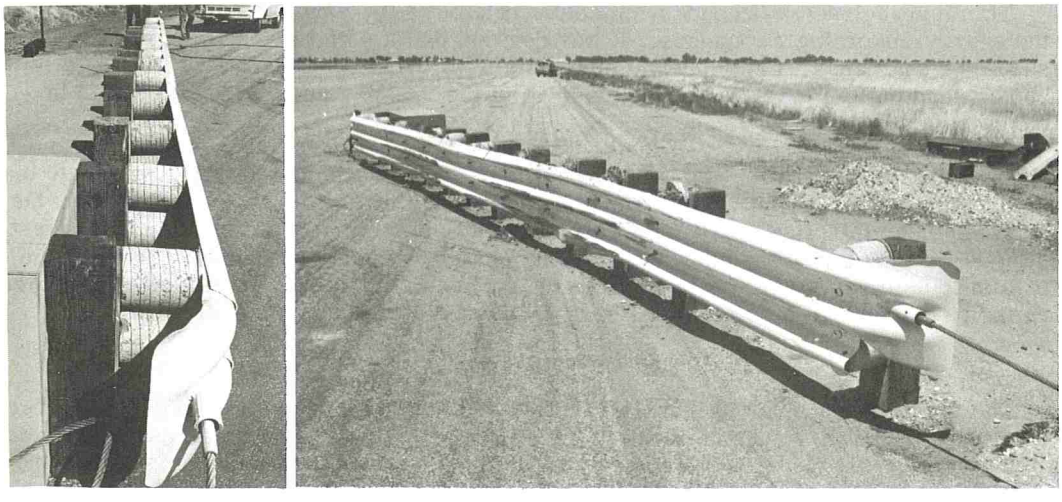

Test 1-15

The minimal vehicle damage and low acceleration loads experienced in the previous tests suggested that tests with a properly restrained human driver could be run safely.

In this test, a 1955 Chrysler Windsor hardtop convertible weighing 4,000 lb and carrying a human driver impacted the rail at a speed of 50 mph and an angle of 21 deg, with a 8-deg exit angle. One purpose of this test was to determine whether an amateur driver, after impacting the rail on a typical hit, would be able to bring the car to a safe stop. The driver controlled the car following impact, steering the car to a stop approximately 200 yd from point of impact on a predetermined alignment.

Damage to the car was limited to sheet metal and suspension bending. The car was steerable following impact, rolling on all four wheels. The amateur driver, restrained by aircraft-type lap and double shoulder harness, reported no discomfort from restraint loading.

Three rail bolts snagged the body and wheel of the test car. There was no post deflection. Rail contact was 13.7 ft. Maximum compression of the rail was about 5 in. Six energy-absorbing cartridges were activated between 10 and 70 percent.

Test 1-22

In this test, a 1959 Studebaker Lark 4-door sedan weighing approximately 3,200 lb, including a human driver, impacted the rail at a speed of 60 mph and an angle of 21 deg.

This test included a secondary objective related to the vertical stiffness gradient in the energy-absorbing cartridges. It was decided that a soft-top, stiff bottom cartridge should be evaluated. Cartridges employing a wrap-wire spacing of 1, 1, and $\frac{5}{8}$ in. (top, center, and bottom cells) were used instead of the $\frac{5}{8}$-, $\frac{5}{8}$-, and $\frac{5}{8}$-in. wrap used in other tests.

The high center of gravity of the vehicle plus the greater resistance of the bottom energy-absorbing vermiculite concrete cell may have caused the 15- to 20-deg into the rail. This roll made the vehicle more difficult to control following impact. Nevertheless, the vehicle rolled on all four wheels and was steerable. The results of this test suggest that the top of the energy-absorbing cartridge should be made stiffer than the bottom to help rotate the car away from the rail and attempt to hold the left side wheels on the pavement. The soft-top stiffness gradient is not recommended.

DISCUSSION OF RESULTS

The overall objectives of the design have been satisfied. Penetration depth has been controlled by effective use of about 10 in. of lateral distance. Although the lateral loads applied to the test vehicles were greater than those experienced in impacts with more flexible guardrails, the longitudinal impulses and the damage to safety-sensitive vehicular components (steering, suspension, tires, and wheels) were significantly reduced. In tests with human drivers at speeds of about 50 mph and entry angles greater than 20 deg, steering control has been recovered after the impacts and the vehicles brought to a safe stop without overturning. This was effected in large part by the broadened force distribution resulting from the lapped W-beam and by the reduction in lateral loads provided by the energy-absorbing cartridges.

Expected exposure in service of the helicell units to moisture and freezing temperatures suggests that some steps should be taken to prevent intrusion of moisture. This has been accomplished by coating the helicell with asphalt emulsion and enclosing it in an aluminum foil skin. Repeated water-soak and freeze-thaw testing of treated cells indicates that the treatment is effective in preventing water intrusion, giving adequate water protection to prevent deterioration of helicell performance. The foil skin also help to contain the helicell debris during and after use.

Investigation of the effect of vertical stiffness gradient in the energy-absorbing cartridges suggests that better performance will result from a gradient that increases with increasing height. In Test 1-22, a decreasing gradient appeared to encourage the vehicle to roll toward the rail, making run-out recovery more difficult. It is expected that a rail system that is stiffer on top will keep the vehicle wheels more firmly loaded during impact. More extensive testing is needed to fully evaluate this secondary effect.

These test results, together with those published elsewhere (2), for a vermiculite concrete modified W-4 guardrail system, show satisfactory performance for both relatively stiff and relatively soft backup systems.

The vermiculite concrete cartridge is conceptually simple and easy to use. It may be used to construct guardrail systems that provide the graduated stiffness called for at rail-to-bridge transitions and, at the same time, hold vehicle crash loading at an acceptable level.

SYSTEM CHARACTERISTICS: REFURBISHMENT

Three factors about this system seem to contribute to ease of refurbishment. First, the use of energy-absorbing cartridges, coupled with strong-post design, tends to minimize the post refurbishment required. In these tests, no post was found to shift more than 1 in. in its earthen foundation. The time-consuming labor of resetting posts, and the attendant realignment, was greatly reduced. A second factor that improves the refurbishment posture is the use of guardrail and post components already on hand. Third, the bolt-sleeve attachment system adopted to reduce snagging during impact also reduces bending of attachment bolts.

In all but the severest impacts, one could reasonably expect to refurbish by simply removing the spent cartridges and permanently deformed W-beam and bolting replacement components in place. All refurbishment in this test series was accomplished by hand without the use of power machinery. After Test 1-22 was completed, the system was refurbished by simply jacking the steel rail into place and replacing five vermiculite concrete cartridges. The estimated total cost of refurbishment was less than $125, including on-site labor.

CONCLUSIONS

The results of the tests discussed in this paper allow the following conclusions to be made:

1. The system presented in this paper has thus far proved to effectively prevent excessive rail deflection without destruction of safety-related vehicle components. Insofar as has been determined, overall acceleration loads and velocity changes are reduced while post-crash controlability is increased, as compared to the performance of W-4 guardrail systems.
2. Overall cost of the system will vary with intended application. First cost will probably not greatly exceed that of the W-4 guardrail in comparable installations. Maintenance costs, including the cost of replaceable energy-absorbing cartridges, may be less than those for the W-4 because of the decreased post displacement.
3. The tests have demonstrated the feasibility of this system for safe, no-penetration deflection as is required in many median barriers and bridge transitions.
4. These tests and those presented elsewhere (2) are representative of performance that would be expected at the stiff and soft ends of a transition section. The test results indicate that vermiculite cartridges can be used effectively to improve the performance of guardrail systems in cramped medians and at bridge transitions.

REFERENCES

1. Michie, J. D., and Calcote, L. R. Location, Selection, and Maintenance of Highway Guardrails and Median Barriers. NCHRP Report 54, 1968.
2. Warner, C. Y., and Walker, G. W. Crash Test Performance of a Prototype Lightweight Concrete Energy-Absorbing Guardrail System. Highway Research Record 343, 1971, pp. 13-18.
3. Bronstad, M. E., and Burkett, R. B. Evaluation of Timber Weak-Post Guardrail Systems. Highway Research Record 343, 1971, pp. 34-56.

DYNAMIC TESTS OF THE CALIFORNIA TYPE 15 BRIDGE BARRIER RAIL

Eric F. Nordlin, J. Robert Stoker, Raymond P. Hackett, and Robert N. Doty, California Division of Highways

The results of two full-scale vehicle impact tests of the California Type 15 bridge barrier rail are reported. The Type 15 bridge rail is a semirigid system consisting of two 3½-in. square structural steel tubular rails mounted 14 and 27 in. above the pavement on 6-WF-25-steel posts bolted to the edge of the reinforced concrete bridge deck. The post spacings tested were 6 ft 3 in. and 9 ft 4½ in. This bridge barrier rail was designed for use on secondary California highways with maximum bridge widths of 32 ft. The tests were conducted at impact velocities of approximately 60 mph and approach angles of approximately 15 deg. The test results indicate that the bridge rail designs tested will retain and redirect a 4,500-lb passenger vehicle impacting at a speed of 60 mph and an angle of 15 deg. Tolerable deceleration rates, moderate vehicle damage, and minor to moderate barrier damage will be sustained. However, it was concluded that a post spacing of 8 ft 0 in. would provide an effective, economical, and aesthetically pleasing compromise between the relatively rigid 6-ft 3-in. post spacing and the more flexible, but marginal, 9-ft 4½-in. post spacing. It was also concluded that, with a post spacing of 8 ft 0 in. or less, the California Type 15 bridge barrier rail is satisfactory for use on federal-aid secondary highways and other secondary California State highways.

•THE California Type 15 bridge barrier rail was designed by the California Division of Highways' Bridge Department to provide an effective and economical railing for use on bridges on secondary roads.

The metal beam bridge railing frequently used on California's secondary roads in the past was developed and tested in 1959 (1) as part of a test series to investigate existing and proposed bridge rail designs. This metal beam bridge railing consisted of a single steel W-section beam mounted 24 in. high on steel H-section posts bolted to the outside edge of the concrete bridge deck at 6 ft 3 in. on centers (Fig. 1).

In the 1959 tests, a 4,000-lb passenger vehicle was impacted into the bridge railing at a speed of 55 mph and an angle of 30 deg. The crash produced severe wheel-post entrapment and excessive rail deflections (Fig. 2). Although this design was not judged adequate for freeway use, it was considered suitable at that time for placement on federal-aid secondary highways and certain California state highways where only lower speed, flat, oblique-angle collisions were expected. It proved to be an economical and effective barrier under these conditions. However, as heavier, higher speed vehicles became more prevalent on these secondary highways, failures began occurring even at low, oblique impact angles. These failures were attributed to the inability of the single W-section beam to adequately distribute the larger impact loading outside the immediate impact area. Thus, only the posts very close to the impact area were being loaded, and failures were occurring at the post-to-deck connections in much the same manner as had been observed in the 1959 test series.

Sponsored by Committee on Traffic Safety Barriers and Sign, Signal and Lighting Supports and Committee on Bridge Design.

In 1967, the single W-section beam was replaced with two 3½-in. square structural steel tubular rails in an effort to correct this deficiency. This provided a post and rail system that conforms to the requirements of the 1969 AASHO Specifications for Highway Bridges. However, these specifications stipulate loading requirements for bridge railings attached to "surface mount" posts. Thus, the adequacy of the AASHO Specifications as applied to the Type 15 bridge rail, with the posts attached to the edge of the bridge deck, had not been evaluated. This exact system had never been subjected to controlled full-scale vehicle impact tests.

A bridge rail system of this type was tested by the New York State Department of Public Works Bureau of Physical Research in 1963 and reported on in 1967 (2). Although somewhat similar in overall appearance, the details of the New York barrier and the Type 15 barrier varied significantly. It was felt that no analogy could be made between the two. Therefore, a series of dynamic tests was deemed necessary to accurately evaluate the effectiveness of the California Type 15 bridge barrier rail.

OBJECTIVES

The primary objectives of this research project were to (a) test the ability of the California Type 15 bridge barrier rail to effectively retain and redirect a 4,500-lb vehicle impacting at a speed of 60 mph and an angle of 15 deg, (b) determine the structural capabilities of the California Type 15 bridge approach guardrail and its connection to the bridge abutment wing wall, and (c) develop and test subsequent systems design modifications as dictated by the results of the initial impact tests.

TEST CONDITIONS

Barrier Design

The test installation consisted of 67 ft of Type 15 bridge barrier rail and 52 ft of Type 15 bridge approach guardrail (Fig. 3).

The initial Type 15 design consisted of two structural steel tubular rails mounted 14 and 27 in. above the pavement on steel posts spaced at 6 ft 3 in. on centers. On the bridge rail portion of the installation, the WF posts were bolted to the edge of a cantilevered reinforced concrete bridge deck (Fig. 4). The steel posts for the bridge approach guardrail (BAGR) were embedded in concrete footings. The posts for both the bridge rail and the BAGR were 6-WF-25-structural steel members conforming to the requirements of ASTM Designation A 36.

Each bridge rail post was attached to the edge of the deck with two high-strength threaded rods 1 in. in diameter and 2 ft long and two high-strength bolts (⅝ in. in diameter and 1 ft long) cast into the reinforced concrete. The high-strength steel rods conformed to the requirements of ASTM Designation A 108, grade 1144. The high-strength bolts conformed to the requirements of ASTM Designation A 325.

The rails were 3½-in. square, 10½-lb structural steel tubing that conformed to the requirements of ASTM Designation A 500, grade B. The interior sleeve-type rail splice (Fig. 5) and the ¾-in. welded stud rail-to-post connectors that proved effective in a previous test series (4) were again used.

The bridge barrier rail was bolted to the outside edge of a reinforced concrete bridge deck 12 in. thick and 67 ft long cantilevered 36 in. off a 24-in. by 30-in. by 68-ft reinforced concrete anchor block. A 6 sack mix was used for the concrete. The 28-day compressive strength of the concrete was 4,735 psi.

The posts for the bridge approcah guard railing were set in concrete footings (5 sack mix) 24 in. in diameter and 36 in. deep. The leading, or upstream, ends of the tubular rails were curved down and anchored to two reinforced concrete footings (6 sack mix) 18 in. in diameter and 36 in. deep.

The type 15 bridge barrier rail design[1], other than the post-to-deck connection, was

[1]The original manuscript of this paper included detailed drawings of the Type 15 bridge barrier rail design, the photographic instrumentation used in the tests, and the vehicle transducer instrumentation. These drawings are available in Xerox form at cost of reproduction and handling from the Highway Research Board. When ordering, refer to Xerox Supplement 39, Highway Research Record 386.

Figure 1.

Figure 2.

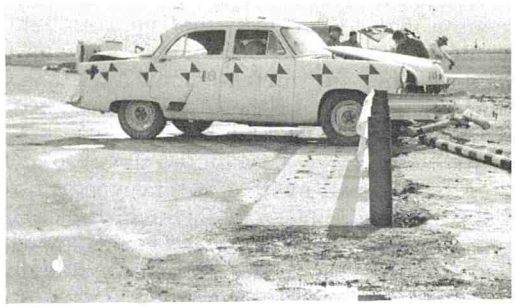

Figure 3.

Figure 4.

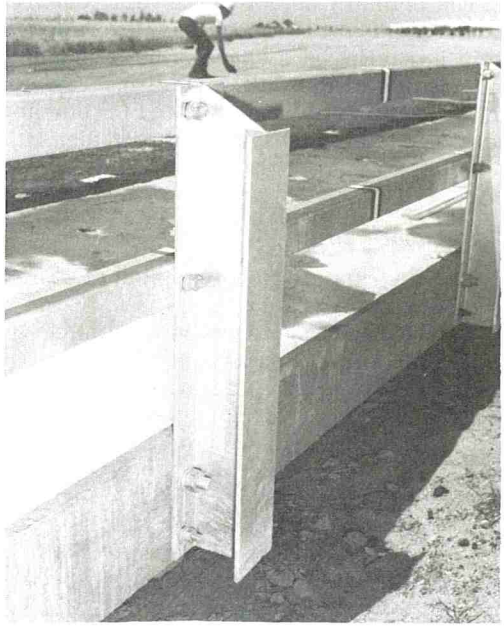

Figure 5.

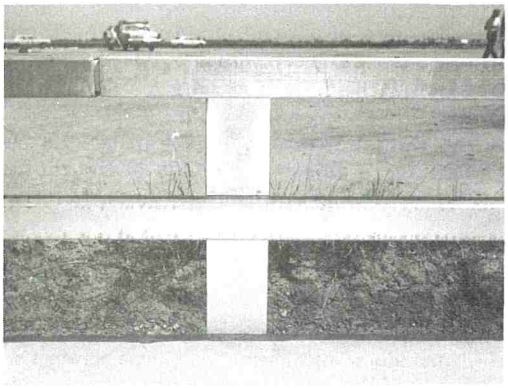

designed in accordance with the requirements of the Standard Specifications for Highway Bridges adopted by the American Association of State Highway Officials in 1969.

Test Parameters

Test guidelines established by the Highway Research Board Committee on Guardrails and Guideposts (11) specify the use of a ±4,000-lb vehicle, an impact velocity of 60 mph, and an impact angle of 25 deg. For the tests reported here, the vehicle weighed 4,550 lb including an anthropometric dummy and on-board instrumentation. Although this weight exceeds HRB guidelines, it is more representative of the more severe conditions currently being encountered on California highways.

The planned impact velocity and impact angle for these tests were 60 mph and 15 deg. These values were selected because the bridge barrier rail design tested is intended for use on secondary California highways with maximum bridge widths of 32 ft. It was estimated that, under these conditions, 60-mph/15-deg collisions were representative of the more severe accidents that would actually occur.

Test Procedures

A description of the procedures used to modify the test vehicles for remote radio control is given elsewhere (5). A description of the photographic and electronic data acquisition systems used during the tests reported here is given in the original report (6).

TEST RESULTS

Test 251

Test 251 was conducted to test the ability of the initial Type 15 bridge barrier rail design (6-ft 3-in. post spacing) to redirect a passenger vehicle impacting at a moderate velocity and approach angle (Fig. 6).

Initial barrier contact occurred at midspan between posts B-4 and B-5. The impact velocity and approach angle were 64 mph and 12 deg. The height of the barrier rail elements was such that upon impact the vehicle bumper and leading chassis members rode up and over the lower rail and the upper rail knifed into the body sheet metal just below the headlight. However, there was no further penetration because the lower rail effectively deflected the left front wheel, thus precluding any serious vehicle-barrier entrapment. There was only a 5-deg roll toward the barrier (Fig. 7), and the vehicle was effectively redirected to an exit angle of 3 deg with the barrier.

The total vehicle-barrier contact was approximately 10 ft. The post-impact vehicle trajectory was satisfactory with a maximum vehicle rebound into the traveled lanes of 13 ft.

Barrier damage was relatively minor. Two rail sections and three posts were deformed and would have required replacement for aesthetic reasons. However, all the barrier components were intact structurally and the barrier was still functional. The maximum residual lateral rail deflections occurred at post B-5, approximately 3 ft downstream of initial impact. The permanent deformations of the upper and lower rails were 0.21 ft and 0.14 ft respectively (Fig. 8).

The flanges of the three deformed posts were bent above their upper post-to-deck connections. Maximum residual lateral post deflections, measured from the upper edge of the deck, were (a) post B-4, 3.0 ft upstream of impact, ¼ in., (b) post B-5, 3.2 ft downstream of impact, ½ in., and (c) post B-6, 9.4 ft downstream of impact, ⅜ in. There was no damage to any of the post-to-deck connectors, rail stud bolts, or splice sleeves, and except for insignificant surface spalling, there was no concrete damage.

Vehicle damage was moderate, consisting of paint scratches and sheet metal deformation at the left front corner, along the left side, and at the left rear fender. The grill, headlights, and fender at the left front end were extensively deformed, a portion of the front bumper was torn away, and the bumper mounting brackets and leading frame members were distorted back toward the front wheel. However, the deformation was essentially superficial, and, except for the possible rubbing of distorted sheet metal against the front tire, the vehicle appeared to be operable (Fig. 9).

Figure 6.

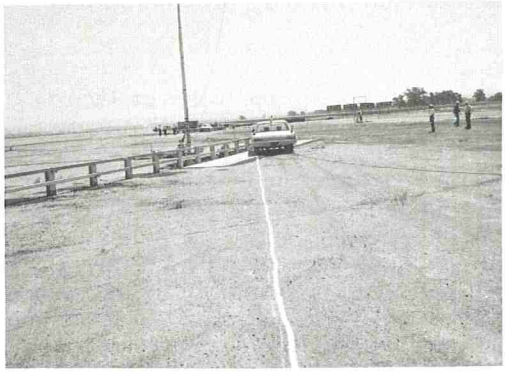

Figure 7.

Figure 8.

Figure 9.

Figure 10.

Inside the passenger compartment, there was no appreciable deformation of the steering wheel rim or of the left front door frame to indicate that the dummy had been subjected to high deceleration forces (Fig. 10). However, deceleration recording instrumentation indicated that the deceleration forces, particularly in the lateral direction, were higher than anticipated or desired. Records of the instrumentation data are contained elsewhere (6). A summary of these data is as follows:

1. The highest 50-msec average vehicle deceleration (longitudinal) was 4.7 g (using two accelerometers);
2. The highest 50-msec average vehicle deceleration (lateral) was 9.0 g (using two accelerometers);
3. The highest 50-msec average dummy (head) deceleration was 25.0 g (using three accelerometers); and
4. The highest 50-msec average dummy (chest) deceleration (longitudinal) was 4.6 g (using one accelerometer).

The maximum seat belt load was 1,350 lb. The Gadd Severity Index was 278.

Test 252

Analysis of the results of Test 251 led to the modification of the test barrier installation to provide a post spacing of 9 ft 4½ in. The post spacing was increased to introduce more flexibility into the barrier rail system, thereby lessening the severity of a collision with the barrier. To achieve this modification, seven posts were removed and 2-ft square sections of the cantilevered bridge deck were removed at three locations. New post anchor bolts were installed at these locations, the deck edges within the removed sections were coated with epoxy, and new concrete was cast using a 6 sack mix. The 28-day compressive strength of the concrete was 4,540 psi. The steel rail sections from the original barrier were modified to provide stud bolts and rail splices at the new locations as required. This resulted in a discontinuity in the lower rail. However, this discontinuity was far enough from the location of impact such that it did not affect the test results. The height of the upper and lower rails was identical to that tested in Test 251 (Fig. 11).

Initial barrier contact occurred 2.7 ft upstream of post B-5 at a speed of 59 mph and an angle of 14 deg. Vehicle-barrier interaction was similar to that observed in Test 251.

Vehicle tire scrub marks on the bridge deck indicated that the left front wheel had come dangerously close to the edge of the bridge deck. If the wheel had dropped off the deck, serious wheel-post entrapment could have resulted.

Again, vehicle dynamics through impact were good. A 7-deg roll toward the barrier occurred (Fig. 12) and the vehicle was effectively redirected to an exit angle of 2 deg with the barrier. The total vehicle-barrier contact was approximately 14 ft. The maximum vehicle rebound into the traveled lanes was 22 ft. In view of the low 2-deg exit angle, the overall post-impact vehicle trajectory was considered satisfactory.

The barrier damage was more severe than that which was observed after Test 251. Two rail sections and two posts were deformed and would have required replacement. Although all of the principal barrier components remained physically intact, it is doubtful that the barrier could have sustained a subsequent impact into the damaged section without failure. The maximum residual lateral rail deflections occurred at midspan between posts B-5 and B-6, approximately 7.4 ft downstream of initial impact. Deflection of the top rail was 0.56 ft and of the bottom rail 0.43 ft (Fig. 13). Maximum residual lateral post deflections, measured from the upper edge of the deck, were (a) post B-5, 2.7 ft downstream of impact, 1⅞ in. and (b) post B-6, 17.1 ft downstream of impact, 1⅞ in. Although the post deflections are numerically equal, thus indicating similar loadings, at post B-6 the downstream upper post-to-deck connector (high-strength threaded rod 1 in. in diameter) failed in tension and, consequently post flange deformation was absent at that point. Minor post flange deformation did occur on that side of the post just above the lower connector (Fig. 14). On the upstream side, post flange deformation occurred above the upper post-to-deck connector, which remained intact (Fig. 15).

At post B-5, all post-to-deck connectors were intact and both post flanges deformed above the upper connectors (Fig. 16). However, a flange-web fracture (0.1-in. by 3-in.

Figure 11.

Figure 12.

Figure 13.

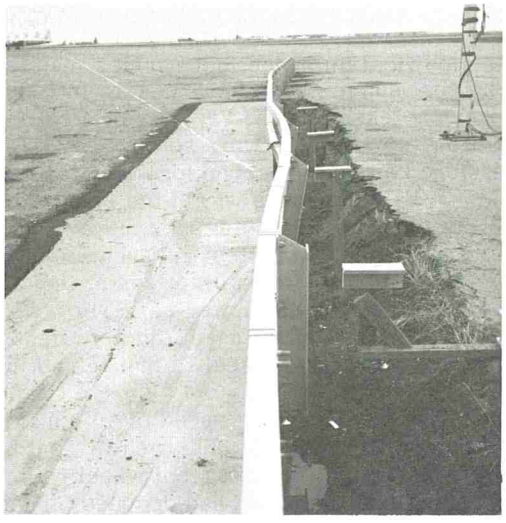

Figure 14.

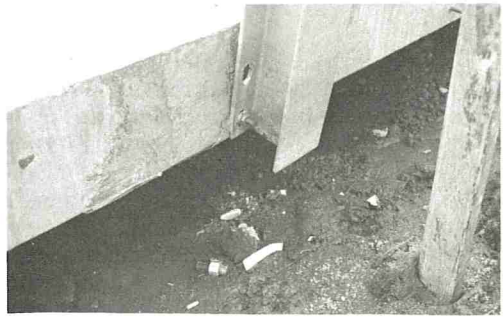

Figure 15.

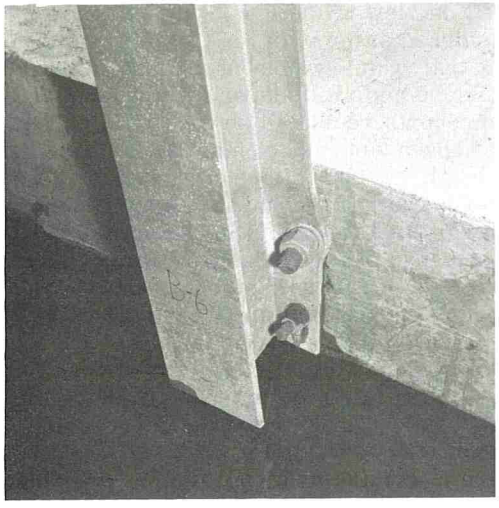

Figure 16.

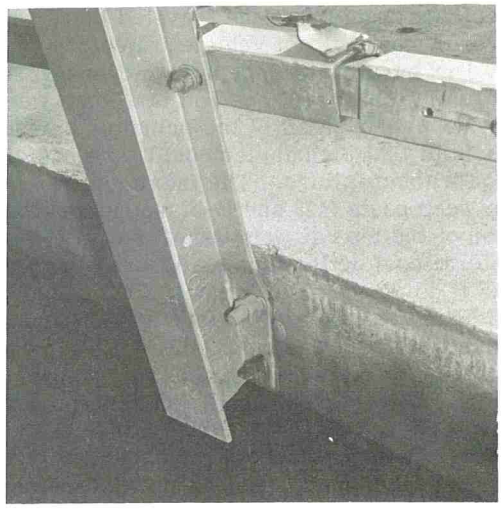

Figure 17.

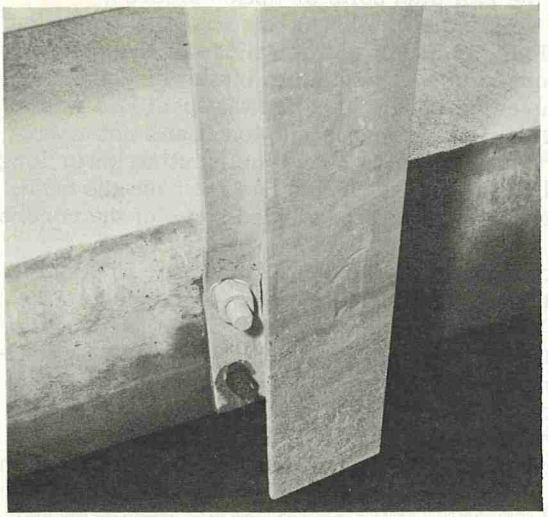

Figure 18.

Table 1. Vehicular decelerations.

Accelerometer Orientation in Vehicle	No. Accele-rometers	Highest 50-msec Average Deceleration (g)		Highest 200-msec Average Deceleration[a] (g)		
		Test 251	Test 252	Unre-strained	Lap Belt	Lap Belt and Shoulder Harness
Lateral	2	9.0	3.9	3	5	15
Longitudinal	2	4.7	3.1	5	10	25

[a] Ref. 8.

separation) occurred adjacent to the downstream upper post-to-deck connector (Fig. 17). There was no damage sustained by any of the rail stud bolts or splice sleeves.

Concrete damage was limited to minor spalling at the lower anchor bolts and on the underside of the bridge deck at post B-6 (Figs. 14 and 15). The failure of the upper post-to-deck connector at this post transferred impact loading to the lower connector and contributed to the concrete damage. However, it should be noted that post B-6 was at one of the rebuilt sections of the bridge deck. During reconstruction it was not always possible to install the new lower post-to-deck connectors above the existing lower longitudinal deck reinforcing steel as specified on the plans. If this had not been the case, the load transfer capability of the deck reinforcing may have precluded some of the concrete spalling.

Laboratory tests of the failed barrier components from Test 252 were conducted to check on the possibility of defective material. A hardness test was performed on the sheared-off end of the failed post-to-deck connector from post B-6. This produced an average Brinell reading, with a $\frac{1}{16}$-in. ball, of 94 on the B scale. This value approximates a tensile value of 100,000 psi, which is comparable with the minimum specified tensile strength requirement for the anchor bolts of 105,000 psi. However, because it was both an approximate value and slightly below specification, the remainder of this connector was jackhammered from the bridge deck for further testing. A standard tensile test resulted in values of 108,700 psi ultimate and 91,300 psi yield. Both values are well above the specified minimum strength for this material. A tensile specimen was also cut from the failed post (B-5). The test results were 67,400 psi ultimate and 41,400 psi yield. Both of these values were well above the minimum specified values for the post material. The failures were therefore attributed to the inability of the rails to transmit the impact loading to a sufficient number of posts due to the greater post spacing in this design.

Vehicle damage was generally similar to that observed in Test 251 and consisted of paint scratches and sheet metal deformation at the left front corner, along the left side, and at the left rear fender. At the left front corner, sheet metal deformation was slightly less than that observed in the first test. However, the bumper mounting brackets and leading frame members were more extensively distorted, the left front wheel rim was deformed, and the tire was ruptured. Damage along the left side was also similar to that observed in the first test. However, the left rear fender damage was more severe than that observed after Test 251. This indicated that a harder rear end slap occurred as the vehicle was being redirected (Fig. 18). Data film alalysis revealed that this was due to the larger rail deflections in this test. These large deflections permitted the vehicle to pocket into the barrier and follow the deflecting rails rather than rebound, or "bounce," off as observed in Test 251 on the more rigid initial design. Although vehicle body damage was essentially superficial, the damaged left front wheel rendered the vehicle inoperable. There was no evidence inside the vehicle passenger compartment to indicate that the dummy driver was subjected to excessive deceleration forces. This was verified by the accelerations recorded, which were generally less than those recorded in Test 251 (6). A summary of the data is as follows:

1. The highest 50-msec average vehicle deceleration (longitudinal) was 3.1 g (using two accelerometers);
2. The highest 50-msec average vehicle deceleration (lateral) was 3.9 g (using two accelerometers);
3. The highest 50-msec average dummy (head) deceleration was 24.0 g (using three acelerometers); and
4. The highest 50-msec average dummy (chest) deceleration was 4.4 g (using one accelerometer).

The maximum seat belt load was 120 lb, and the Gadd Severity Index was 234.

DISCUSSION OF FINDINGS

General

The initial Type 15 bridge barrier rail design, impacted in Test 251, appeared to be effective in redirecting a passenger vehicle impacting at a moderate velocity and angle.

Vehicular redirection was smooth, barrier damage was minor, and vehicle damage was moderate. However, it was also apparent, from the post-impact vehicle trajectory and the low residual barrier deflections, that the system was more rigid than necessary. Spacing was therefore increased from 6 ft 3 in. to 9 ft 4½ in., which would result in lower decelerations in the vehicle passenger compartment because of the increased barrier flexibility and an economic saving through a 33 percent decrease in the number of barrier posts used. The 9-ft 4½-in. post spacing was arbitrarily selected as an economic expedient because this modification could easily be effected on the existing test installation by removing every second and third post and replacing them with a single post.

Test 252, conducted on this modified system, substantiated the desirability of increasing the barrier's flexibility. However, the barrier damage, particularly at the post-to-deck connection, and the proximity of the left front wheel of the vehicle with the edge of the deck during vehicle redirection was such that the 9-ft 4½-in. post spacing was considered marginal. Thus a post spacing of 8 ft 0 in. was chosen to obtain the desired flexibility and yet retain sufficient rigidity within the barrier system to effectively contain and redirect an impacting vehicle with moderate vehicle damage, minor barrier damage, and tolerable passenger decelerations.

Neither the bridge approach flare nor the approach flare wing wall were impact tested in this study even though both were included in the initial project proposal. It was decided that the design assumptions that were verified by the results of the tests reported here could be utilized in the design of these appurtenances. Also, because the Type 15 BAGR was structurally similar to the successfully tested Type 8 BAGR (3), it was felt that the results of the Type 8 BAGR tests would be applicable. The Type 8 BAGR utilizes the same 6-WF-25-post and concrete post footing as does the Type 15 BAGR. However, the Type 8 post spacing is 10 ft on centers as compared to the 6-ft 3-in. spacing utilized for the Type 15. The Type 8 rail element is a 6-in. by 2-in., 12.02-lb structural steel tube that conforms to the requirements of ASTM Designation A500, grade B, whereas the Type 15 rail element is a 3½-in. square, 10.50-lb structural steel tube that conforms to the requirements of ASTM Designation A500, grade A or B, or A501. The section modulus of the Type 15 rail is approximately 70 percent that of the Type 8 rail. However, the 6-ft 3-in. post spacing of the Type 15 system is approximately 63 percent that of the Type 8. Therefore, the forces required to exceed the ultimate strength of the Type 15 and Type 8 rail elements are reasonably comparable ($F_{15} = 0.86F_8$). By increasing the post spacing of the Type 15 BAGR from 6 ft 3 in. to 8 ft 0 in. we can decrease this ratio to 0.67. However, the lateral kinetic energy imparted to the barrier during a 15-deg impact is only 37 percent of that imparted to the barrier at the 25-deg impact angle used for the tests of the Type 8 BAGR. Thus, an 8-ft 0-in. post spacing should be adequate for the Type 15 BAGR as well as for the Type 15 bridge rail.

Observation of the effect of the impact load distribution into the reinforced concrete bridge deck led to the decision that the structural design criteria utilized for the deck could be applied to the design of the approach flare reinforced concrete wing wall. It was felt that this would be an appropriate application, thus obviating the necessity of constructing a test installation and performing a full-scale impact test.

One problem encountered during construction or reconstruction of the bridge barrier installation was with the interior sleeve rail splice. It was reported by construction personnel that the lateral sliding tolerance between the sleeve and the interior of the tubular rail was too great; thus rail alignment at the splices was not as close as was desired. However, it should be noted that this clearance must be adequate to permit the splice sleeve to slide readily inside the tube for ease of barrier construction and rail replacement.

Another point of concern was the dimensional tolerances for the slotted hole in the tubular rail. When repairs were made the splice sleeves were not readily interchangeable, particularly when a tube that had been bent from the previous impact was used. This, however, could easily be remedied by increasing the slot width from 7/16 in. to ½ in. This should provide the needed tolerance for interchangeability.

Also, some method of sliding the sleeve other than hammering on the bolt head should be devised. The use of either a slot in the adjoining tube, with a corresponding hole in the splice sleeve, or a slot and corresponding hole on the opposite side of the

slotted tube would suffice. This would provide for the use of a drift pin to slide the splice sleeve and would facilitate assembly and disassembly of the barrier. Except for the aforementioned items, barrier construction and collision repairs were relatively easy and economical.

Interpretation of Instrumentation Data

The severity of the 50-msec vehicular decelerations reported here was determined by comparing the deceleration magnitudes with the recommended 200-msec deceleration tolerance limits proposed by Cornell. Injury severity predictions are related only to the direction of deceleration that appears to be most critical (i.e., no vectorial addition of deceleration was accomplished unless otherwise noted). A discussion of deceleration tolerances and the reasoning behind the choice of these values are given elsewhere (5). These limits define what would be, in the opinion of the researchers, a survivable environment under almost all circumstances when applied to the 50-msec time period (Table 1).

Filtered records of vehicular deceleration (100 Hz for Test 251 and 176 Hz for Test 252) were used to compute the highest 50-msec average values (average of ten continuous 5-msec intervals).

The dummy used in Tests 251 and 252 was restrained with a conventional lap belt. Only the vehicular lateral deceleration in Test 251 (9g) exceeded the recommended value for passengers restrained with lap belts (Table 1). This higher value was probably due to the closer post spacing and, hence, more rigid bridge rail system impacted in Test 251.

Longitudinal, lateral, and vertical components of deceleration from the dummy's head were vectorially combined to obtain a resultant value of deceleration. The Gadd Severity Index was

$$\int_{t_1}^{t_2} a^{2.5}\, dt$$

computed for the 50-msec period with the highest average resultant values of head deceleration using 20 time intervals, i.e., dt = 0.0025 sec. A discussion of the Gadd Severity Index and the tolerance of the human head to deceleration is contained elsewhere (9). The Gadd Severity Index (10), based on the resultant deceleration of the dummy's head, was 278 for Test 251 and 234 for Test 252. The lower threshold of fatal head injuries is 1,000 if we assume that penetration of the skull does not occur; therefore, the dummy would only have suffered moderate injuries in both tests, provided the impact occurred on the dummy's forehead or an equally strong portion of the skull and was distributed such that no penetration of the skull occurred.

The maximum seat belt loads measured were 1,350 lb for Test 251 and 120 lb for Test 252, which are not excessive values. The reason for the wide variation in seat belt loads is not readily apparent. It appears that the magnitude of these loads is independent of the 6-g maximum longitudinal dummy chest decelerations, which are almost identical for both tests. It is possible that there was a malfunction in the instrument for one or both tests that caused the wide variation in recorded seat belt loads.

An estimate of injury severity for both collisions can be inferred from the preceding results. Passengers restrained with lap belts and shoulder harnesses would probably have incurred minor or no injuries, passengers with lap belts would have sustained moderate injuries, and passengers who were unrestrained could have suffered serious injuries, particularly in Test 251.

The preceding results indicate that the bridge rail system used for Test 252 was slightly preferable to that used for Test 251 with regard to injury potential because of the lower vehicle decelerations recorded in Test 252 (particularly in the lateral direction). However, the dummy decelerations were approximately the same for both tests and are therefore inconclusive with regard to barrier preference.

The vehicle accelerometer records show that the vehicular backslap decelerations in the longitudinal direction for both tests were less than those recorded during the in-

itial impact. However, the lateral decelerations recorded during both the initial impact and the backslap were approximately equal in both tests.

CONCLUSIONS

The following conclusions are based on an analysis of the results of the full-scale vehicle impact tests reported here:

1. The initial California Type 15 bridge barrier rail design impacted in Test 251 will retain and redirect a 4,500-lb passenger car impacting at a velocity of 60 mph and an approach angle of 15 deg. Barrier damage can be expected to be minor and vehicle damage moderate. Because of the rigidity of this design (6-ft 3-in. post spacing), however, very little impact energy will be absorbed by the barrier. Thus, vehicle deceleration rates, particularly in the lateral direction, will be somewhat higher than desirable.
2. The modified California Type 15 bridge barrier rail design impacted in Test 252 will retain and redirect a 4,500-lb passenger car impacting at a velocity of 60 mph and an approach angle of 15 deg. Moderate vehicle damage and tolerable passenger compartment deceleration rates will be experienced. Barrier damage, particularly at the post-to-deck connection, will be significant and the barrier deflection will be such that the wheel (s) of the vehicle on the impact side will be very close to the edge of the bridge deck at the time of maximum barrier deflection. Thus, the 9-ft 4½-in. post spacing used in this design is considered marginal.
3. The California Type 15 bridge barrier rail design with post spacing of 8 ft on centers should produce both the desired flexibility within the barrier system and yet retain sufficient rigidity to effectively contain and redirect a 4,500-lb vehicle impacting at a speed of 60 mph and an angle of 15 deg. This 8-ft post spacing will also provide an economical and aesthetically pleasing compromise between the 6-ft 3-in. and the 9-ft 4½-in. post spacings tested.
4. The California Type 15 bridge approach guardrail (BAGR) with a post spacing of 8 ft 0 in. will effectively contain and redirect a passenger vehicle impacting at speeds of up to 60 mph and angles of 15 deg. This conclusion is based not only on the results of the bridge barrier rail tests reported here but also on the results of a previous series of tests of the structurally similar California Type 8 BAGR (Test 174) (3).
5. The assumptions used for the design of the barrier rail-bridge deck connection, which were verified by the results of the tests reported here, can be applied to the design of the approach rail-wing wall connection, thus eliminating the need to construct and test this appurtenance.

ACKNOWLEDGMENTS

This work was accomplished in cooperation with the U. S. Department of Transportation, Federal Highway Administration, as item D-4-90 of Work Program HPR-PR-1 (7). Part 2, Research. The opinions, findings, and conclusions expressed in this publication are those of the authors and not necessarily those of the Federal Highway Administration.

REFERENCES

1. Beaton, J. L., and Field, R. N. Dynamic Full Scale Tests of Bridge Rails. California Division of Highways, Dec. 1960.
2. Graham, M. D., et al. New Highway Barriers, The Practical Application of Theoretical Design. State of New York, Department of Public Works, May 1967.
3. Nordlin, E. F., Ames, W. H., and Hackett, R. P. Dynamic Tests of Type 9 Bridge Barrier Rail and Type 8 Bridge Approach Guardrail. California Division of Highways, June 1969.
4. Nordlin, E. F., and Field, R. N. Dynamic Full Scale Impact Test of Steel Bridge Barrier Rails, Series XI. California Division of Highways, June 1967.
5. Nordlin, E. F., Woodstrom, J. H., and Hackett, R. P. Dynamic Tests of the California Type 20 Bridge Barrier Rail, Series XXIII. California Division of Highways, Sept. 1970.

6. Nordlin, E. F., Stoker, J. R., Hackett, R. P., and Doty, R. N. Dynamic Tests of the California Type 15 Bridge Barrier Rail, Series XXV. California Division of Highways, June 1971.
7. Field, R. N., and Prysock, R. H. Dynamic Full Scale Impact Tests of Double Blocked-Out Metal Beam Barriers and Metal Beam Guardrail, Series X. California Division of Highways, Feb. 1965.
8. Highway Barrier Analysis and Test Program. Sumary Report, July 1960 to July 1961, Cornell Aeronautical Laboratory Report VJ-1472-V-3, July 1969.
9. Nordlin, E. F., Stoker, J. R., and Doty, R. N. Dynamic Tests of An Energy Absorbing Barrier Employing Sand-Filled Frangible Plastic Barrels, Series XXIV. California Division of Highways, April 1971.
10. Gadd., C. W. Use of a Weighted-Impulse Criterion for Estimating Injury Hazard. Proc., 10th Stapp Car Crash Conf., SAE, Nov. 1966.
11. Highway Research Board Committee on Guardrails and Guideposts, HRB Circular 482, Sept. 1962.

TENTATIVE CRITERIA FOR THE DESIGN OF SAFE SLOPING CULVERT GRATES

Hayes E. Ross, Jr., and Edward R. Post, Texas Transportation Institute, Texas A&M University

Some highway drainage structures have a geometrical configuration that can cause an errant automobile to come to an abrupt stop or veer out of control. One such structure is the end culvert inlet with or without headwalls. In recent years, highway engineers have used sloping inlet and outlet grates that allow an automobile to traverse the culvert opening rather than come to an abrupt stop. Sloping grates are currently designed on the basis of judgment and experience because objective criteria are practically nonexistent. By using a mathematical simulation technique, we were able to investigate the dynamic behavior of a selected standard-size automobile traversing a median containing a crossover and a sloping culvert inlet grate. Twenty-three computer simulations were made. It was determined that 8:1 ditch side slopes and 10:1 culvert grate slopes produced tolerable automobile accelerations to an unrestrained occupant. Steeper combinations of side and grate slopes were found to produce severe accelerations and/or roll-over and should be avoided where possible. For purposes of structural design, it was found that the dynamic tire load on 8:1 and flatter grate slopes was about five times the automobile curb weight. For 6:1 and steeper grate slopes, the dynamic tire load reached values of about 10 times the automobile curb weight.

•AS discussed in a recent publication (1), some highway drainage structures are potentially hazardous and, if located in the path of an errant vehicle, can substantially increase the probability of an accident. These structures consist of cross drains and their appended culvert end structures, median and curb inlets, roadside channels or ditches, and other special drainage structures.

An objective for which the highway engineer should strive has been defined as follows:

> A traffic-safe drainage structure is one which does not inhibit the driver's ability to regain control of his vehicle—permitting him either to return to the traveled roadway or to stop safely without damage or injury (1).

General guidelines that aid the highway engineer in the design of a traffic-safe drainage structure have been presented elsewhere (1). These guidelines reflect the best knowledge available concerning those measures that have proved to be the most successful in minimizing the potential hazards associated with drainage structures and maintaining hydraulic efficiency.

A sloping inlet or outlet grate is a structure occasionally used in place of the abrupt culvert inlet with or without headwalls. Figure 1 shows a typical sloping grate installation. This study provides criteria for the design of a traffic-safe sloping culvert grate.

A mathematical simulation technique was used to study the traffic-safe characteristics of a sloping grate-slope configuration. The simulation provided information on the motion, forces, and accelerations of an automobile that could be expected during the event. Twenty-three different events were studied to identify important parameters

Sponsored by Committee on Traffic Safety Barriers and Sign, Signal and Lighting Supports.

Figure 1. Typical sloping culvert grate.

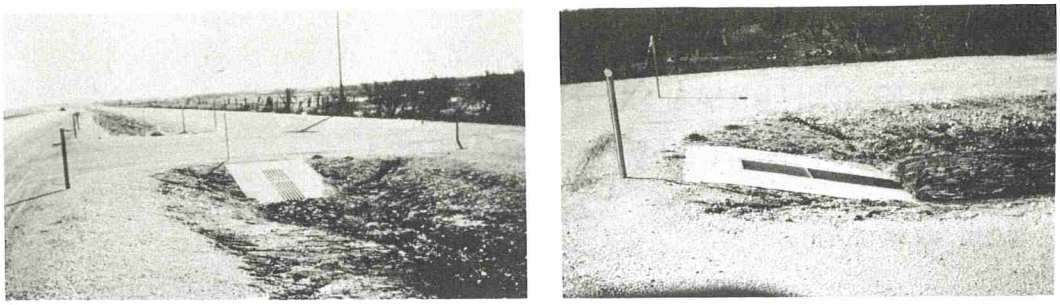

Figure 2. Idealization of automobile (2, 3).

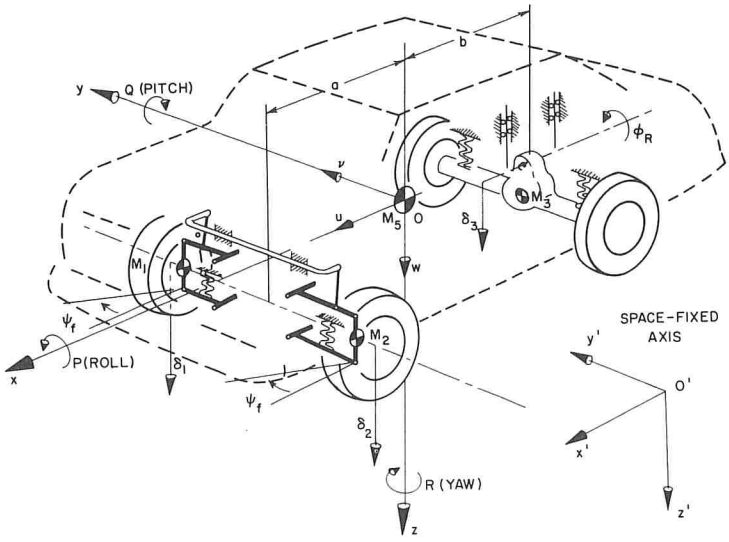

Figure 3. Simulated median terrain configuration and selected automobile paths.

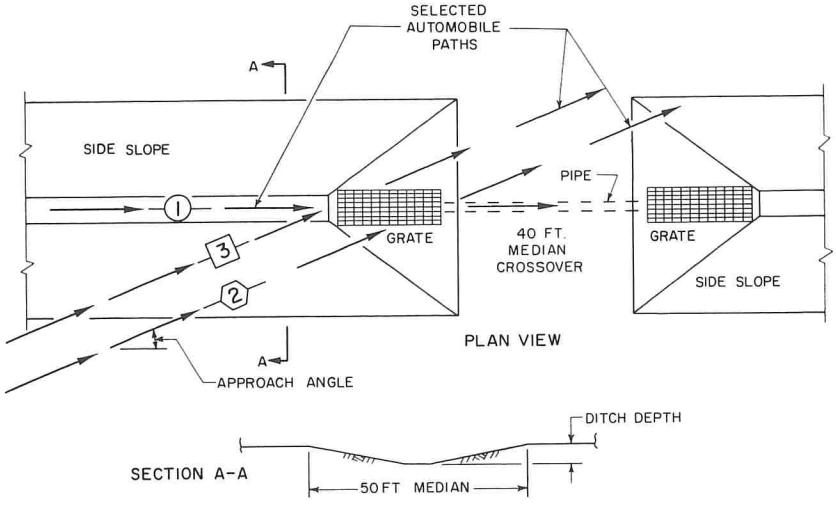

and to make recommendations concerning grate design. The information provided, when used in conjunction with the data in Ref. 1, will help the highway engineer ensure that an errant automobile can safely traverse a defined side slope and adjoining grate slope configuration.

MATHEMATICAL MODEL OF AN AUTOMOBILE

In the evaluation and design of a roadway and its environment, it is important to understand the effects of various roadway geometric features on the dynamic response of an automobile and its occupants.

The mathematical model described here was used to investigate the dynamic response of an automobile negotiating various side slope and adjoining sloping grate terrain configurations. The model can also be used to investigate various other problems associated with the roadway environment, such as highway traffic barrier collisions, rapid lane change maneuvers, handling response on horizontal curves, and drainage-ditch cross sections.

The mathematical model was developed by Cornell Aeronautical Laboratory (CAL) (2, 3) and later modified for specific problem studies by the Texas Transportation Institute (TTI) (4). A conceptual idealization of the model is shown in Figure 2. The model is idealized as four rigid masses, which include (a) the sprung mass (M_s) of the body supported by the springs, (b) the unsprung masses (M_1 and M_2) of the left and right independent suspension system of the front wheels, and (c) the unsprung mass (M_3) representing the rear axle assembly. The 11 degrees of freedom of the model include translation of the automobile in three directions measured relative to some fixed coordinate axes system; rotation about the three coordinate axes of the automobile; independent displacement of each front wheel suspension system; suspension displacement and rotation of the rear axle assembly; and steering of the front wheels. A more detailed discussion of the mathematical model is given elsewhere (2, 3, 4).

The validity of the model is dependent to a large extent on the accuracy of the input parameters pertaining to the automobile selected. In this study, a 1963 Ford Galaxie four-door sedan was selected because of (a) the availability of data on the automobile parameters, (b) the excellent comparisons obtained by CAL (2, 3) between full-scale tests and mathematical simulation during a variety of maneuvers, and (c) its representativeness of a large population of automobiles with regard to size, weight, and suspension.

Very good comparisons were observed between full-scale ramp traversal tests and corresponding simulated tests conducted by CAL (3). The nature of a ramp traversal by an automobile is very similar to that experienced during traversal of a sloping grate.

Mathematical simulation provides a rapid and economical method to investigate the many parameters involved as an automobile traverses some defined ground forms. Once the limiting parameters are identified, it may be desirable to conduct a limited number of full-scale tests prior to final selection of a particular design. This approach, in contrast to a full-scale trial-and-error approach, will yield more meaningful results with considerably less resource expenditure.

The mathematical simulation was facilitated by the use of an IBM 360 computer. Approximately 1 min of computer time is required for 1 sec of event time. On the average, it takes 3 sec for an automobile departing the roadway at a speed of 60 mph and at an angle to traverse some defined side and sloping grate ground form. The computer cost for 3 min of time is approximately $25.

EVALUATION CRITERIA

The criteria used in this study to investigate the traffic-safe characteristics of a ground form in the vicinity of sloping grate culvert were (a) automobile stability, (b) automobile airborne distance, and (c) automobile acceleration severity index.

The stability criterion requires that an automobile, subsequent to becoming airborne on the sloping grate, remain in an upright position. Roll-over was considered sufficient to classify a terrain configuration as being not traffic-safe. Roll-over was observed to occur in one of two ways. First, side roll-over occurred about the X-axis

of the automobile. Second, front-end roll-over occurred about an axis parallel to the Y-axis (pitch) upon contacting the terrain after being airborne.

The distance airborne criterion requires that the automobile, subsequent to becoming airborne on the sloping grate, land in a location that would not endanger the lives of motorists in the opposing traffic lanes of travel.

The acceleration severity index requires that the combined longitudinal, lateral, and vertical accelerations of the automobile at its center of mass have a severity index equal to or less than unity. A severity index of less than unity indicates that serious or fatal injuries will probably not occur. The equation used to determine the severity index is discussed in some depth elsewhere (5). The severity index equation is as follows:

$$SI = \sqrt{\left(\frac{G_{long}}{G_{XL}}\right)^2 + \left(\frac{G_{lat}}{G_{YL}}\right)^2 + \left(\frac{G_{vert}}{G_{ZL}}\right)^2}$$

where

G_{long} = actual automobile acceleration in longitudinal Z-axis, g;
G_{lat} = actual automobile acceleration in lateral Y-axis, g;
G_{vert} = actual automobile acceleration in vertical Z-axis, g;
G_{XL} = limit automobile acceleration in longitudinal X-axis, g;
G_{YL} = limit automobile acceleration in lateral Y-axis, g; and
G_{ZL} = limit automobile acceleration in vertical Z-axis, g.

The limit accelerations in the preceding equation were defined as the highest automobile accelerations that an occupant could sustain without serious or fatal injury. The limit acceleration values used in this study for an unrestrained occupant were G_{XL} = 7 g, G_{YL} = 5 g, and G_{ZL} = 6 g.

It is well known that the actual accelerations of an automobile can reach high values over a small time interval (from roughly 2 to 10 msec). Such accelerations are commonly referred to as "spikes." There is much discussion among highway and research engineers as to whether automobile acceleration spikes are actually felt by the occupants. In a recent publication (6), it was concluded that the accelerations of an automobile at its center of mass should be measured as an average over a time interval of 50 msec. The acceleration values reported in this study are in accordance with those findings (6).

MATHEMATICAL SIMULATION RESULTS

In this study, information is provided on a common type of culvert end structure protected by a sloping grate. This information was obtained from a mathematical simulation of a selected 1963 Ford Galaxie traversing various side and sloping grate ground forms at a median crossover.

A median width of 50 ft and, for all but one case, a ditch depth of 3 ft were selected to limit the number of parameters to be studied. The departure speed of the automobile from the roadway was taken as 60 mph, whereas the departure angle was treated as a variable. Figure 3 shows a typical roadway site terrain configuration. The results of this study also apply to at least two other roadway sites: (a) where two sloping grates collect and distribute water into a culvert pipe placed under the traveled roadway to a drainage ditch in the right-of-way as shown in Figure 4, and (b) where the culvert end structure is placed parallel to the traveled roadway under a driveway or roadway that abuts the main highway.

A total of 23 mathematical simulations was investigated in arriving at an optimum design for the median side slope and grate slope terrain configuration shown in Figure 3.

The first group, consisting of six mathematical simulations, was designed to determine the effect of the grate slope, ditch depth, and departure path on the automobile's response. A median side slope of 6:1 and a departure angle of 25 deg were maintained for each run. The slope of the culvert grate was varied from 4:1 to 10:1. Side roll-over occurred in traversing 10:1 and steeper grate slopes for a path 2 departure

Figure 4. Modification of existing culvert crossover with headwalls (1).

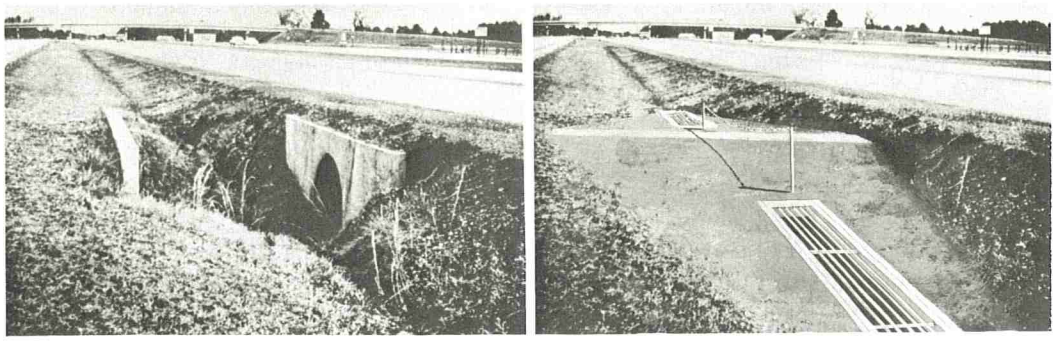

Figure 5. Simulation of automobile negotiating 6:1 side slope and 6:1 culvert grate slope at a speed of 60 mph and an angle of 25 deg.

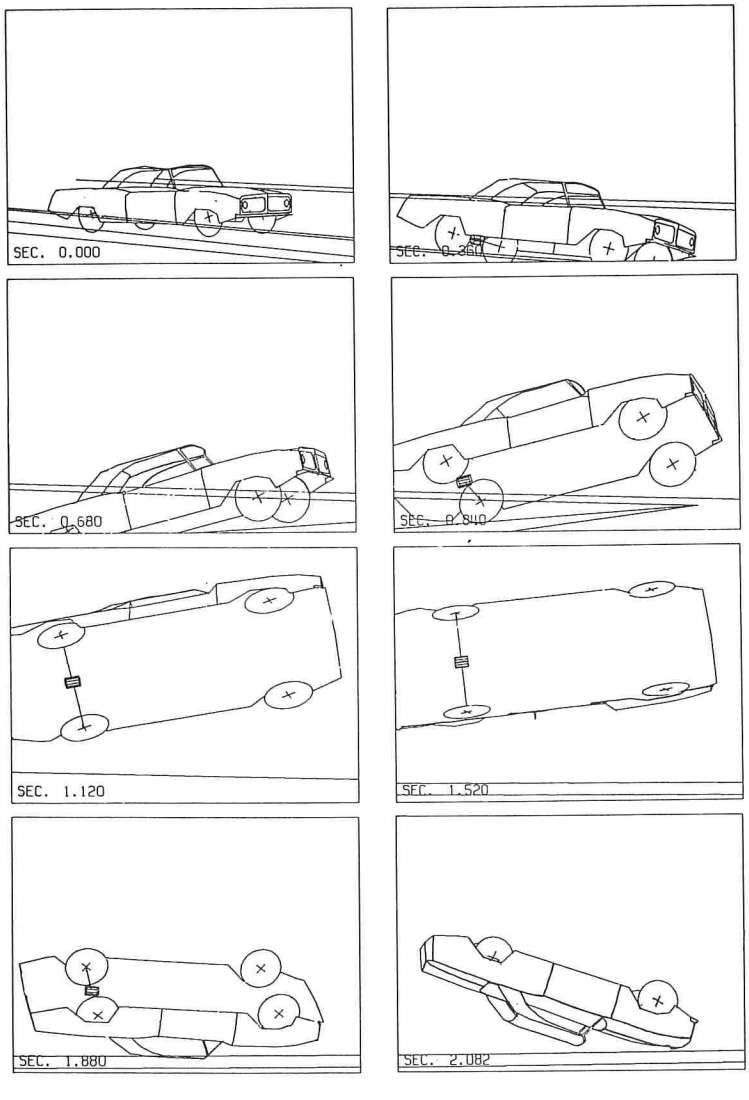

(Table 1). Figure 5 shows the side roll-over of an automobile traversing path 2 after negotiating a 6:1 grate slope. Side roll-over did not occur when the automobile departure path (path 3, Fig. 3) from the roadway was such that the automobile encountered the flat ditch prior to traversing the grate slope. With regard to ditch depth, a change from 3 to 2 ft did not prevent roll-over. Ditch depths greater than 3 ft were not considered because of the limitations imposed by the 50-ft median width. Also, greater ditch depths on wider medians should not appreciably alter the relative angle between the side slope and the grate slope, so that a path similar to that which produced roll-over would be possible.

The second group, consisting of two simulations, involved a median side slope of 8:1 and a grate slope of 6:1. Side roll-over did not occur in either of these cases, but the magnitude of the accelerations was sufficient to probably inflict serious injuries. Also, for the 25-deg departure angle, the airborne criterion was not satisfied; the automobile landed in the opposing traffic lane.

The third group, consisting of four simulations, concerned head-on traversals in which the grate slope was varied from 4:1 to 10:1, and all other variables were held constant. The results obtained from the head-on simulations are given in Table 1 and shown in Figure 6. The steeper the grate slope is, the greater are the automobile accelerations, dynamic vertical tire loads, and height and distance airborne. At a grate slope of 6:1, the automobile, upon contacting the terrain after being airborne, rolled over about its front end (Fig. 7). For the path 1 traversals, the accelerations for a 10:1 grate slope are on the border line, and the severity index indicates that severe injuries can occur; whereas, for grate slopes steeper than 10:1, the severity index indicates that severe injuries will occur.

The fourth group, consisting of six simulations, was run to determine the feasibility of using a median side slope of 8:1 and a grate slope of 8:1. The departure angle of the automobile was treated as a variable. Roll-over occurred at a very shallow departure angle of 5 deg in traversing path 2 as shown in Figure 3. However, when the automobile encountered the flat ditch prior to traversing the grate slope (path 3, Fig. 3) at the same shallow departure angle of 5 deg, roll-over did not occur.

It appeared at this point that an 8:1 side slope and 10:1 grate slope would be a reasonable combination that would satisfy the safety criteria in addition to the economic and hydraulic requirements. The fifth and last group, consisting of five simulations, involved a median side slope of 8:1 and a grate slope of 10:1. The automobile departure angle was treated as the variable. The acceleration severity index of the automobile was unity or less for all cases. As mentioned earlier, however, the acceleration severity index slightly exceeded unity for a head-on 10:1 grate slope simulation, which indicates that severe injuries may occur. The terrain locations where the automobile will land after being airborne are shown in Figure 8. For departure angles of 20 deg or less, the automobile will land within the median on the other side of the 40-ft crossover; whereas, for a departure angle of 25 deg, the automobile will land on the outside edge of the opposite traffic lane shoulder. Simulations were not made for automobile departure angles of more than 25 deg because of the findings of Hutchinson (7), which show that only a small percentage (about 11 percent) of the median encroachments exceed 25 deg. In this study the maximum roll angle of 50 deg occurred at a shallow departure angle of 5 deg (Table 1).

This study also provides information on the dynamic loads imposed by the automobile tires on the culvert grate. Load impact factors, which are defined as the ratio of the dynamic tire loads to the static tire loads, were computed and are given in Table 1. In the absence of additional data it may be assumed that these load impact factors for a standard-size automobile would pertain to any automobile.

SUMMARY AND CONCLUSIONS

The objective of this study was to develop criteria for designing traffic-safe sloping grate configurations. To accomplish this task, we used a mathematical computer simulation technique to investigate the dynamic behavior of a standard-size automobile traversing various terrain configurations in the vicinity of a sloping culvert grate.

Figure 6. Head-on 60-mph simulations of automobile traversing various sloping grate configurations.

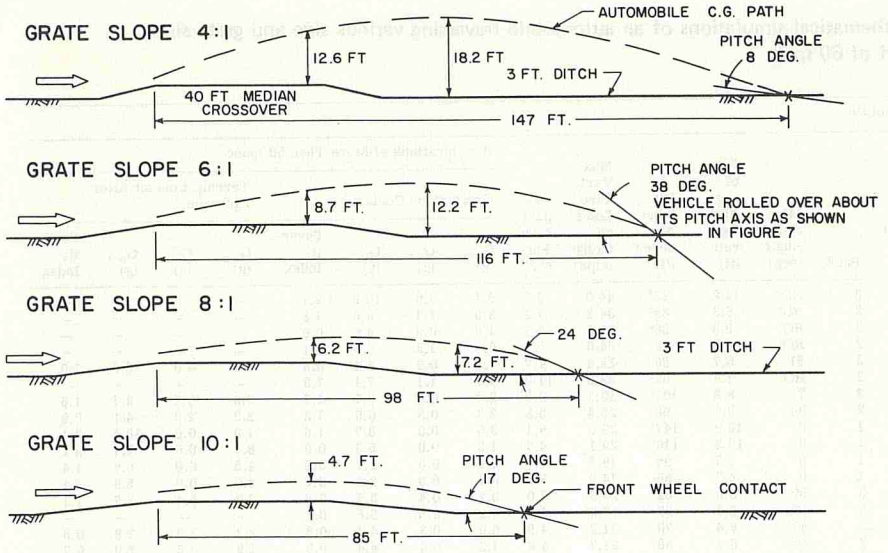

Figure 7. Head-on 60-mph simulation of automobile negotiating a 6:1 culvert grate slope.

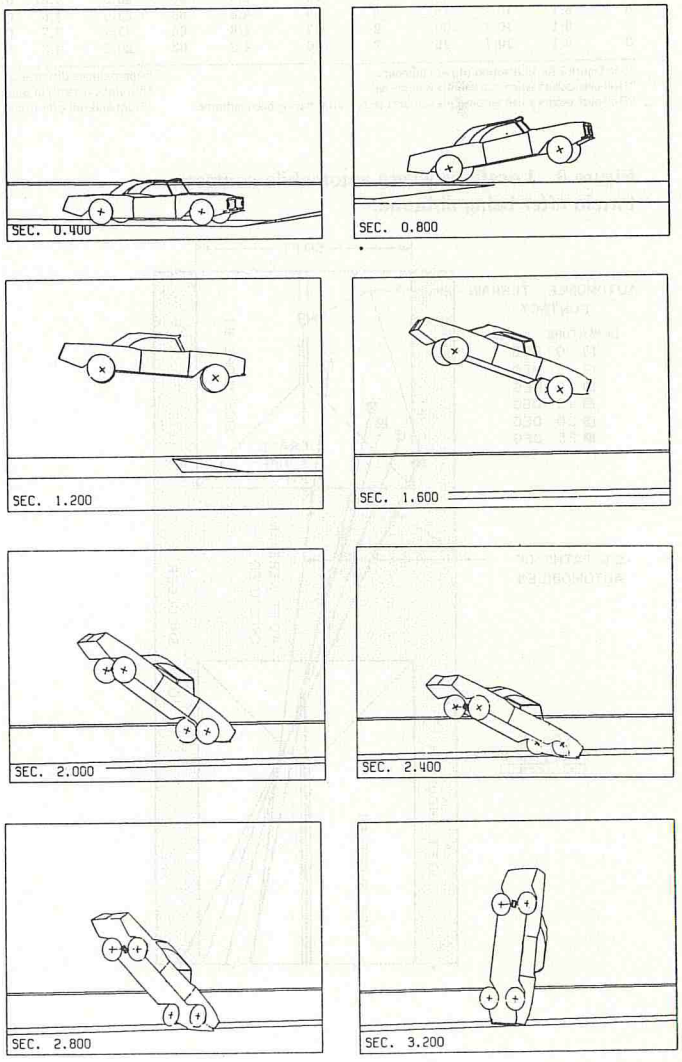

Table 1. Results of mathematical simulations of an automobile traversing various side and grade slope configurations at a speed of 60 mph.

Terrain			Automobile							Accelerations of More Than 50 msec							
										Grate Slope Contact				Terrain Contact After Airborne			
Ditch Depth (ft)	Side Slope	Grate Slope	Approach Angle (deg)	Path[a]	Max. Roll Angle (deg)	Rise of c.g. Above Terrain (ft)	Distance Airborne (ft)	Max. Vert. Tire Load on Grate (kips)	Impact Load Factor	G_{Long} (g)	G_{Lat} (g)	G_{Vert} (g)	Severity Index	G_{Long} (g)	G_{Lat} (g)	G_{Vert} (g)	Severity Index
3	6:1	4:1	25	2	RO[b]	11.8	93[d]	44.0	9.3	5.1	1.9	10.8	2.1	—	—	—	—
3	6:1	6:1	25	2	RO[b]	6.3	85[d]	34.2	7.2	3.5	1.1	6.8	1.3	—	—	—	—
3	6:1	8:1	25	2	RO[b]	5.8	58[d]	31.9	6.7	1.8	0.9	4.6	0.9	—	—	—	—
3	6:1	10:1	25	2	RO[c]	4.7	52	24.6	5.2	0.3	1.3	6.5	1.1	—	—	—	—
3	6:1	6:1	25	3	51	6.7	86	22.4	4.7	1.1	0.6	4.4	0.8	1.3	4.8	3.9	1.0
2	6:1	6:1	25	2	RO[b]	7.8	87[d]	52.3	11.0	1.9	1.1	7.1	1.3	—	—	—	—
3	8:1	6:1	25	2	7	8.8	101[e]	30.1	6.3	2.8	0.4	9.1	1.7	0.3	0.7	9.7	1.6
3	8:1	6:1	15	2	34	9.9	98	25.4	5.3	2.3	0.3	6.9	1.2	2.2	2.9	4.1	0.9
3	—	4:1	0	1	0	18.2	147	29.0	6.1	3.6	0.0	8.7	1.6	1.9	0.0	18.4	3.1
3	—	6:1	0	1	0	12.2	116[f]	22.1	4.7	1.3	0.0	5.3	0.9	8.4	0.0	7.7	2.1
3	—	8:1	0	1	0	7.2	98	19.3	4.1	0.6	0.0	3.7	0.6	4.5	0.0	6.6	1.4
3	—	10:1	0	1	0	4.7	86	14.9	3.1	0.1	0.0	3.1	0.5	3.0	0.0	5.9	1.1
3	8:1	8:1	5	3	50	6.6	82	23.9	5.0	0.2	0.4	3.6	0.8	2.9	5.4	2.7	1.1
3	8:1	8:1	5	2	RO[c]	6.1	97	18.9	4.0	0.2	0.5	3.6	0.6	—	—	—	—
3	8:1	8:1	10	2	40	6.4	78	21.2	4.5	0.9	0.3	4.4	0.8	2.2	3.7	2.9	0.8
3	8:1	8:1	15	2	50	6.3	68	22.7	4.8	1.2	0.4	4.4	0.8	1.9	3.2	2.0	0.7
3	8:1	8:1	20	2	21	6.2	78	21.2	4.5	1.4	0.3	6.3	1.1	1.2	1.2	2.4	0.5
3	8:1	8:1	25	2	12	6.2	81[e]	23.6	5.0	1.5	0.3	7.1	1.2	1.1	1.0	2.4	0.5
3	8:1	10:1	5	2	50	4.8	73	17.8	3.7	0.1	0.5	3.4	0.6	2.7	4.8	2.4	1.0
3	8:1	10:1	10	2	32	5.0	68	20.3	4.3	0.1	0.4	3.6	0.6	1.8	2.5	2.6	0.7
3	8:1	10:1	15	2	34	4.8	62	21.6	4.6	0.7	0.3	3.5	0.6	1.7	3.0	3.3	0.8
3	8:1	10:1	20	2	17	4.8	65	17.7	3.7	0.9	0.3	5.2	0.9	0.3	0.7	4.9	0.8
3	8:1	10:1	25	2	26	4.8	63	20.5	4.3	0.9	0.3	5.4	0.9	0.3	0.6	3.6	0.6

[a]See Figure 3 for illustration of path numbers.
[b]Roll-over occurs when automobile is airborne.
[c]Roll-over occurs when automobile contacts terrain after having been airborne.
[d]Approximate distance when top of automobile contacts terrain.
[e]Automobile lands in opposing traffic lane.
[f]Front-end roll-over occurs when automobile contacts terrain after having been airborne.

Figure 8. Locations where automobile contacts terrain after being airborne.

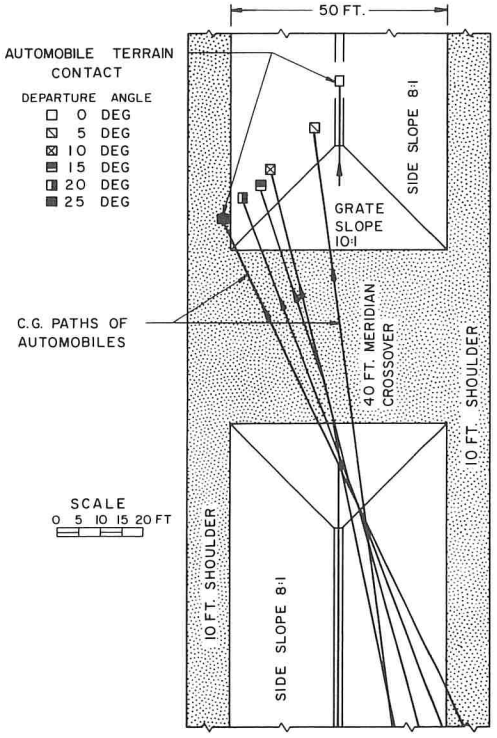

A typical roadway site was selected to limit the number of parameters studied. The site consisted of a divided roadway, a median crossover, and sloping inlet and outlet grates to allow water to flow under the crossover. A median width of 50 ft and, for all but one case, a ditch depth of 3 ft were selected. The speed at which the automobile departed from the roadway was taken as 60 mph.

Parameter studies were conducted to determine what influence departure angle and path, median side and grate slopes, and ditch depth had on the response of an automobile and occupant. Both head-on and angle departures were studied. For evaluation criteria, the configurations were judged on the basis of minimizing automobile accelerations as measured by a severity index, preventing roll-over, and minimizing the chance of the automobile landing in the opposite lane of traffic after being airborne. Specific findings of this study are as follows:

1. For side slope and grate slope traversals, the tendency of an automobile to roll over increases as the angle of departure from the roadway decreases;
2. For head-on traversals, the acceleration severity index for a grate slope of 10:1 may be questionable; whereas, for grate slopes steeper than 10:1, the severity index indicates that severe injuries would probably occur; and
3. When used in conjunction with 10:1 and steeper grate slopes, wide roll-over will occur on a 6:1 slope with ditch depths of 2 and 3 ft.

The simulation results further indicate that, during a departure angle of 25 deg or less, an automobile could safely traverse a terrain configuration having side slopes of 8:1 and a culvert grate slope of 10:1. Findings on the dynamic response of an automobile as it traverses this particular ground form are summarized as follows:

1. The acceleration severity index indicates that an unrestrained occupant would probably not be seriously injured;
2. The maximum roll angle of 50 deg occurred at a shallow departure angle of 5 deg;
3. The distance airborne was sufficiently low such that the automobile would land on the shoulder of the opposing traffic lane or median and hence probably not endanger traffic in the opposing lanes of travel; and
4. The dynamic vertical tire load on the sloping grate was about 5 times greater than the static weight of the automobile.

Guidelines that suggest that side slopes and culvert sloping grates should be 10:1 and flatter are presented elsewhere (1). The findings of this study tend to substantiate those guidelines.

ACKNOWLEDGMENT

The consultation and suggestions of Mr. John Nixon and Mr. Dave Hustace of the Texas Highway Department and Mr. Edward Kristaponis of the Federal Highway Administration during the course of this study were appreciated. Mr. Wayne Lammert's assistance in conducting computer runs and in data reduction is acknowledged.

REFERENCES

1. Traffic-Safe and Hydraulically Efficient Drainage Practice. NCHRP Synthesis of Highway Practice 3, 1969.
2. McHenry, R. R., and Segal, D. J. Determination of Physical Criteria for Roadside Energy Conversion Systems. Cornell Aeronautical Laboratory, Rept. VJ-2251-V-1, July 1967.
3. McHenry, R. R., and DeLeys, N. J. Vehicle Dynamics in Single Vehicle Accidents: Validation and Extension of a Computer Simulation. Cornell Aeronautical Laboratory, Rept. VJ-2251-V-3, Dec. 1968.
4. Young, R. D., Edwards, T. C., Bridwell, R. J., and Ross, H. E. Documentation of Input for Single Vehicle Accident Computer Program. Texas Transportation Institute, Texas A&M University, Research Report 140-1, July 1969.
5. Ross, H. E., and Post, E. R. Criteria for Guardrail Need and Location on Embankments. Texas Transportation Institute, Research Report 140-4, Oct. 1971, 61 pp.

6. Nordlin, E. F., Woodstrom, J. H., and Hackett, R. P. Dynamic Tests of the California Type 20 Bridge Barrier Rail, Series XXIII. California Division of Highways, Materials and Research Laboratory, Report 636459, Sept. 1970, pp. A6-7.
7. Hutchinson, J. W., and Kennedy, T. W. Medians of Divided Highways—Frequency and Nature of Vehicle Encroachments. Eng. Exp. Station, Univ. of Illinois, Bull. 487, 1966, Figure 17.

MEDIAN DIKE IMPACT EVALUATION: SENSITIVITY ANALYSIS

Duane F. Dunlap and Philip Grote, University of Michigan

An impact sensitivity analysis was performed on earthen drainage dikes that are constructed in the median of divided highways perpendicular to the roadway (1). Six parameters are examined: approach velocity, approach angle, dike lateral impact position, dike approach slope, soil type, and median profile. Results are evaluated by comparing maximum values of acceleration, incremental velocity change, and center-of-gravity height. Dynamic variable data are presented for selected cases. The simulation program is described along with the modifications necessary for simulating travel over soft soil (a common condition in drainage control areas). Conclusions indicate the probable unsafe character of the current dike standard.

•IN current Michigan freeway design practice, dikes are placed in the median perpendicular to the right-of-way to control surface water runoff. Because of the proximity of the dikes to traffic and ramp-like cross sections, a program was initiated to evaluate dike configurations in terms of the dynamic response imparted to an impacting vehicle. The purpose of the evaluation is to define an optimum cross section for both minimizing the hazard to errant vehicles and maintaining positive drainage control.

Dynamic interaction of the vehicle and dike was simulated by means of the Cornell Aeronautical Laboratory Single Vehicle Accident (CALSVA) model. The model is programmed for use on a digital computer and was altered where necessary to simulate specific dike-vehicle interaction phenomena. The primary modification was the inclusion of a high-speed, soft soil subroutine.

PROBLEM DEFINITION

The current standard dike configuration used in Michigan (2) is shown in Figure 1. The approach slope on both sides of the crest is 1:6. The objective of the program is to examine this cross section and variations of it to arrive at a more optimum design standard.

The final section must be evaluated over the range of impact conditions that exist in the operational environment to ensure its adequacy. In addition, criteria for evaluation must be developed that relate impact phenomena to occupant safety.

Operational Impact Conditions

Operational impact conditions fall into four main areas: vehicle type, approach velocity, approach angle, and impact position along the dike. The range of interest for the first three of these can be determined from survey data that have been collected for other purposes.

Vehicle type data in the form of weight frequency and distribution (3) are shown in Figure 2. Because more than 85 percent of all vehicles weigh between 1,500 and 4,500 lb, this weight range was chosen for this study.

Approach velocity data are difficult to ascertain because of the probable differences between highway speeds and actual impact speeds after some braking has occurred. The

Sponsored by Committee on Traffic Safety Barriers and Sign, Signal and Lighting Supports.

Figure 1. Basic median profile with 1:6 dike face slope.

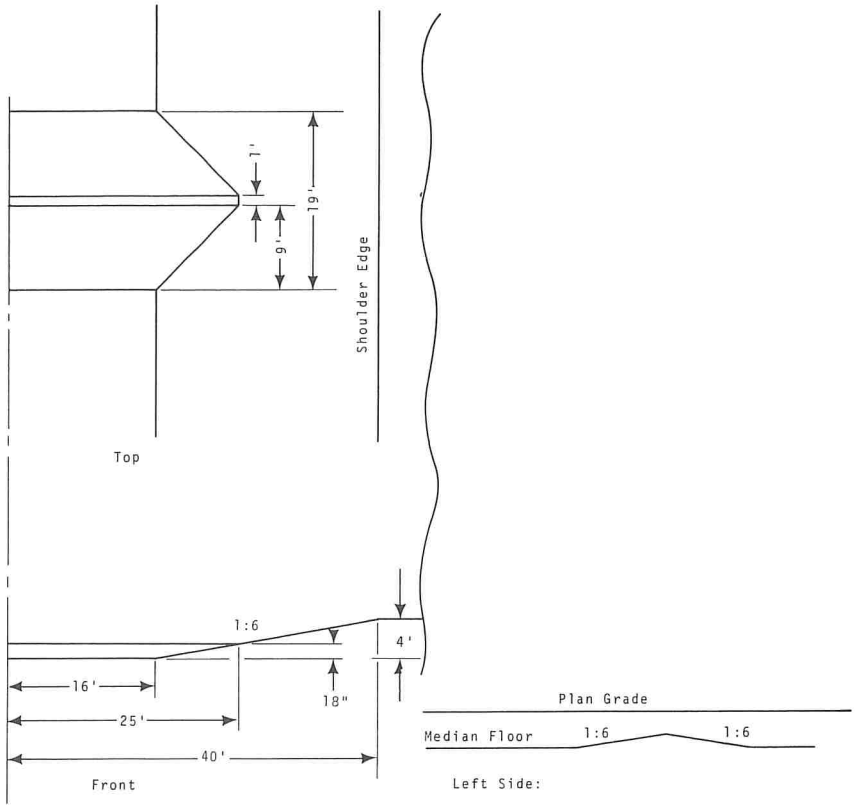

Figure 2. Vehicle weight distribution and frequency.

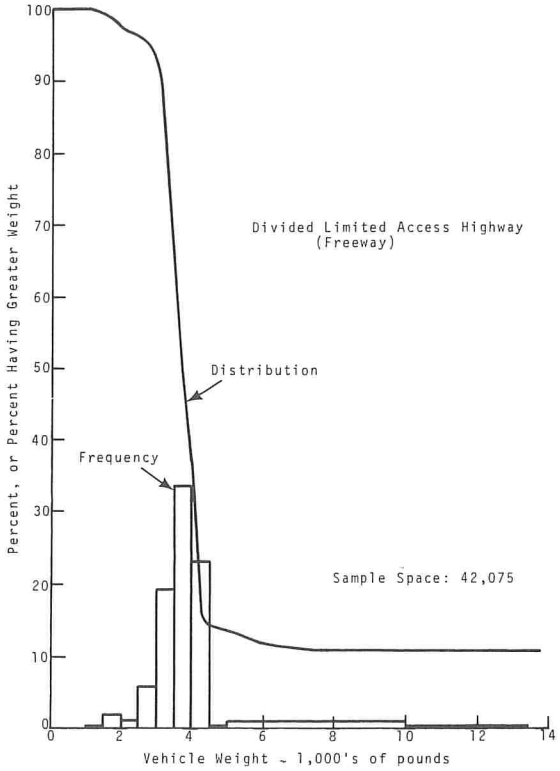

range for approach velocities was therefore taken from two sources: actual highway speed survey data (4) and impact speed data estimated by investigating police officers (5). The two kinds of data are shown in Figures 3 and 4 respectively. From these data the range of applicable impact speeds was chosen to lie between 40 and 80 mph. This covers 98 percent of the vehicles in the highway speed survey and 86 percent of the vehicles in the estimated impact speed range.

The range of approach angles was taken from the Hutchinson data (6) shown in Figure 5. Ninety percent of the roadway exit angles measured in this study were between 0 and 25 deg; this was therefore chosen as the range of interest.

Evaluation Criteria

Criteria for evaluating a particular dike cross section must involve considerations of safety as well as drainage efficacy. Drainage is not an overriding consideration, however, because primary drainage control requirements can be used to calculate minimum dike height. Therefore, if a minimum height constraint exists the controlling factors in dike design are related to the safety of motorists.

Occupant safety, in turn, can be correlated with the time histories of injury-related kinematic variables as the vehicle contacts the dike. According to current understanding (7), the primary kinematic variables that influence occupant injury are incremental change in velocity, acceleration, and acceleration onset. Velocity change manifests itself in the relative velocity of a passenger in a secondary collision with the vehicle interior; acceleration and acceleration onset are shown through the internal loading and deformation of body parts. Of the three, least is known about the effects of acceleration onset.

The level, direction, and duration of action of these variables are generally considered in assigning tolerance levels. The situation is complicated by several factors, however, some of which include passenger restraint, age, vital condition, and body orientation. Therefore, a sharp cutoff between injury and no injury in terms of kinematic variables does not exist, and injury assessment on this basis can only be made in a general sense. Working-range thresholds used in this evaluation are as follows (7, 8):

	Injury Threshold	
Criterion	Magnitude	Duration
ΔV_z	12 fps	—
a_z	10 g	100 to 200 msec

No threshold is listed for da_z/dt (acceleration onset) because of the general lack of applicable experimental data. Therefore, only ΔV_z and a_z were used as injury-related evaluation criteria. Each is associated with vertical motions of the passenger because this is the primary direction of the forces imparted to the vehicle as it crosses the dike.

MATHEMATICAL MODEL

The basic digital computer simulation program used in the study was developed and validated by McHenry and DeLeys at Cornell Aeronautical Laboratory. Briefly, the vehicle is represented in the program by an assemblage of four rigid masses: the main vehicle body, or "sprung mass," a solid rear axle, and two independent front wheels with their attendant suspension systems. The sprung mass has 6 degrees of freedom (roll, pitch, and yaw rotations and longitudinal, lateral, and vertical displacements); the rear axle has two (roll rotation and vertical displacement); and each front wheel has one (vertical displacement). An additional degree of freedom can be associated with the steering system as a user option. Other vehicle simulation features include representations of front-wheel camber, rear-axle roll steer, anti-pitch suspension characteristics, nonlinear suspension springs in both extension and compression (including bump stops), Coulomb and viscous friction in the suspension, elastic roll stiffness, and nonlinear tire aligning torque. A more extensive description of the program is given elsewhere (9, 10, 11).

Figure 3. Vehicle speed distribution and frequency for passenger automobiles.

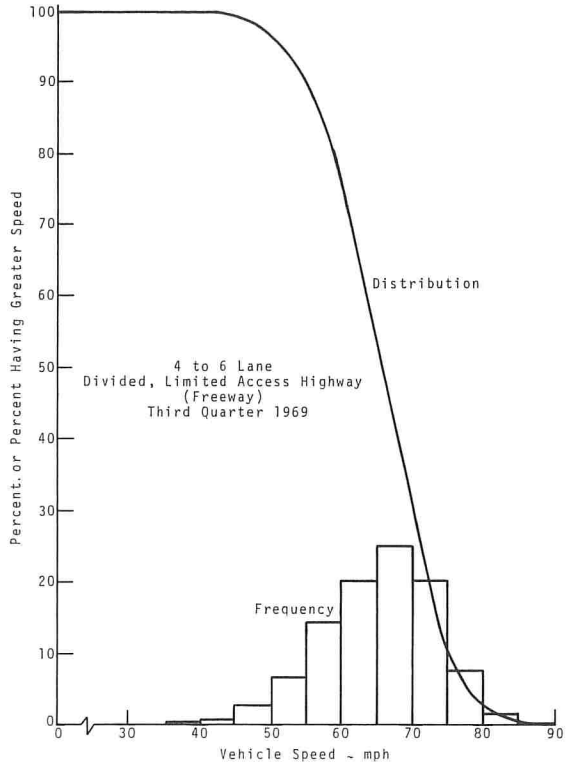

Figure 4. Estimated impact speed distribution and frequency for passenger automobiles.

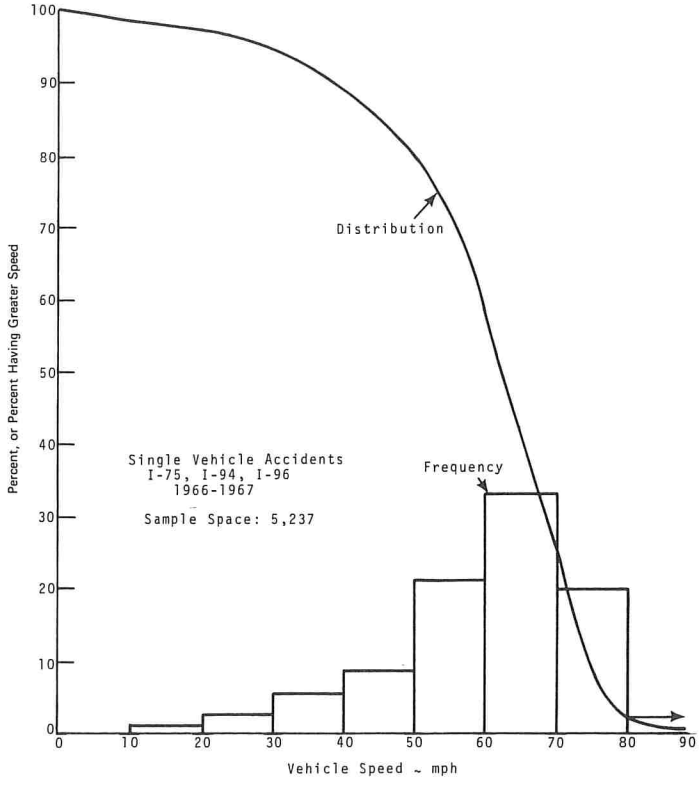

Figure 5. Encroachment angle distribution and frequency.

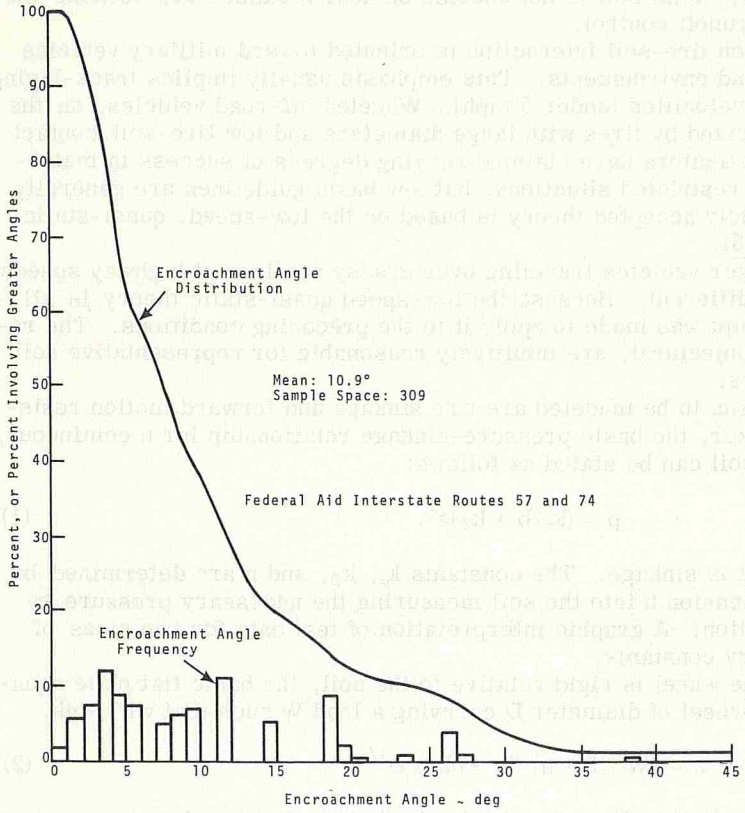

Table 1. Dike interaction sensitivity analysis (simulation exercise program).

Case	α (deg)	V (mph)	Lateral Position	Approach Slope	Soil Type	Approach Profile
1 (Baseline)	0	40	Center	1:6	Hard, frozen	Flat to dike
2	25	40	Center	1:6	Hard, frozen	Flat to dike
3	0	80	Center	1:6	Hard, frozen	Flat to dike
4	0	40	One wheel on flat, one on dike	1:6	Hard, frozen	Flat to dike
5	0	40	Center	1:10	Hard, frozen	Flat to dike
6	25	40	Center	1:6	Hard, frozen	Full median profile
7	0	40	Center	1:6	Soft, moist	Flat to dike
8	25	80	Center	1:6	Hard, frozen	Full median profile

The primary program addition for evaluating earthen dikes was the inclusion of a soft soil subroutine. Soft, moist soil is not uncommon near median dikes because the primary dike function is runoff control.

Most of the literature on tire-soil interaction is oriented toward military vehicles operating in swamp or sand environments. This emphasis usually implies track-laying vehicles traveling at low velocities (under 5 mph). Wheeled off-road vehicles, on the other hand, are characterized by tires with large diameters and low tire-soil contact pressures. Several investigators have claimed varying degrees of success in mathematically modeling these restricted situations, but few basic guidelines are generally agreed on. The most widely accepted theory is based on the low-speed, quasi-static analysis of Bekker (12, 13).

For stiff-tired passenger vehicles traveling over grassy medians at highway speeds, conditions are obviously different. Because the low-speed quasi-static theory is all that is available, an attempt was made to apply it to the preceding conditions. The results, although strictly conjectural, are intuitively reasonable for representative soil characterizing parameters.

The two basic phenomena to be modeled are tire sinkage and forward motion resistance. According to Bekker, the basic pressure-sinkage relationship for a continuous, homogeneous, isotropic soil can be stated as follows:

$$p = (k_c/b + k_\phi)z^n \tag{1}$$

where p is pressure and z is sinkage. The constants k_c, k_ϕ, and n are determined by driving a flat plate of dimension b into the soil measuring the necessary pressure to achieve a certain penetration. A graphic interpretation of test data for two sizes of plates yields the necessary constants.

If it is assumed that the wheel is rigid relative to the soil, the basic flat plate equation can be extended to a wheel of diameter D carrying a load W such that will sink.

$$z = 3W/[(3 - n)\ (k_c + bk_\phi)\ D^{1/2}] \tag{2}$$

Additional assumptions implicit in Eqs. 1 and 2 imply that predicted values become more valid as the soil sinkage approaches zero and the wheel diameter approaches infinity. Practical limits indicate adequate agreement with test data at low speeds for a miximum diameter of 20 in. and a maximum sinkage of one-sixth of the diameter.

As the tire sinks while moving forward, it must displace the soil in its path. The soil is partly compacted beneath the rolling tire surface and partly bulldozed to the side. These two effects are generally lumped together in calculating the forward motion resistance as follows:

$$R = (3W)^\epsilon/[(3 - n)^\epsilon\ (n + 1)\ k^{1/2n+1}\ D^{\epsilon/2}] \tag{3}$$

where

$\epsilon = (2n + 2)/(2n + 1)$ and
$k = k_c + bk_\phi$.

This relationship is derived by considering the ground reaction over the surface of the tire-soil interface and integrating over that area to obtain the equivalent resistance force.

The mathematical relations in Eqs. 1, 2, and 3 were incorporated into the variable terrain profile subroutine of the original simulation and are available on a user option basis.

SENSITIVITY ANALYSIS

The procedure for the sensitivity analysis consisted of making variations on a single standard case. The sensitivity of the vehicle-dike system to a particular parameter was

then determined, in terms of the evaluation criteria, by varying only that parameter from the standard. This resulted in a series of two-point estimates of the true variation for each parameter.

The parameters and the respective values of each that was used in the sensitivity analysis are listed as follows:

1. Approach velocity: 40 mph, 80 mph;
2. Approach angle: 0 deg, 25 deg;
3. Dike approach slope: 1:6, 1:10;
4. Impact position along dike: center, one wheel on flat—one wheel on dike;
5. Approach profile: flat to dike, full median profile; and
6. Soil type: hard-frozen, soft-moist. The first value given for each of the preceding parameters was the standard case value.

The simulation exercise program for the specific cases that were examined is given in Table 1. Parameters and variables that were held constant for these runs are as follows:

1. A dike height equal to 18 in.;
2. A fixed steering-wheel position;
3. An unpowered vehicle;
4. Up to 75 parameters defining the dynamic properties of a 1963 Ford Galaxie, four-door, eight-cylinder sedan; and
5. The median profile as shown in Figure 1.

RESULTS

Study results were derived from kinematic data histories from the vehicle-dike simulation runs. Two samples of the kinematic data are shown in Figures 6 and 7.

Kinematic Data

Kinematic data for case 1 (Table 1) are shown in Figure 6. Vertical acceleration, vertical velocity, and center-of-gravity height are shown. Center-of-gravity height is measured with respect to a flat reference, with zero corresponding to the at-rest center-of-gravity position. The acceleration and velocity variables are measured with respect to a body fixed coordinate system. The arrows attached to the center-of-gravity height points represent the vehicle pitch attitude.

The dike profile is actually about 22 in. below the indicated position because the at-rest center-of-gravity height is taken as zero. The dike profile is also distorted because of the difference in vertical and horizontal scales.

Examination of the data reveals that the vehicle flies into the air to a maximum height of about 5 ft following initial contact with the dike. The vehicle pitch angle reaches an upper value of about 16 deg during this time. A maximum acceleration of about 17 g occurs at the landing point following the initial airborne phase. This acceleration is the peak of a fairly narrow spike, however, and the average acceleration during the 100-msec interval between the time marks within which the spike falls is about 6 g. During this period, the oscillation frequency of the acceleration trace is about 40 Hz. In general, this kind of acceleration would probably not cause injury to a seated passenger.

The maximum change in velocity, about 21 fps, occurs at the impact after the second airborne phase. This would probably cause injury to an unrestrained passenger in a "second colission" with the car interior.

Data for a second example, case 3, are shown in Figure 7. This case differs from case 1 only in that the velocity is 80 mph rather than 40 mph. Vehicle motions are, however, markedly different.

The vehicle travels more than 13 ft into the air following initial contact with the dike and 6 ft during the first rebound. Maximum pitch angle reaches 46 deg. This occurs during the second airborne phase and is responsible for the irregularity in the center-of-gravity trace near the 300-ft position point. The rear end of the vehicle strikes the ground at this location.

Figure 6. Case 1 kinematic data.

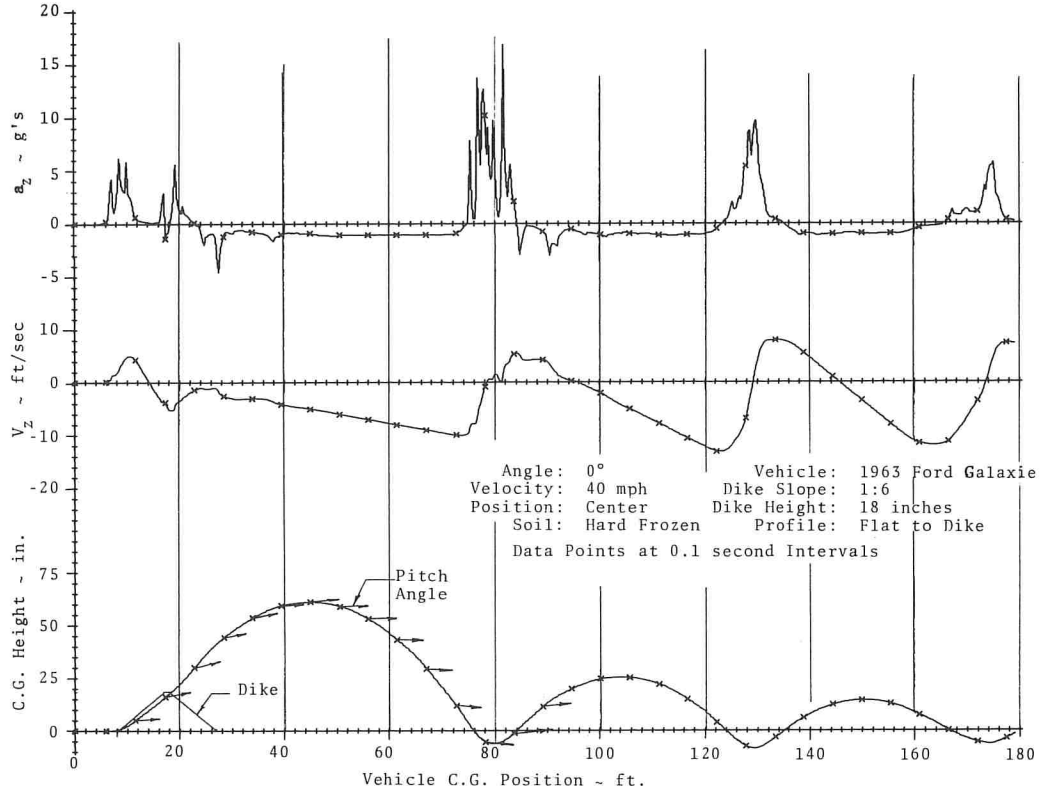

Figure 7. Case 3 kinematic data.

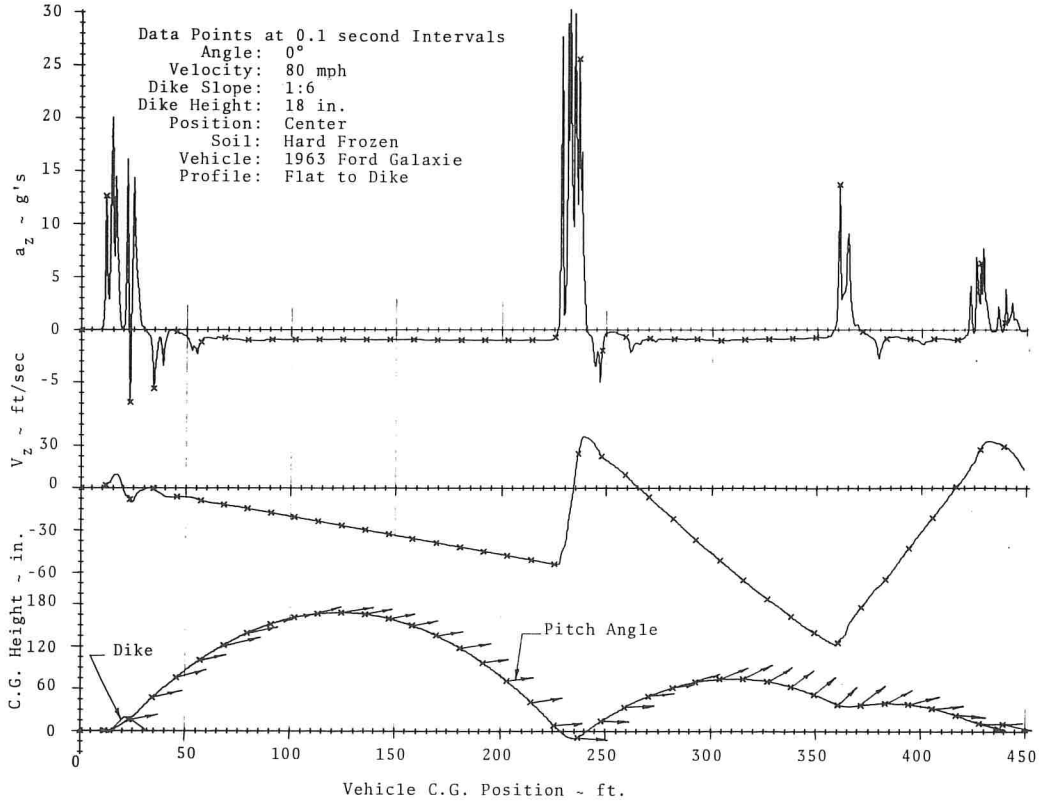

Maximum acceleration is again at the landing point following the initial airborn phase. Peak acceleration is more than 30 g, and the average is about 15 g over a 100-msec interval. The oscillation frequency is about 50 Hz. It is unlikely that an unrestrained passenger could withstand these accelerations without injury.

The maximum change in velocity is about 73 fps. This occurs at the initial landing when the vehicle strikes the ground and rebounds. This velocity change is not entirely vertical because it is measured with respect to a coordinate system fixed in the car. Large pitch angles of the vehicle tend to complicate the situation, with the result that some of the velocity change is a component of forward velocity. The vehicle attached coordinate system is realistic relative to passenger attitute, however, in that the passenger feels these velocity changes through a reorientation of his motion with respect to the vehicle interior. Needless to say, the indicated magnitude of velocity change would very probably cause injury.

Comparative Data

The sensitivity of the vehicle-dike system to a specific parameter was estimated by comparing the variation of selected evaluation measures as the parameter was varied. The measures were maximum vertical acceleration, maximum vertical velocity change, and maximum center-of-gravity height. The first two were compared with the threshold levels given in Table 1 as a means of estimating occupant injury.

Angle Effect—The effect of varying the approach angle to the dike is given in Table 2, in which cases 1 and 2 are compared with approach angles of 0 and 25 deg respectively. Interestingly, case 1 shows larger acceleration and greater center-of-gravity movement, whereas case 2 shows greater velocity change. The effects are due to the roll motion inherent in case 2 and tend to suggest that impact angle has a sizable effect on vehicle kinematics. Results in both cases are in the range of possible passenger injury.

Approach Velocity Effect—The effect of approach velocity on the vehicle-dike system is given in Table 3. Two sets of runs are compared with velocities of 40 and 80 mph. One set is for a 0-deg impact angle (cases 1 and 3), whereas the other is for a 25-deg angle with a full median approach profile (cases 6 and 8).

By examining the 0-deg approach angle first, one can observe that there are marked increases in all three measures when the speed is increased from 40 to 80 mph. Passenger injury is virtually certain in the 80-mph case.

One could get a different impression from the 25-deg approach angle data, however, because the increases here are not nearly as great. Except for the center-of-gravity height, this can be explained by the fact that the case 8 run (V = 80 mph, α = 25 deg) was terminated just after impact with the dike when the vehicle had rolled over on its side. Therefore, the acceleration and ΔV_z values are not strictly comparable. Each of these would undoubtedly have been higher had the run continued. Center-of-gravity height is fairly representative, however, because the vehicle appeared to be near maximum height at the termination point.

Approach velocity has a large effect on all measures, then, except perhaps for center-of-gravity height at high approach angles. In the latter case, much of the energy that would normally cause the car to fly into the air is converted to roll motion.

Lateral Position Effect—The effect of impact position along the dike is given in Table 4, in which cases 1 and 4 are compared. In case 1, the vehicle was directed toward the center of the dike, whereas in case 4 the vehicle was positioned along the median side slope such that one wheel went over the dike while the other just missed. The height of the dike under the traversing wheel was about 10 in.

The data given in Table 4 make it quite clear that there is a dramatic decrease in vehicle loading for the off-center impact. Kinematic values are negligible by comparison, which indicates that position along the dike has a considerable effect on vehicle kinematics.

Dike Approach Slope—The system sensitivity to dike approach slope is given in Table 5. Data for cases 1 and 5 with slopes of 1:6 and 1:10 respectively are compared. In each case, values of acceleration, ΔV_z, and center-of-gravity height for the 1:10 case

are roughly half those for the 1:6 case. Whereas the 1:6 slope might cause injury, the 1:10 slope would probably not. Dike slope is an important factor, then, in vehicle-dike interaction.

Soil Effect—The effect of soil variation on the system is indicated in Table 6, which compares cases 1 and 7. Evidently, soft soil causes a substantial reduction in vehicle acceleration and velocity change—in effect, altering the injury probability from likely to unlikely. The soil is quite soft, however, with the vehicle sinking in up to 8 in. at highway speeds.

As indicated earlier, the soft soil model used in the simulation is strictly an intuitive one. Both theoretical and experimental work are required to develop a truly valid high-speed soil model, and this has not been done. The model appears to be representative, however, and as a minimum gives an indication of the attenuating benefits of softer soil. Soil is therefore an important factor relative to vehicle kinematics.

Median Profile Effect—Case 2 involves a flat approach to the dike, and in case 6 the vehicle approaches over the full median profile. The approach angle in each case is 25 deg. Comparative data are given in Table 7.

Peak accelerations are slightly less for the full median case, whereas the maximum change in velocity is substantially less. Lower values for the full median case are due to the roll attitude of the vehicle as it travels down the median slope. Because the vehicle is approaching the dike at an angle, one front wheel strikes the dike before the other, which causes an initial rolling motion. The vehicle is already rolled by virtue of its traveling down the median slope, however, and the induced roll is less. Resulting impact loads on the front tire are also less. Although the difference in ΔV_z values is substantital, the general agreement is closer than in any of the other cases.

CONCLUSIONS AND RECOMMENDATIONS

Sensitivity analysis has shown that most of the vehicle-dike parameters investigated have a marked influence on vehicle dynamics. It also seems clear that, due to the general nonuse of seat belts, the standard dike profile, with 1:6 approach slope, is unsafe. Indeed, a casual examination of several dike installations indicates that dikes in general are rather nonstandard and that many have steeper slopes than 1:6. Thus, the problem is an acute one. Specific conclusions are listed as follows:

1. Possible injury to unrestrained passengers is indicated at all speeds above 40 mph when a vehicle strikes the middle of a dike similar to the current Michigan standard.
2. Approach velocity, angle, impact position, dike slope, and soil type have sizable effects on vehicle kinematics. Dike approach profile has a lesser effect.
3. An impact velocity of 80 mph produces about twice the passenger loading that is experienced at 40 mph.
4. Striking the dike in the middle is far more traumatic than hitting off to one side. This suggests that the hazardous portion of the dike may be limited to a relatively narrow region.
5. Striking a 1:10 slope reduces passenger loadings by a factor of about one-half when compared to a 1:6 slope.
6. Soft, moist soil attenuates passenger loading on the order of 50 percent when compared with rigid terrain.
7. Approaching the dike from the road shoulder appears to be less traumatic than approaching from a flat surface.

Now that the important interaction parameters have been identified, the next step is to proceed in developing an optimized cross section. This will require a full-scale test program and additional simulation activities.

Further investigation of high-speed, tire-soil interaction is also required. Since this investigation, the tire-soil work of Crenshaw (14) has been published, but further research is still needed.

ACKNOWLEDGMENT

The research reported in this paper was financed under the Highway Planning and Research Program and was sponsored by the Michigan Department of State Highways

Table 2. Approach angle effect on vehicle dynamics.

Case	V (mph)	α (deg)	$a_{z_{max}}$ (g)	$\Delta V_{z_{max}}$ (fps)	z_{max} (in.)
1	40	0	16.9	21.2	60.9
2	40	25	9.9	34.8	50.5

Table 3. Approach velocity effect on vehicle dynamics.

Case	V (mph)	α (deg)	Approach Profile	$a_{z_{max}}$ (g)	$\Delta V_{z_{max}}$ (fps)	z_{max} (in.)
1	40	0	Flat	16.9	21.2	60.9
3	80	0	Flat	30.3	72.6	168.1
6	40	25	Full median	8.2	17.8	50.4
8	80	25	Full median	12.7	59.3	59.1

Table 4. Lateral impact position effect on vehicle dynamics.

Case	V (mph)	α (deg)	Lateral Position	$a_{z_{max}}$ (g)	$\Delta V_{z_{max}}$ (fps)	z_{max} (in.)
1	40	0	Center	16.9	21.2	60.9
4	40	0	One wheel flat, one on dike	1.6	2.8	4.8

Table 5. Dike approach slope effect on vehicle dynamics.

Case	V (mph)	α (deg)	Approach Slope	$a_{z_{max}}$ (g)	$\Delta V_{z_{max}}$ (fps)	z_{max} (in.)
1	40	0	1:6	16.9	21.2	60.9
5	40	0	1:10	9.0	10.4	33.4

Table 6. Soil effect on vehicle dynamics.

Case	V (mph)	α (deg)	Approach Profile	$a_{z_{max}}$ (g)	$\Delta V_{z_{max}}$ (fps)	z_{max} (in.)
2	40	25	Flat	9.9	34.8	50.5
6	40	25	Full median	8.2	17.8	50.4

Table 7. Median profile effect on vehicle dynamics.

Case	V (mph)	α (deg)	Soil Type	$a_{z_{max}}$ (g)	$\Delta V_{z_{max}}$ (fps)	z_{max} (in.)
1	40	0	Rigid	16.9	21.2	60.9
7	40	0	Soft, moist	4.9	13.0	47.6

through a subcontract to the Highway Safety Research Institute from Wayne State University. The opinions, findings, and conclusions expressed in this paper are those of the authors and not necessarily those of the sponsoring agencies.

REFERENCES

1. Zobel, E. C., et al. Investigation of the Dynamic Impact on Roadside Obstacles—Interim Report. Wayne State University, Publication MES-1, Nov. 15, 1971.
2. Dykes in Median Ditches. Road Design Letter No. 525, from P. E. Plambech to Design Supervisors, Squad Leaders, and Consultants, Michigan Department of State Highways, Aug. 10, 1959, revised Aug. 2, 1963.
3. 1968 Truck Weight and Characteristics Study. Michigan Department of State Highways, Bureau of Engineering, MDSH Report No. 63.
4. Speed Report. Michigan Department of State Highways, Report No. 66, Oct. 1969.
5. Accident Master Tapes of Michigan State Highway Department. Michigan Department of State Highways, 1966 and 1967.
6. Hutchinson, J. W. The Significance and Nature of Vehicle Encroachment on Medians of Divided Highways. University of Illinois, Urbana, Highway Engineering Series No. 8, Dec. 1962.
7. Snyder, R. G. State-of-the-Art—Human Impact Tolerance. SAE Reprint 700398, revised Aug. 1970.
8. Patrick, L. M., Mertz, H. J., Jr., and Kroell, C. K. Cadaver Knee, Chest and Head Impact Loads. 11th Stapp Car Crash Conference, Oct. 10-11, 1967.
9. McHenry, R. R., Segal, D. J., and DeLeys, N.J. Determination of Physical Criteria for Roadside Energy Conversation Systems. Cornell Aeronautical Laboratory, CAL No. VJ-2251-V-1, July 1967.

THE National Academy of Sciences is a private, honorary organization of more than 800 scientists and engineers elected on the basis of outstanding contributions to knowledge. Established by a congressional act of incorporation signed by Abraham Lincoln on March 3, 1863, and supported by private and public funds, the Academy works to further science and its use for the general welfare by bringing together the most qualified individuals to deal with scientific and technological problems of broad significance.

Under the terms of its congressional charter, the Academy is also called upon to act as an official—yet independent—adviser to the federal government in any matter of science and technology. This provision accounts for the close ties that have always existed between the Academy and the government, although the Academy is not a governmental agency and its activities are not limited to those on behalf of the government.

The **National Academy of Engineering** was established on December 5, 1964. On that date the Council of the National Academy of Sciences, under the authority of its act of incorporation, adopted articles of organization bringing the National Academy of Engineering into being, independent and autonomous in its organization and the election of its members, and closely coordinated with the National Academy of Sciences in its advisory activities. The two Academies join in the furtherance of science and engineering and share the responsibility of advising the federal government, upon request, on any subject of science or technology.

The **National Research Council** was organized as an agency of the National Academy of Sciences in 1916, at the request of President Wilson, to provide a broader participation by American scientists and engineers in the work of the Academy in service to science and the nation. Its members, who receive their appointments from the President of the National Academy of Sciences, are drawn from academic, industrial, and government organizations throughout the country. The National Research Council serves both Academies in the discharge of their responsibilities. Supported by private and public contributions, grants, and contracts and by voluntary contributions of time and effort by several thousand of the nation's leading scientists and engineers, the Academies and their Research Council thus work to serve the national interest, to foster the sound development of science and engineering, and to promote their effective application for the benefit of society.

The **Division of Engineering** is one of the eight major divisions into which the National Research Council is organized for the conduct of its work. Its membership includes representatives of the nation's leading technical societies as well as a number of members-at-large. Its Chairman is appointed by the Council of the Academy of Sciences upon nomination by the Council of the Academy of Engineering.

The **Highway Research Board** is an agency of the Division of Engineering. The Board was established November 11, 1920, under the auspices of the National Research Council as a cooperative organization of the highway technologists of America. The purpose of the Board is to advance knowledge of the nature and performance of transportation systems through the stimulation of research and dissemination of information derived therefrom. It is supported in this effort by the state highway departments, the U.S. Department of Transportation, and many other organizations interested in the development of transportation.

HIGHWAY RESEARCH BOARD
NATIONAL ACADEMY OF SCIENCES—NATIONAL RESEARCH COUNCIL
2101 Constitution Avenue Washington, D. C. 20418

ADDRESS CORRECTION REQUESTED

CIVIL ENGR
ENS 3/14